Searches for CPT and Lorentz Invariance Violation with Fermilab Muon g-2

Breese Quinn, University of Mississippi

University of Liverpool Seminar

5 July 2024

CPT and Lorentz Symmetry

- Transformations
  - **Lorentz** (foundation of relativity)
    - Rotations about and boosts along 3 spatial directions
  - **CPT** (foundation of Quantum Field Theory)
    - C: Charge (particle → antiparticle)
    - P: Parity (spatial inversion: mirror + upside down)
    - T: Time (flip direction of time flow)

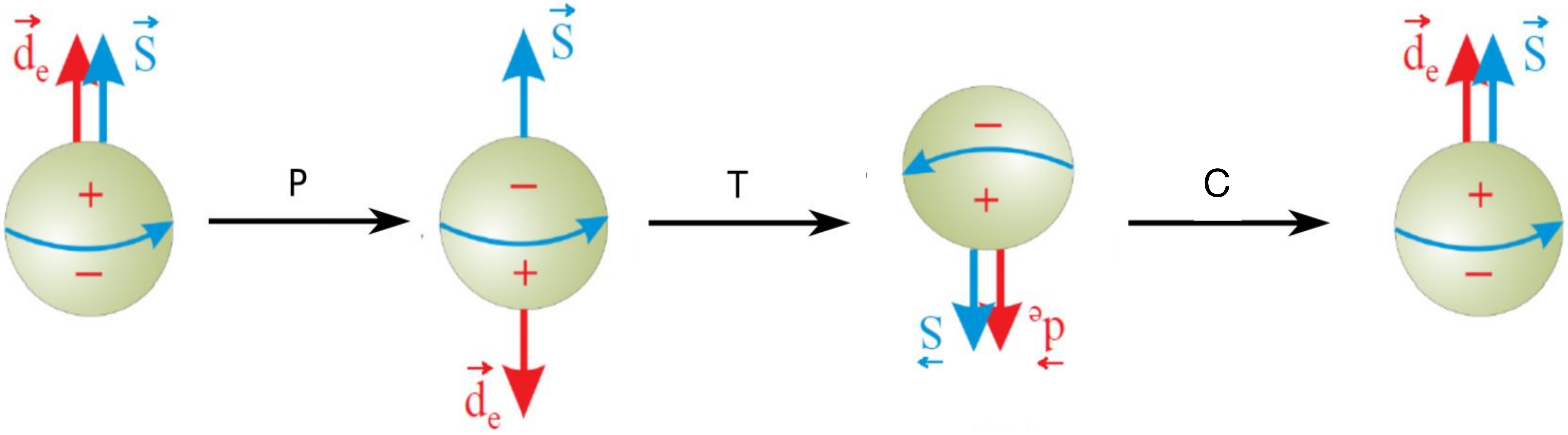

CPT and Lorentz Symmetry

- **Symmetry or Invariance**
  - Laws of physics are unaffected by transformations
  - All symmetries are **ONLY** as good as the **EXPERIMENTAL** evidence for them! (i.e. we assume L and CPT invariance in our theories simply because there is no evidence that they are violated)

- **Why are we always speaking of CPT and L together (CPTLIV)?**
  - **CPT Theorem**: certain theories (local QFT) with Lorentz Symmetry must also have CPT Symmetry (e.g. QED, SM, GUTs)
    - Implies particles and antiparticles have the same m, τ, q, μ

CPT and Lorentz Symmetry

- No evidence for CPTLIV (doesn't mean it's not there!)

- Relatively easy to form a phenomenological description of CPTLIV, but hard to do so with an underlying theory framework that is compatible with
  - Experimental evidence in our universe
  - Established QFT (e.g. SM) and GR (both with Lorentz Symmetry)

- **SME: Standard Model Extension** (Colladay and Kostelecky, Phys.Rev.D58:116002,1998)
  - Includes all conventional SM and GR properties
  - Allows for CPTLIV that is quantitatively described by coefficients to be determined experimentally
    - Only "particle LIV", not "observer LIV"

Lorentz Violations

- **Observer Lorentz Transformation**
  - Relate measurements of an experiment made from different reference frames (i.e. the experiment stays put)
  - David and Breese must agree because simply a change of coordinates

- **Particle Lorentz Transformation**
  - Identical experiments are rotated or boosted relative to each other
  - David's 2 expts may or may not agree
  - Conventional vacuum: OLT and PLT are just inverse of each other
  - Fixed background field: source of Lorentz Violation. Creates preferred direction. If an experiment sensitive to such field is transformed, measurable effects can be observed.

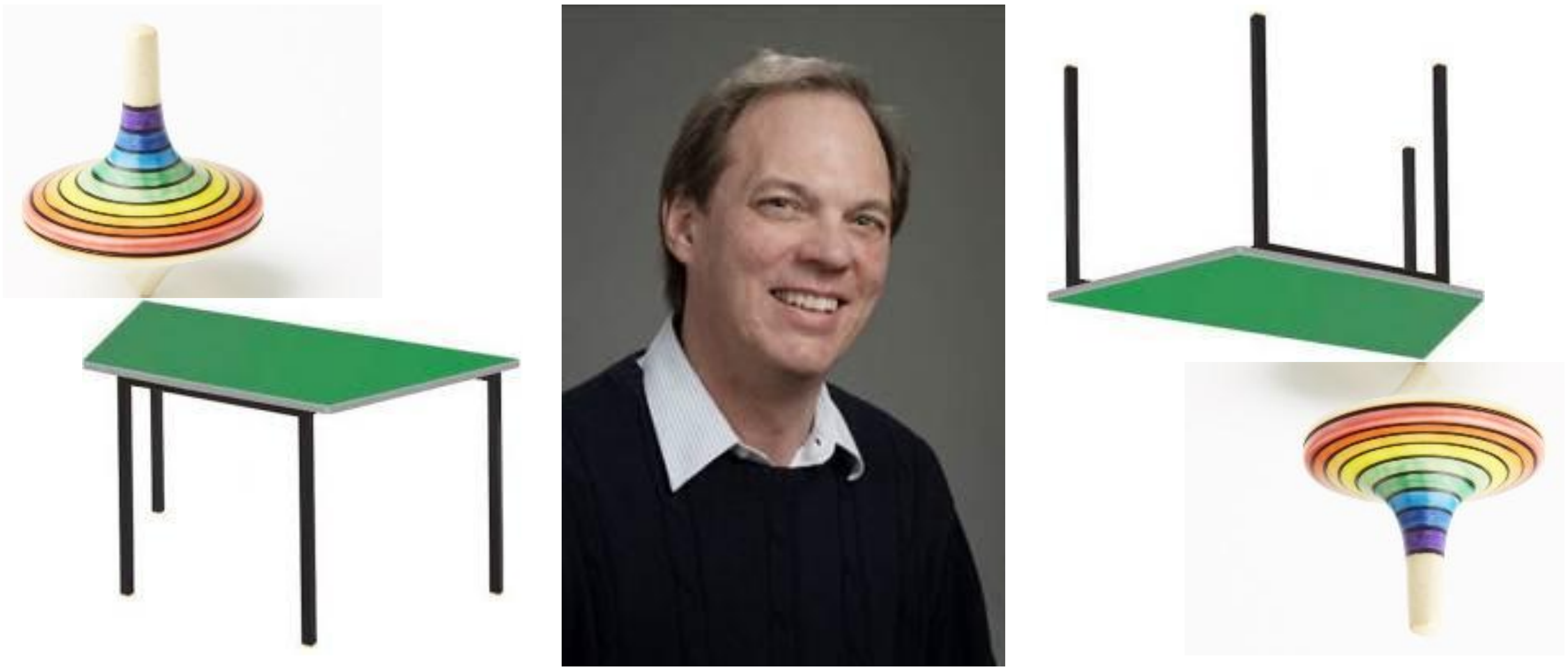

CPT and Lorentz Violations

- **Lorentz Violation – existence of a preferred direction**
  - Uniform background vector, *b*
  - What could it come from? Spontaneous Symmetry Breaking, e.g.
    - **SM:** In EWSB, scalar field gets non-zero vacuum expectation value, filling vacuum with *Lorentz Symmetric quantities*
    - **SME:** Can have Lorentz SB, where vector field gets non-zero vev, filling vacuum with *4-dimensionally oriented quantities* → preferred direction in space → **LIV!**
    - Possibilities: string theory, loop-quantum gravity, etc.

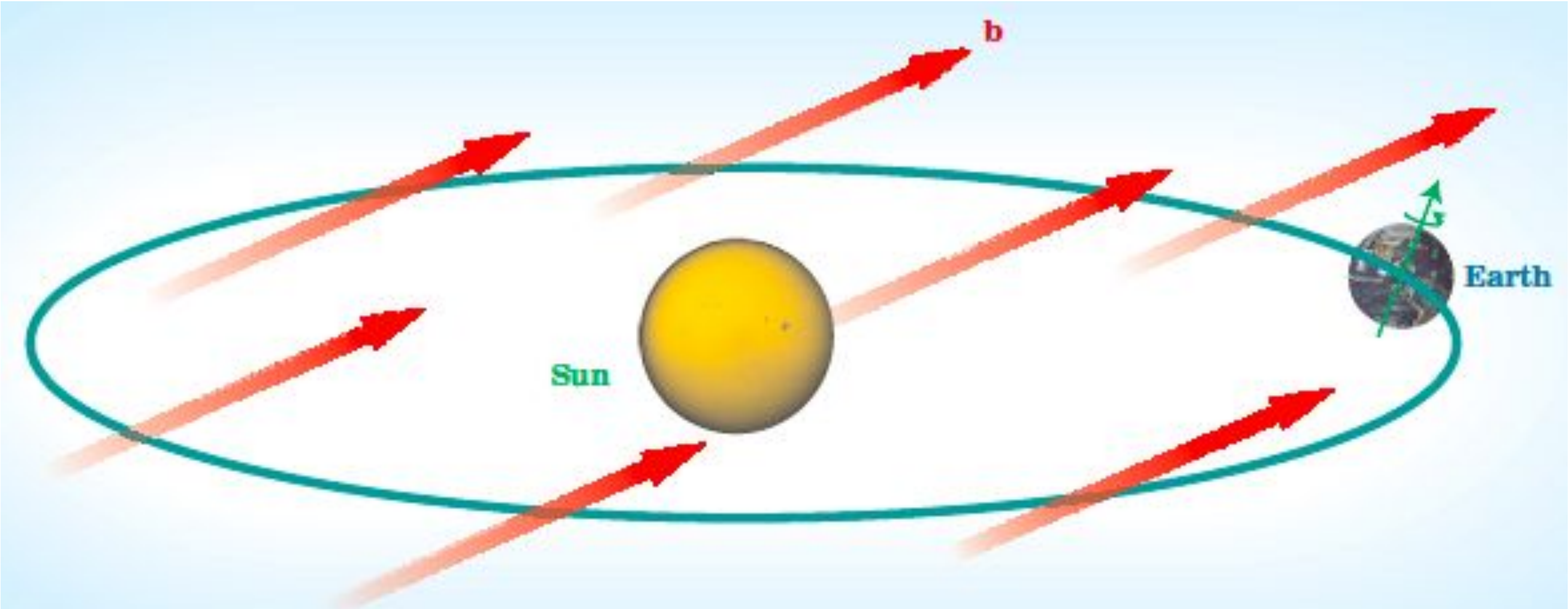

- **CPT Violation**
  - LIV *allows* but does not *require* CPTV, because CPT Theorem no longer holds (but CPTV does require LIV)

Brillet-Hall: Anisotropy of Space

VOLUME 42, NUMBER 9 PHYSICAL REVIEW LETTERS 26 FEBRUARY 1979

Improved Laser Test of the Isotropy of Space

A. Brillet[a] and J. L. Hall
Joint Institute for Laboratory Astrophysics, National Bureau of Standards and University of Colorado, Boulder, Colorado 80309

(Received 20 November 1978)

Extremely sensitive readout of a stable "etalon of length" is achieved with laser frequency-locking techniques. Rotation of the entire electro-optical system maps any cosmic directional anisotropy of space into a corresponding frequency variation. We found a fractional length change $\Delta l/l = (1.5 \pm 2.5) \times 10^{-15}$, with the expected $P_2(\cos\theta)$ signature. This null result represents a 4000-fold improvement on the best previous measurement of Jaseja *et al.*

$$ds^2 = dt^2 - c^2(dx^2 + dy^2 + dz^2)$$

$$ds'^2 = (g_0 dt')^2 - c^2\left[(g_1 dx')^2 + g_2^2(dy' + dz'^2)\right]$$

$$\mathrm{SR} \Rightarrow g_0 = g_1 = g_2 = g_3 = 1$$

$$\frac{g_2}{g_1} - 1 = (3 \pm 5) \times 10^{-15} \qquad \frac{\Delta\ell}{\ell} = (1.5 \pm 2.5) \times 10^{-15}$$

Hughes-Drever: Anisotropy of Inertial Mass

- Search for change in $\vec{\mu} \cdot \vec{B}$ interaction energy as $\vec{B}$ rotates wrt the galaxy center
  - Recall there is a mass in the interaction term

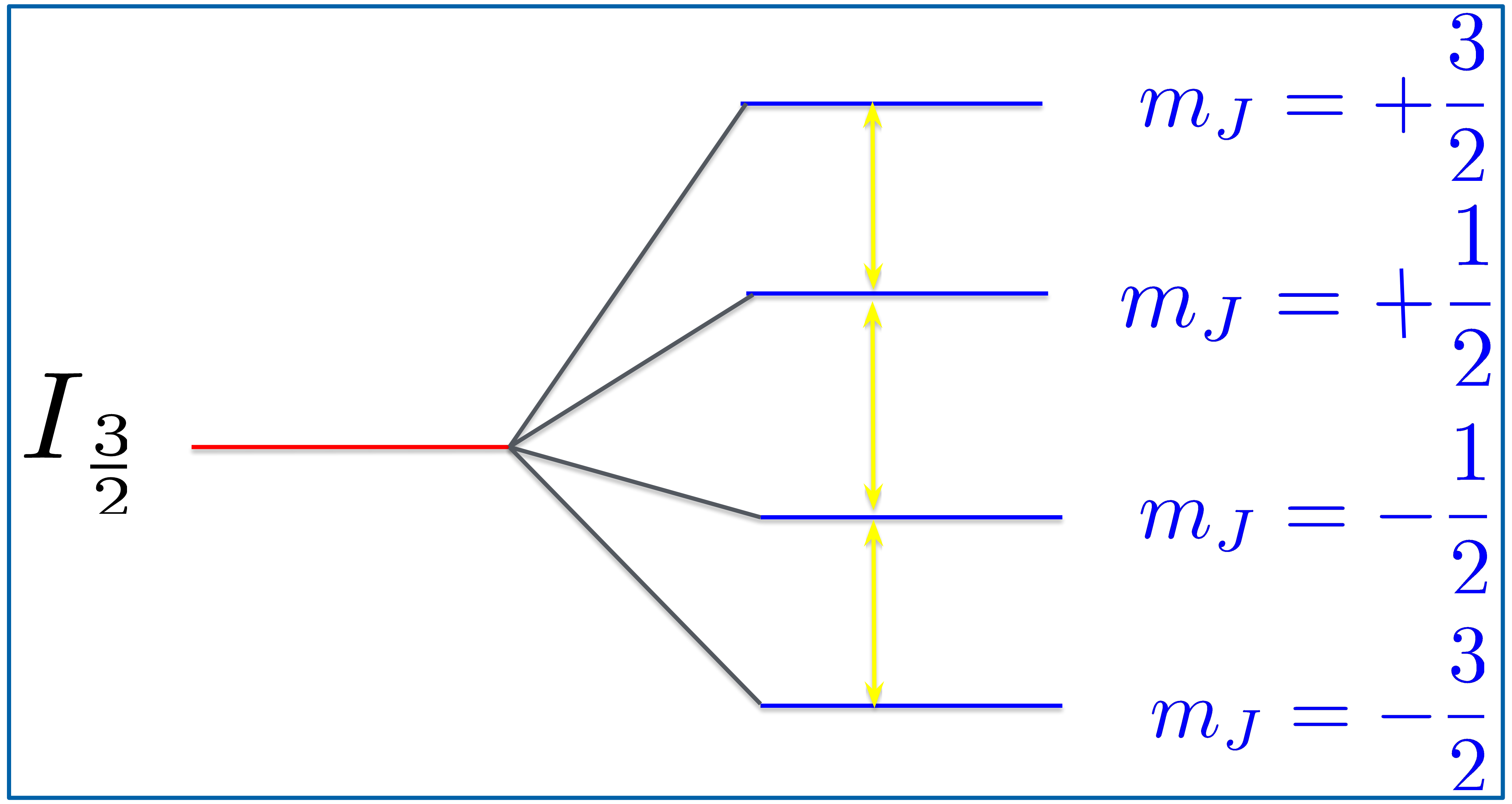

- Hughes: ^{7}Li
  - 4 equally split levels
  - See 1 line (all three transitions are equal)
  - If they are shifted by different amounts see triplet, or broadened structure

- Only a single line was observed to their uncertainty of 5 ppm, which was dominated by $\Delta \boldsymbol{B}$

$$\frac{\Delta m}{m} \leq 10^{-20}$$

Magnetic Moment: g factor

$$\vec{\mu} = g\frac{e}{2m}\vec{S}$$

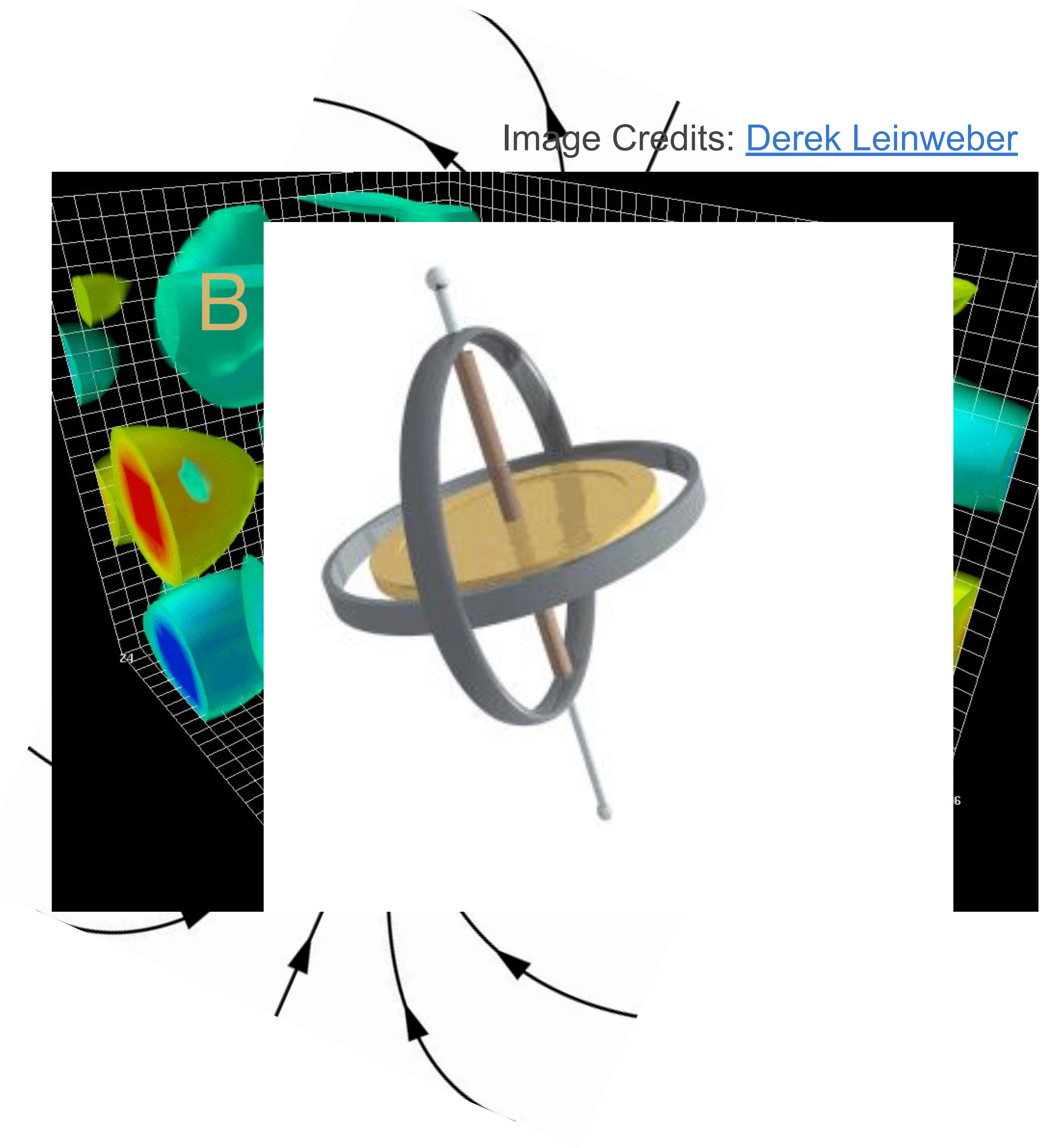

Image Credits: Derek Leinweber

- Classical physics: $g = 1$
- Relativistic quantum mechanics prediction for a point-like particle: $g = 2$ (Dirac, 1928)
- For electron, experimentally found to be $g_e = 2.00238(10)$ (Foley & Kusch, 1948)
- Schwinger figures out why: QED

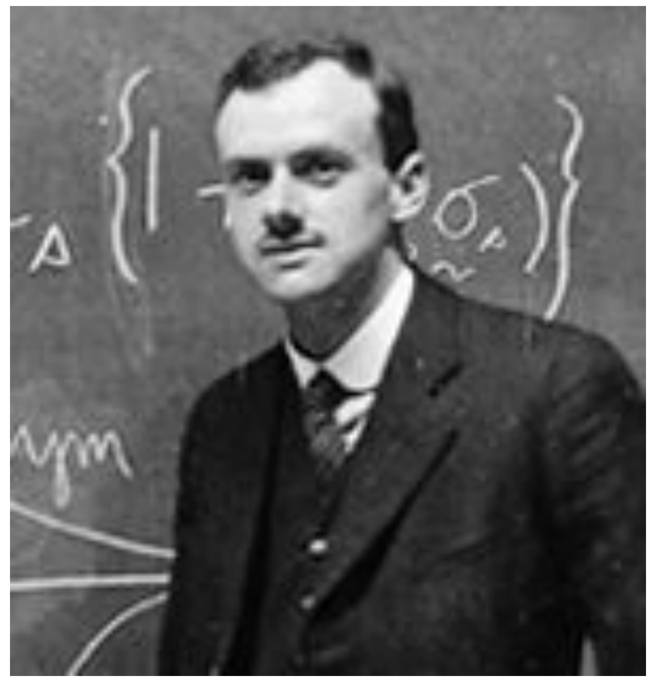

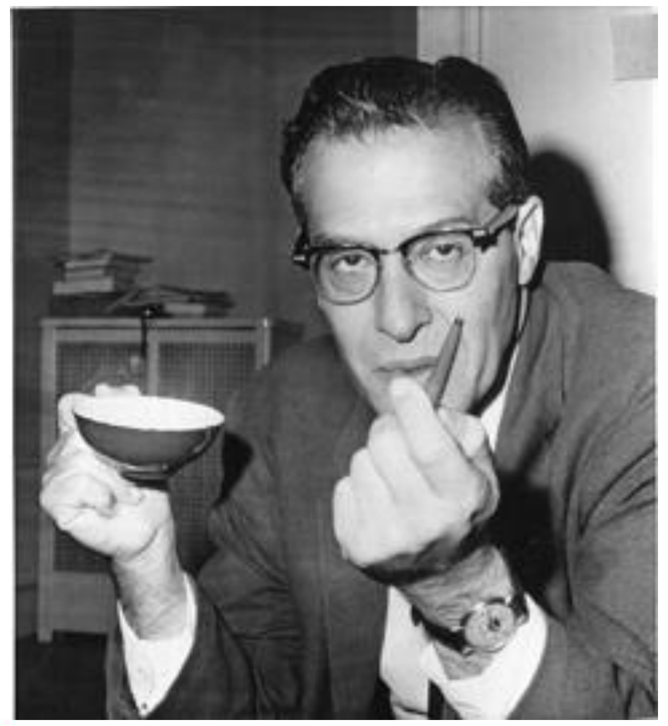

- Anomalous magnetic moment

$$\vec{\mu} = g\frac{e}{2m}\vec{S} = 2(1+a)\frac{e}{2m}\vec{S}$$

$$a = \frac{g-2}{2}$$

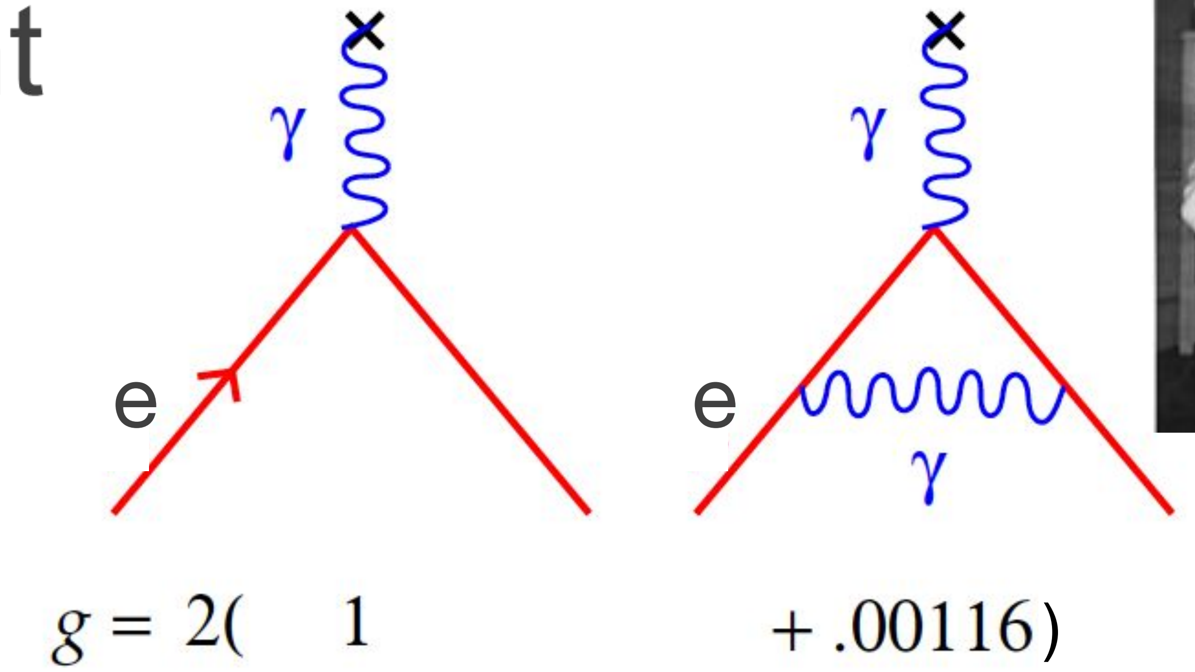

- Interactions proportional to m^2 → muons

The Key Principles of Storage Ring Muon g-2

1. Muons from forward decay of pions produced from a proton beam on target are about 97% polarized.

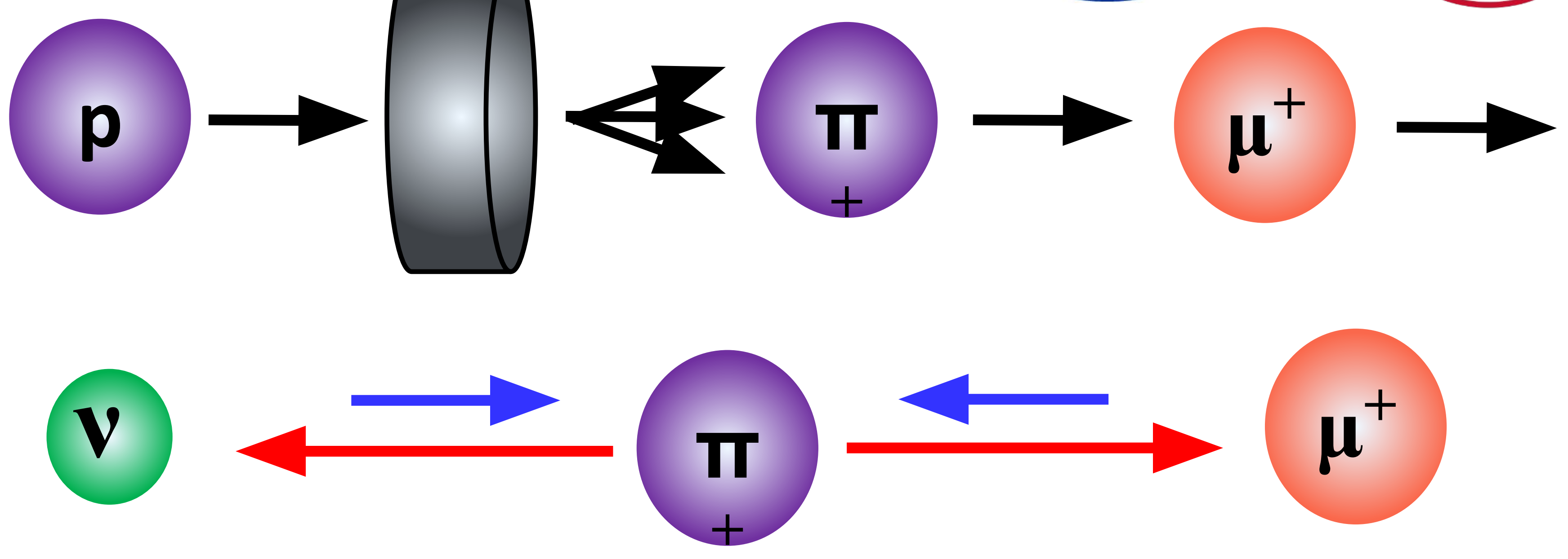

2. The **anomalous magnetic moment** is roughly proportional to the **anomalous precession frequency**

Cyclotron (mom. precession) freq: $\omega_c = \frac{eB}{m_\mu c\gamma}$

Spin precession freq: $\omega_s = \frac{g_\mu eB}{2m_\mu c} + (1-\gamma)\frac{eB}{m_\mu c\gamma}$

Anomalous precession freq: $\boldsymbol{\omega_a} = \omega_s - \omega_c = \boldsymbol{a_\mu}\frac{e}{m_\mu c}\boldsymbol{B}$

(simplified)

To get this

Measure these

- 800x more sensitive than rest muon experiments that measure g

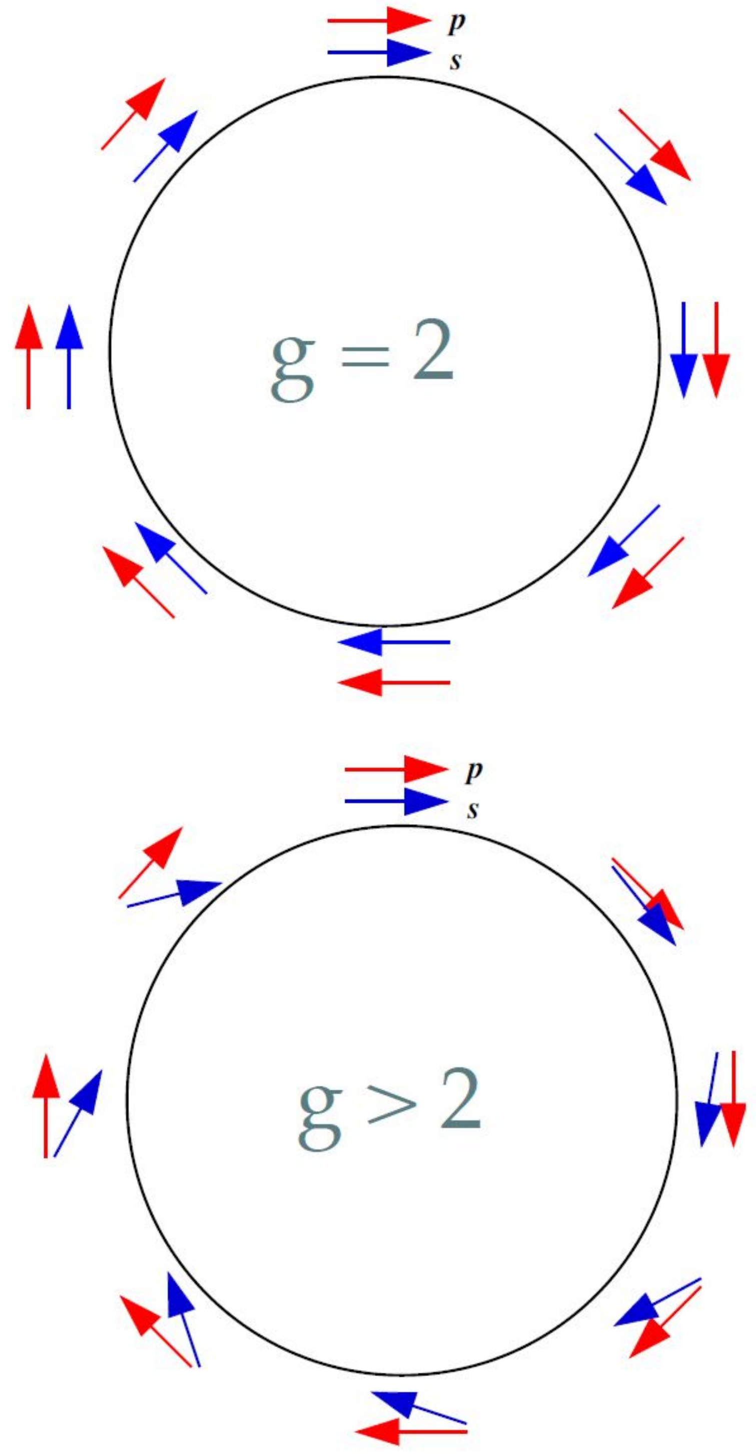

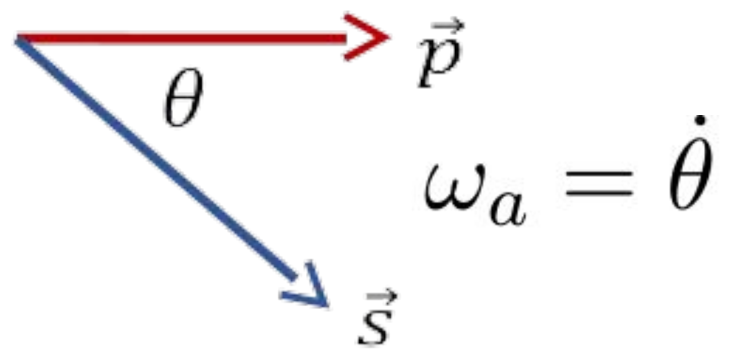

The Key Principles of Storage Ring Muon g-2

3. There is *some* vertical beam motion, so need to use electric quadrupole fields to contain the beam vertically (the *B* field holds them in horizontally). But these facts complicate the expression for the **anomalous precession frequency:**

$$\vec{\omega}_a = \vec{\omega}_s - \vec{\omega}_c = -\frac{e}{mc}\left[a_\mu \vec{B} - a_\mu\left(\frac{\gamma}{\gamma+1}\right)(\vec{\beta}\cdot\vec{B})\vec{\beta} - \left(a_\mu - \frac{1}{\gamma^2-1}\right)(\vec{\beta}\times\vec{E})\right]$$

- If the muons are at just the right "magic" momentum ($\gamma = 29.3$ $(0.9994c), p_\mu = 3.09\ \mathrm{GeV}/c$), then the last term cancels!
- Since the beam is not perfectly planar and the muons' momenta are not all exactly at the magic momentum, pitch and *E* field corrections are needed for the 2nd and 3rd terms.

The Key Principles of Storage Ring Muon g-2

4. Muon decays are self-analyzing: due to parity violation, the highest energy decay positrons are preferentially emitted in the direction of the muon spin.

$$\mu^+ \rightarrow e^+ \nu_e \bar{\nu}_\mu$$

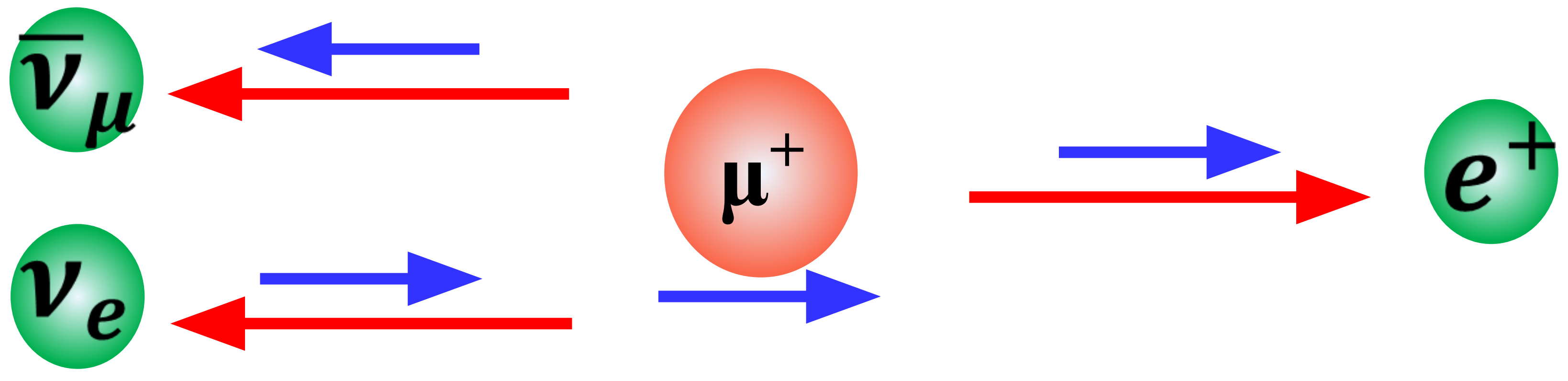

Real data from Run-3

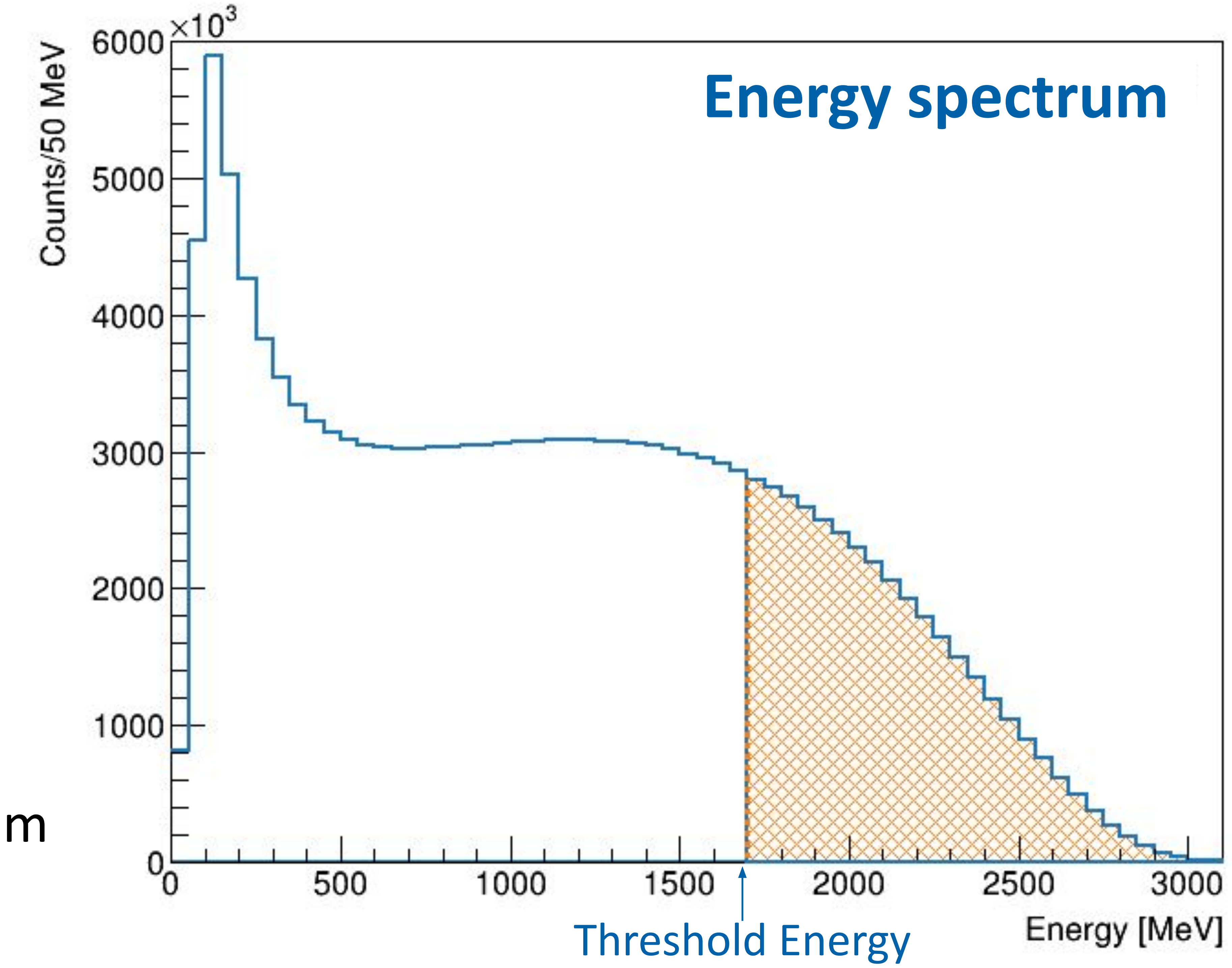

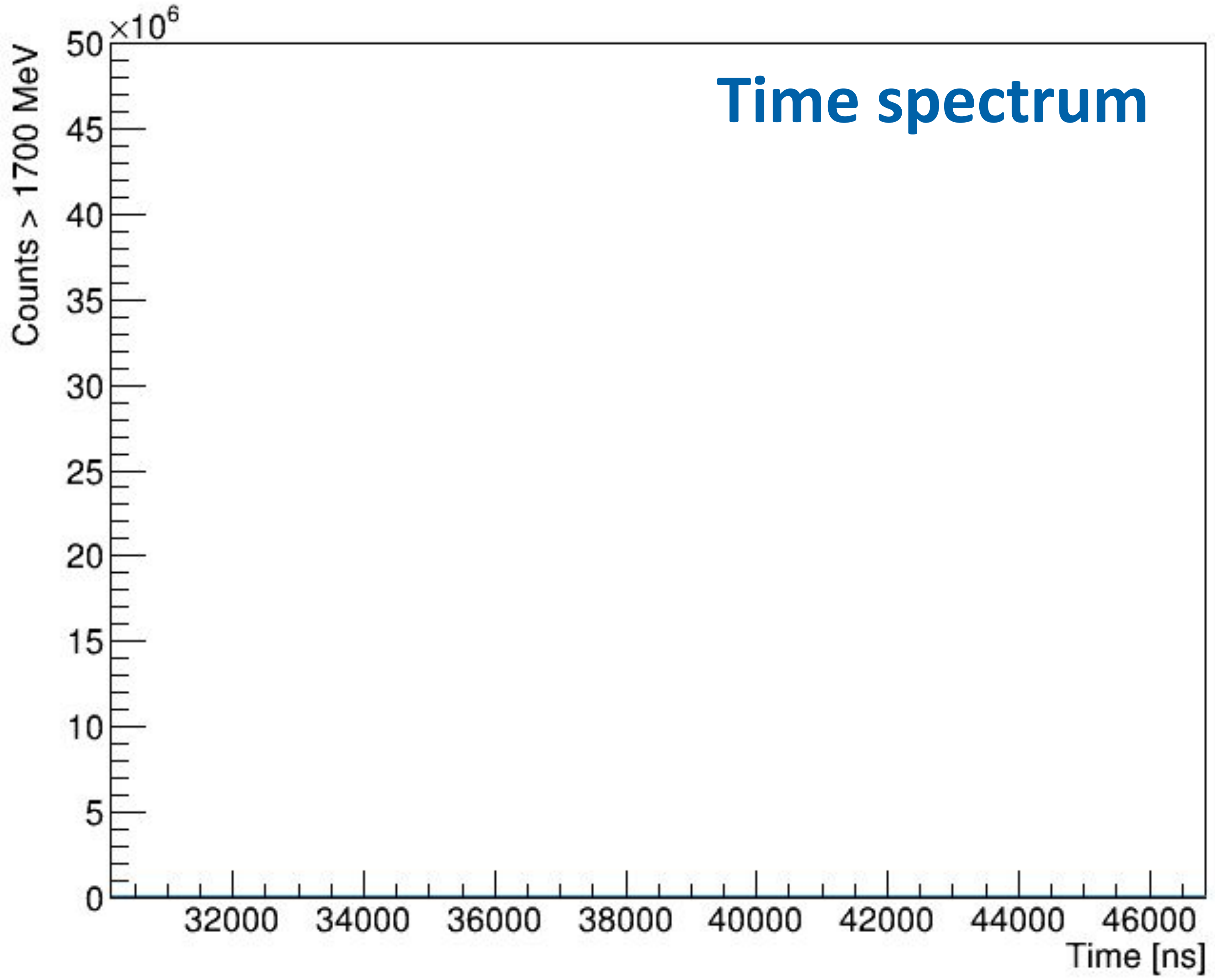

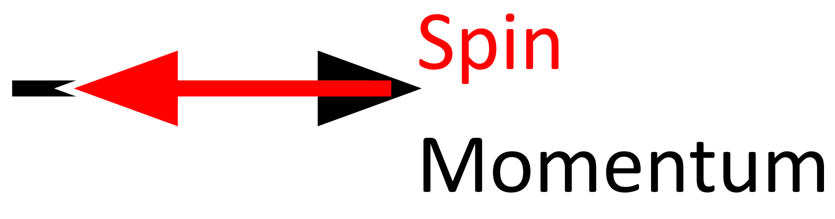

Measuring Muon g-2

- Store polarized muon beam in the storage ring
- The spins precess like a top about the magnetic field as they circulate around the ring
- Count the rate of decay positrons to get a_μ

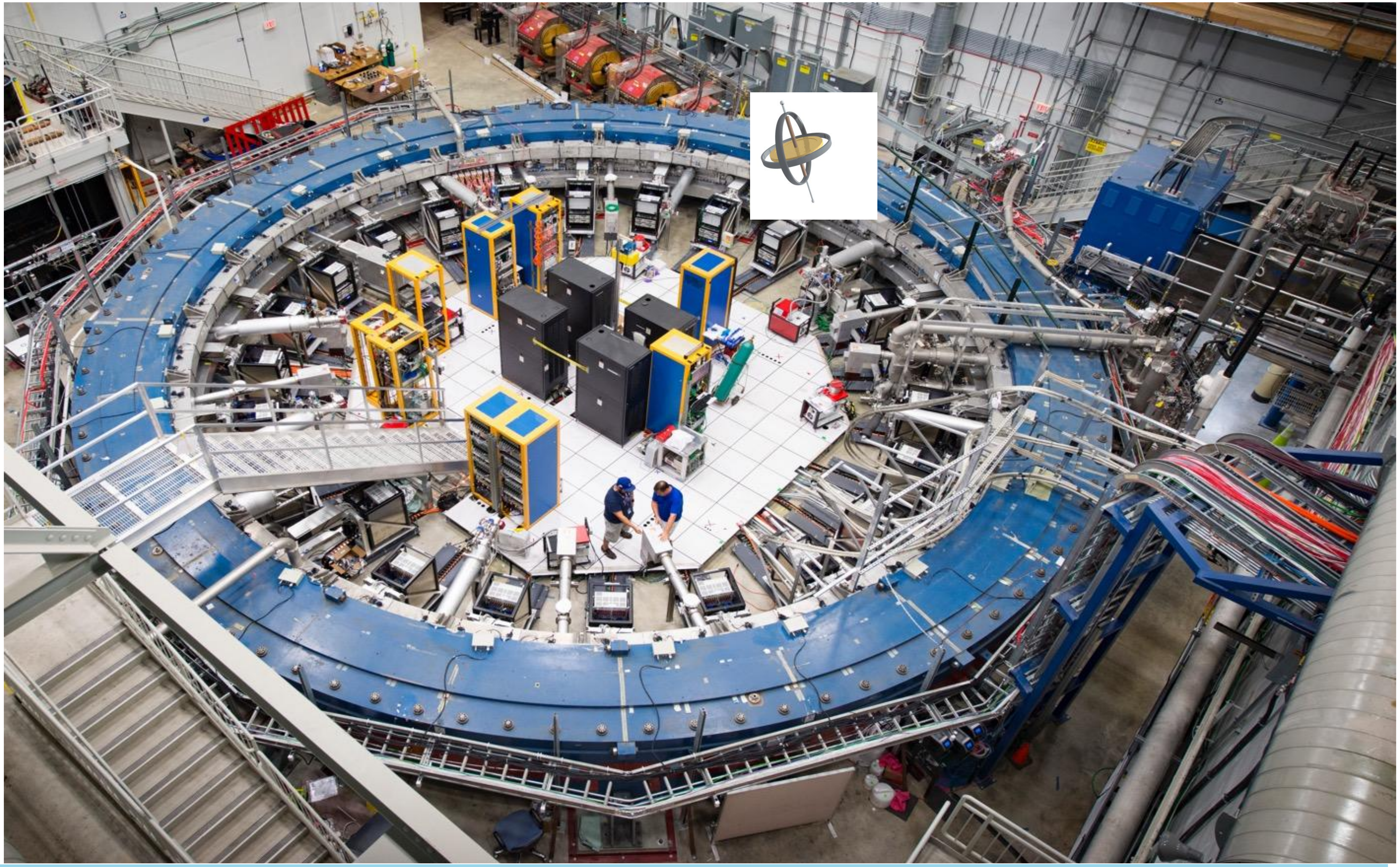

Magnetic Field

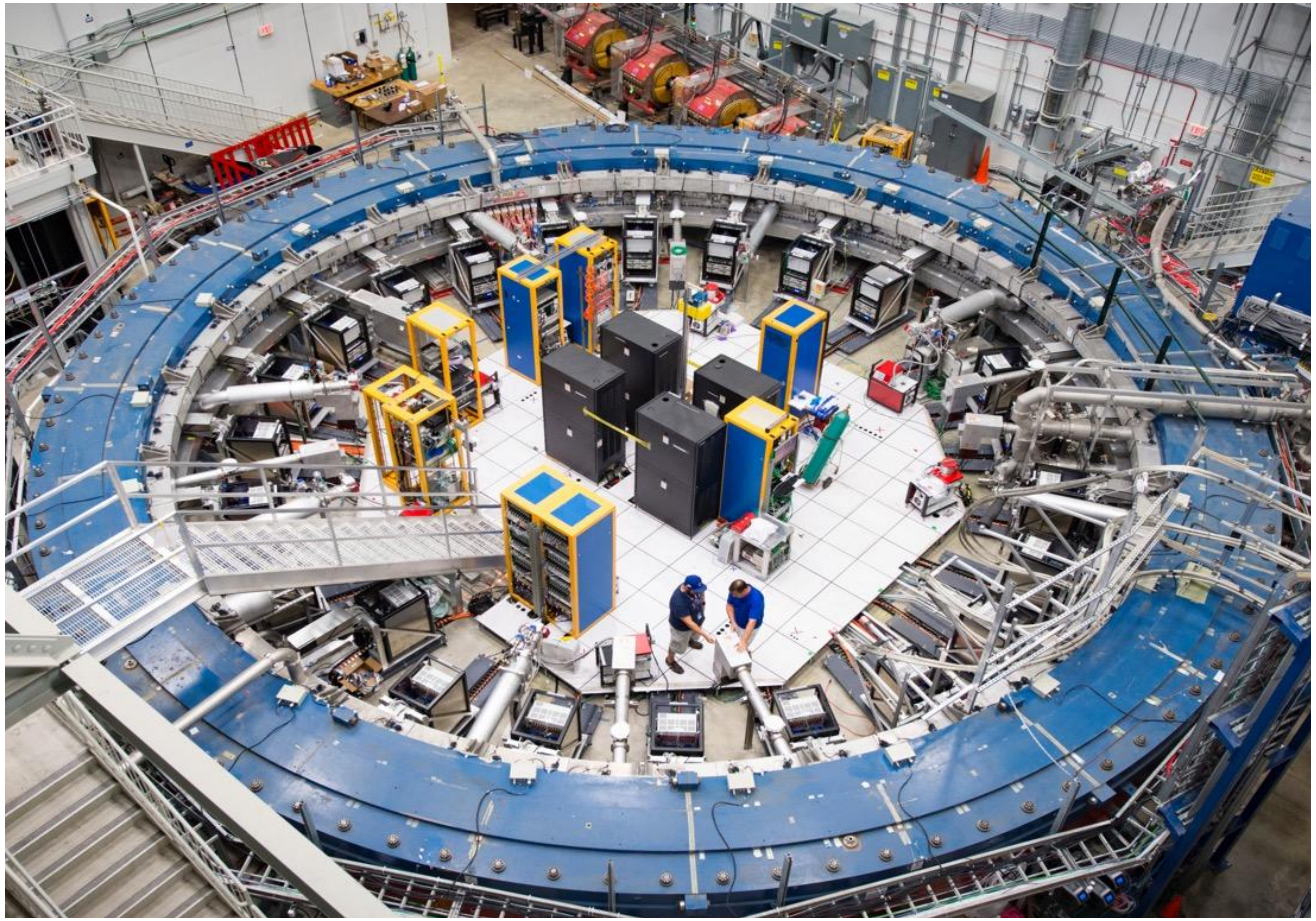

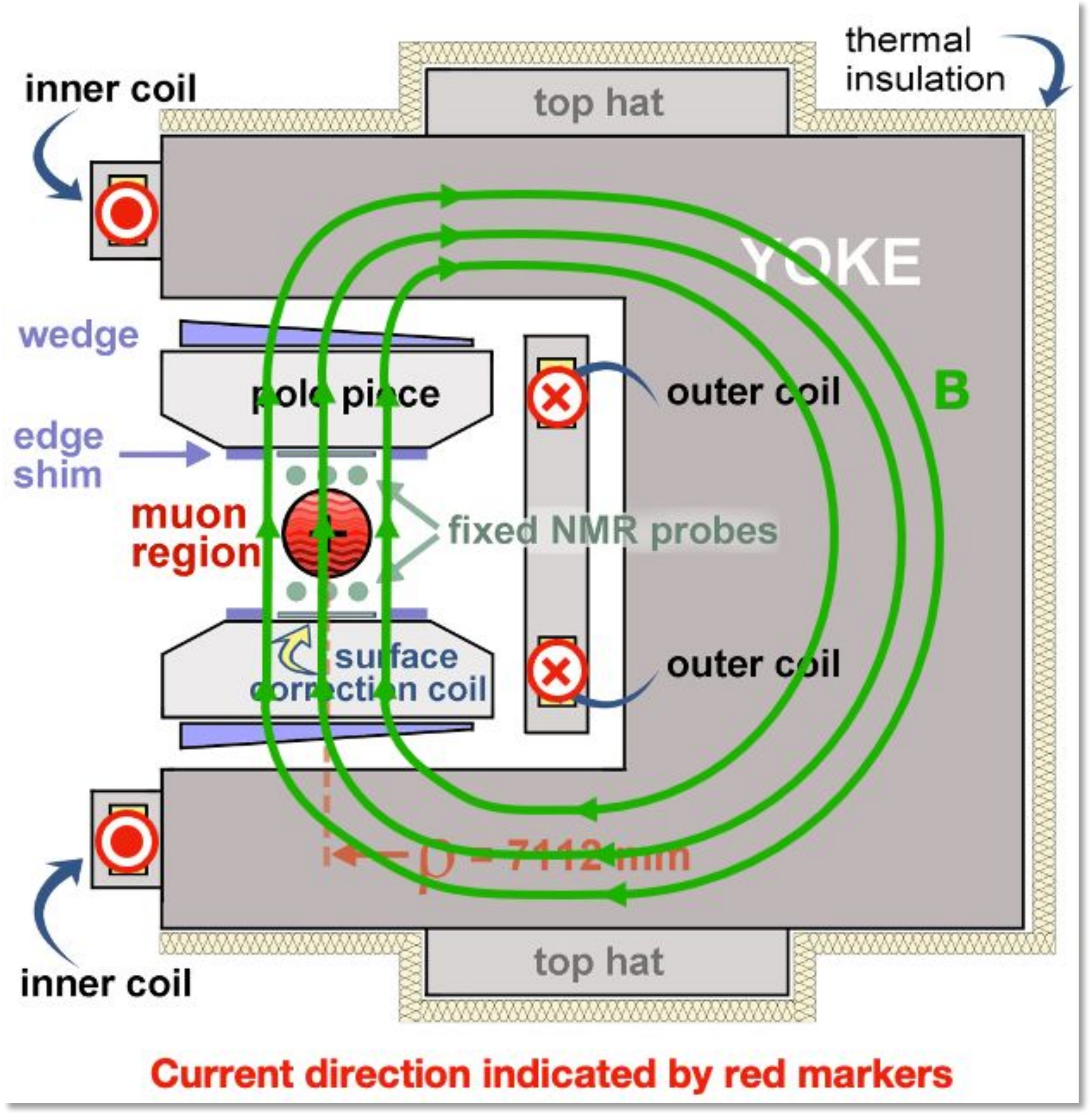

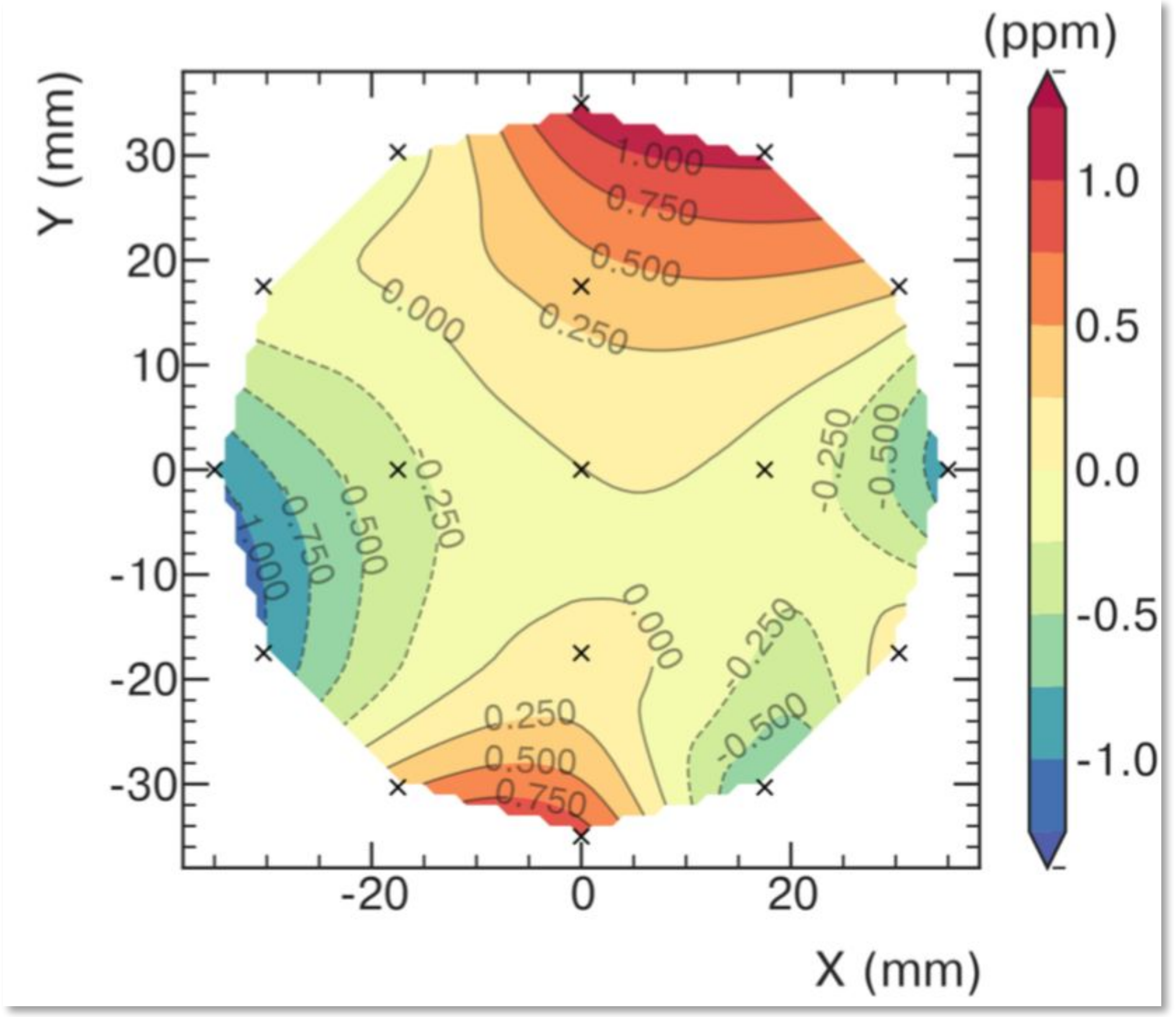

1.45 T Superferric Magnet

- 14 m diameter
- 12 iron yokes excited by superconducting coils
- Iron top hats (24), poles (72), wedges (864), foil laminations (8000), edge shims and surface coils for field shaping

Beam Injection

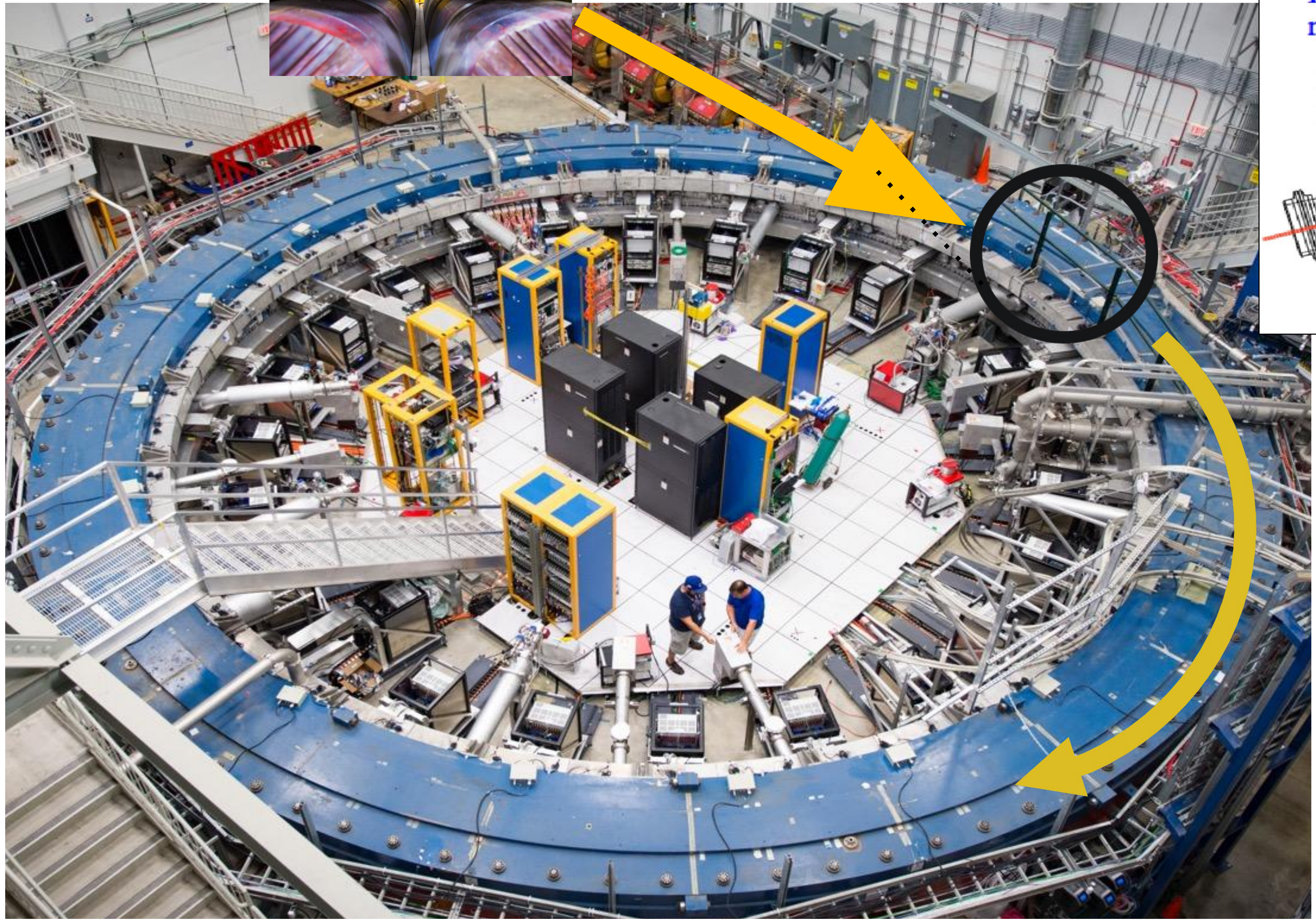

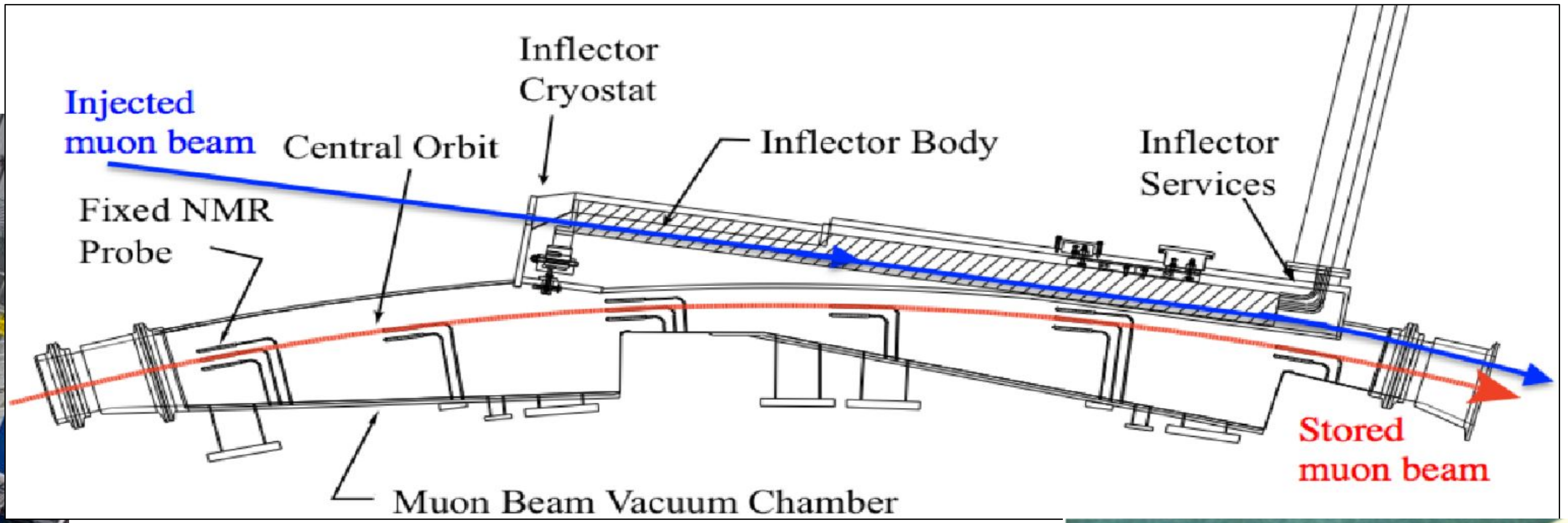

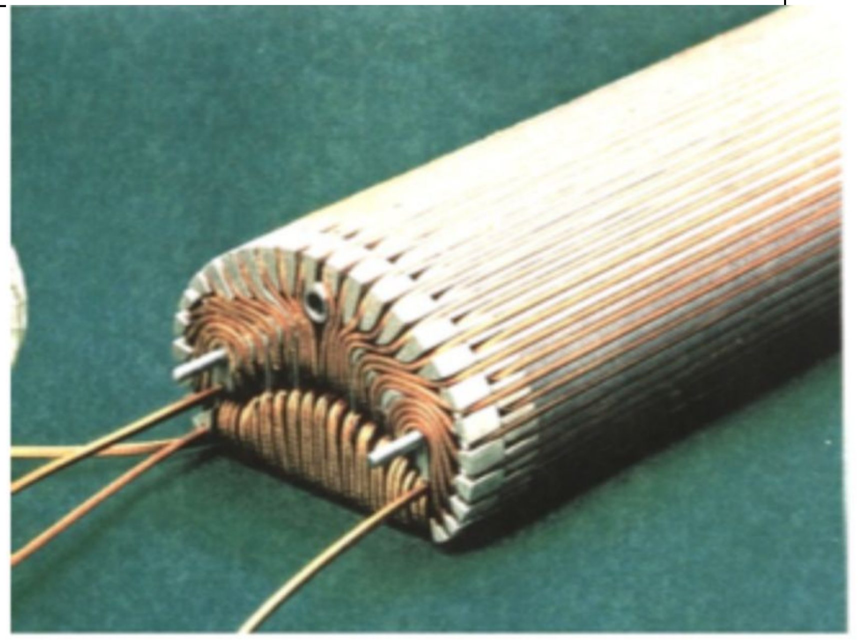

Inflector Magnet

- Provides field free region to deliver beam to edge of storage region
- Stops strong deflection of the beam
- Injected beam center 77mm off from storage region center

Kick Beam Onto Stable Orbit

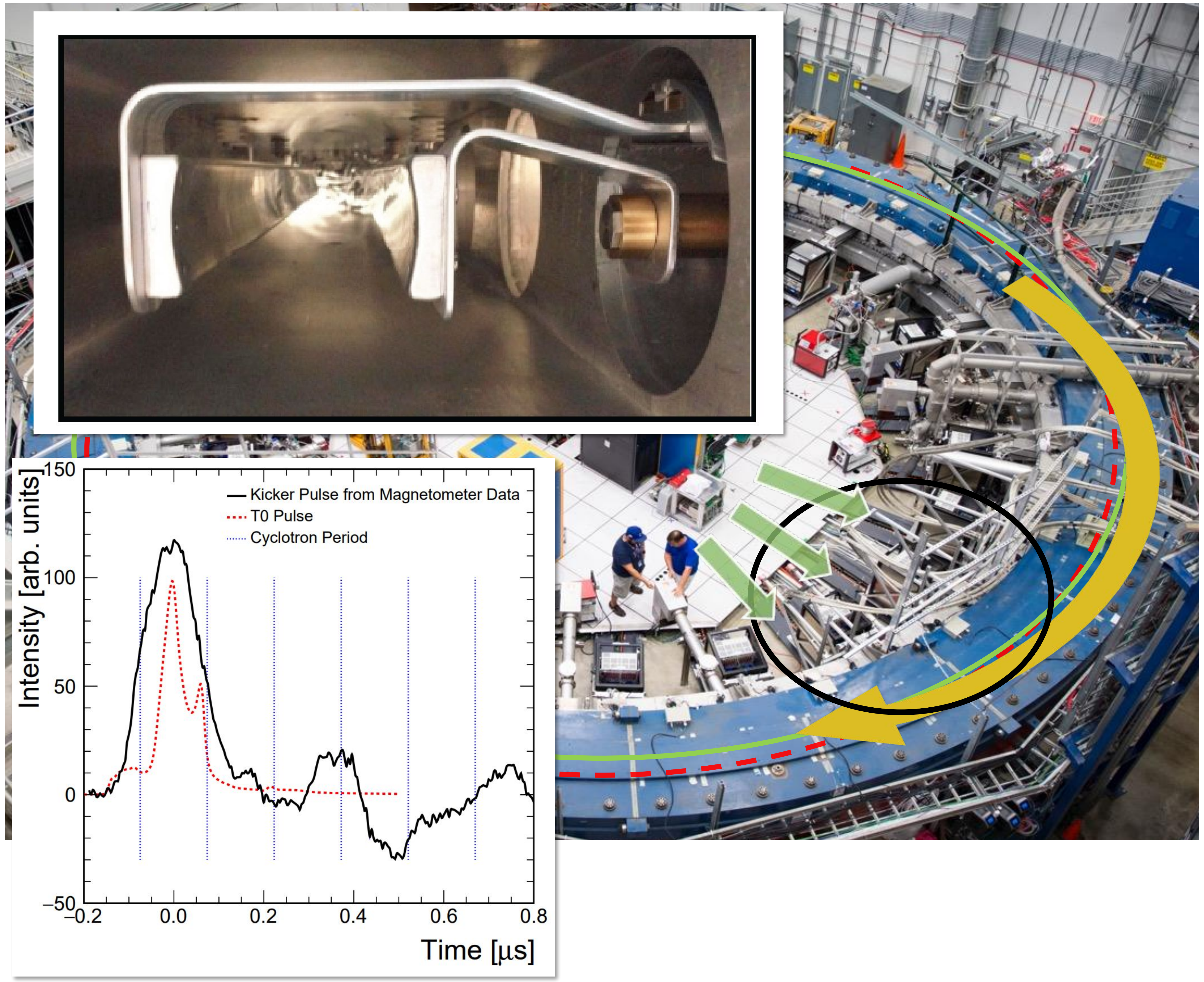

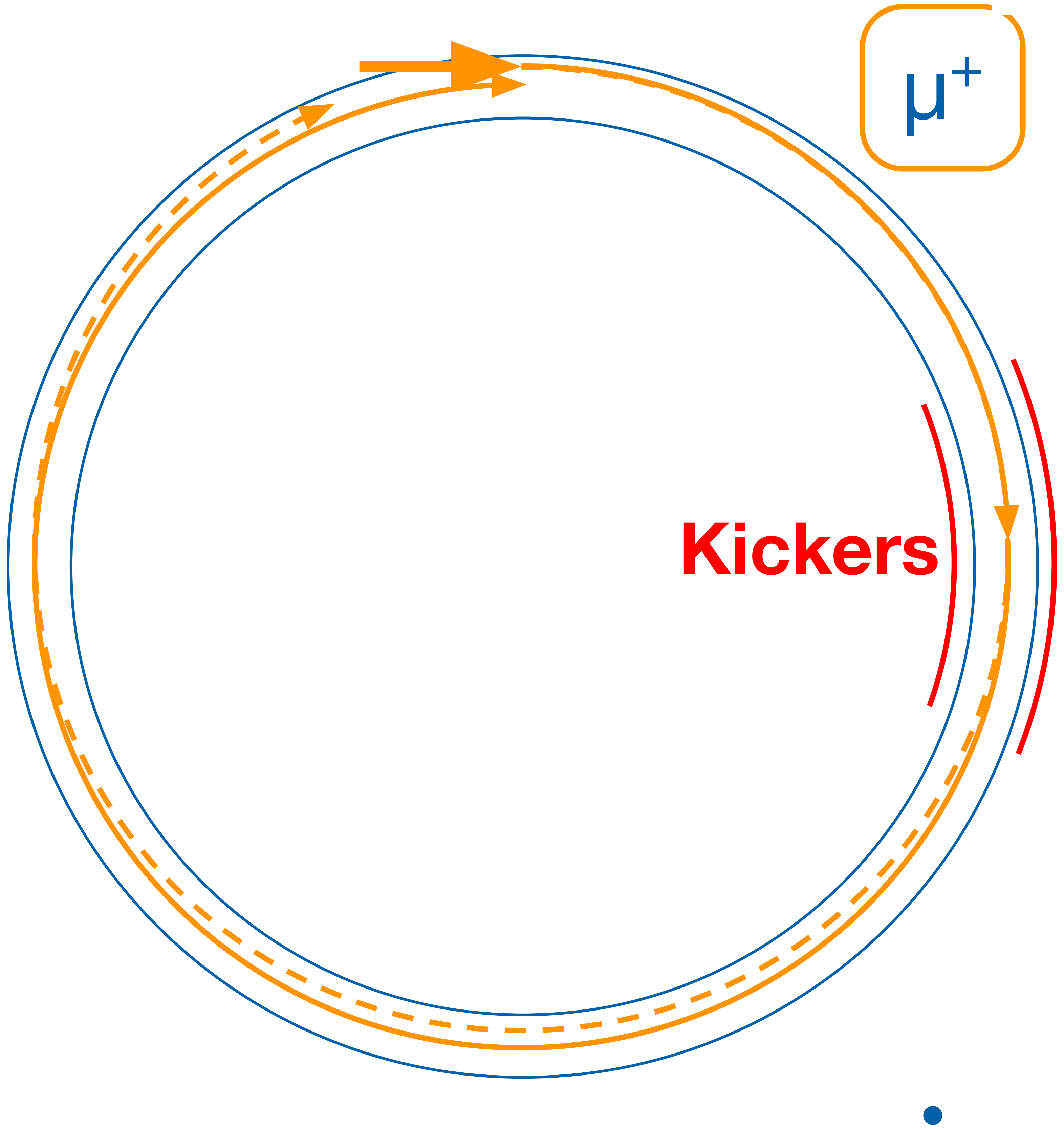

3 Pulsed Kicker Magnets

- Provide 10.8 mrad “kick” to direct muons into ideal orbit (< 149 ns)

Vertical Focusing with Quadrupoles

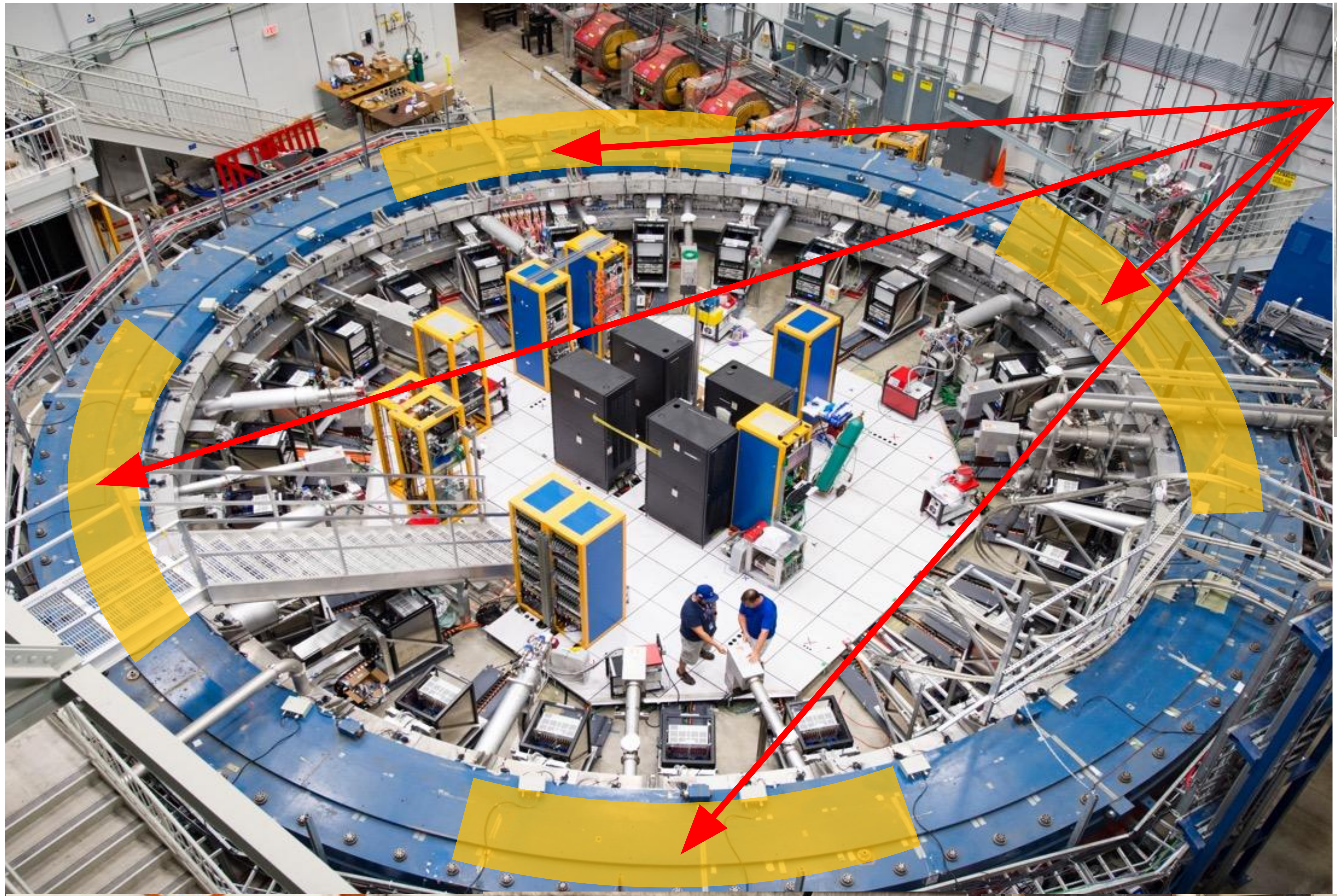

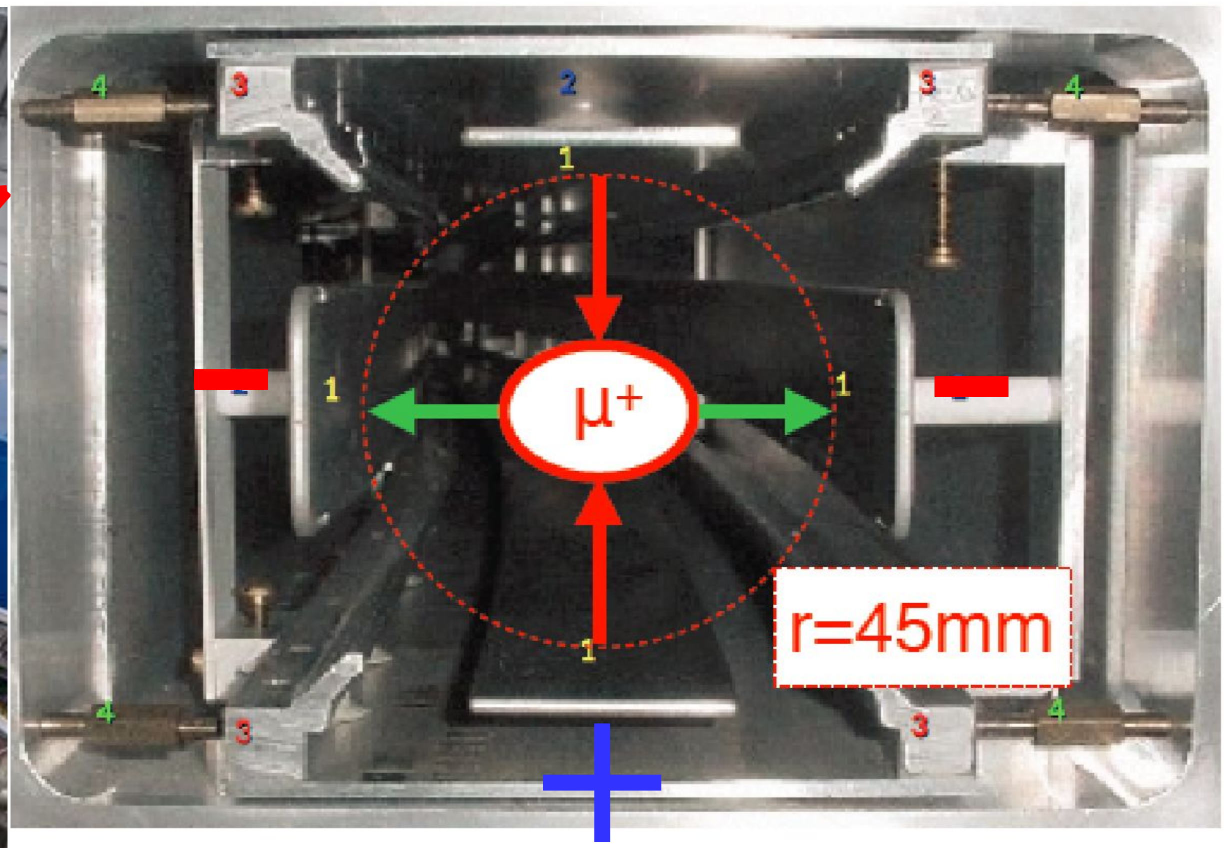

4 Electrostatic Quadrupole (ESQ)

- Provide weak vertical focusing of the beam
- 4 sections cover 43% of ring circumference

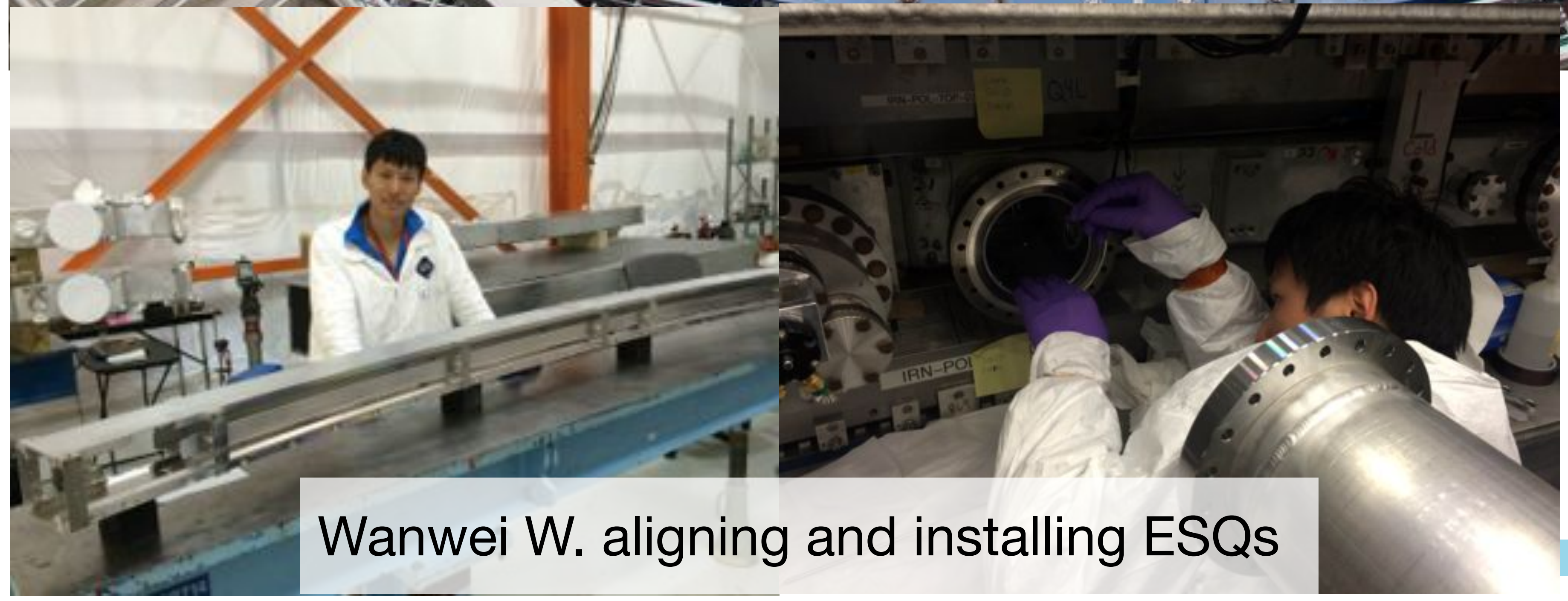

Wanwei W. aligning and installing ESQs

Jason C. teaching us to use them

Meghna B. performing upgrades

Beam Positions with Trackers

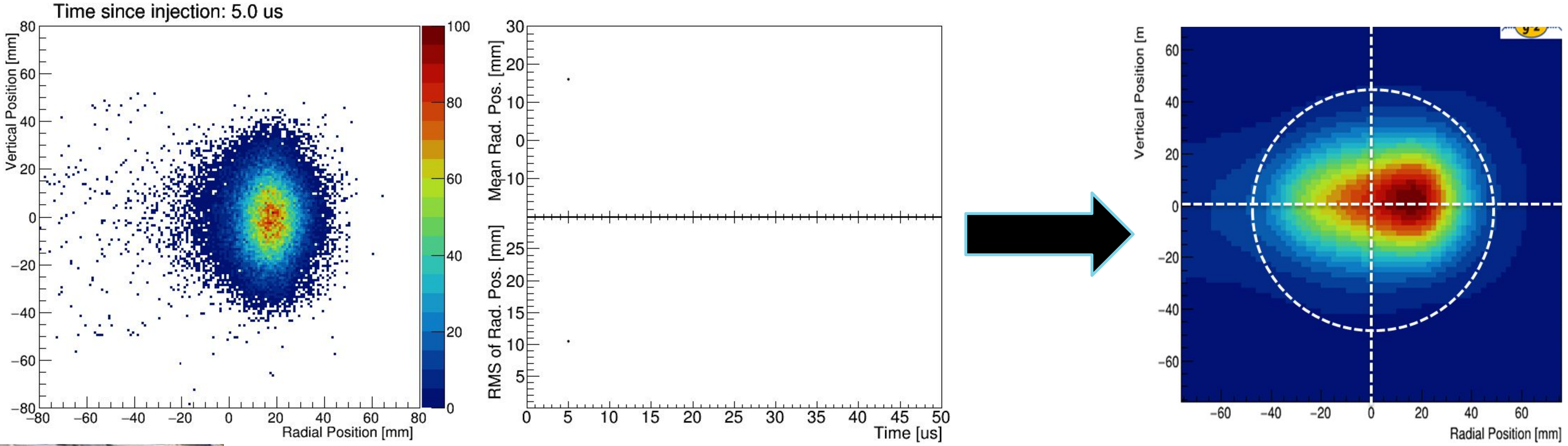

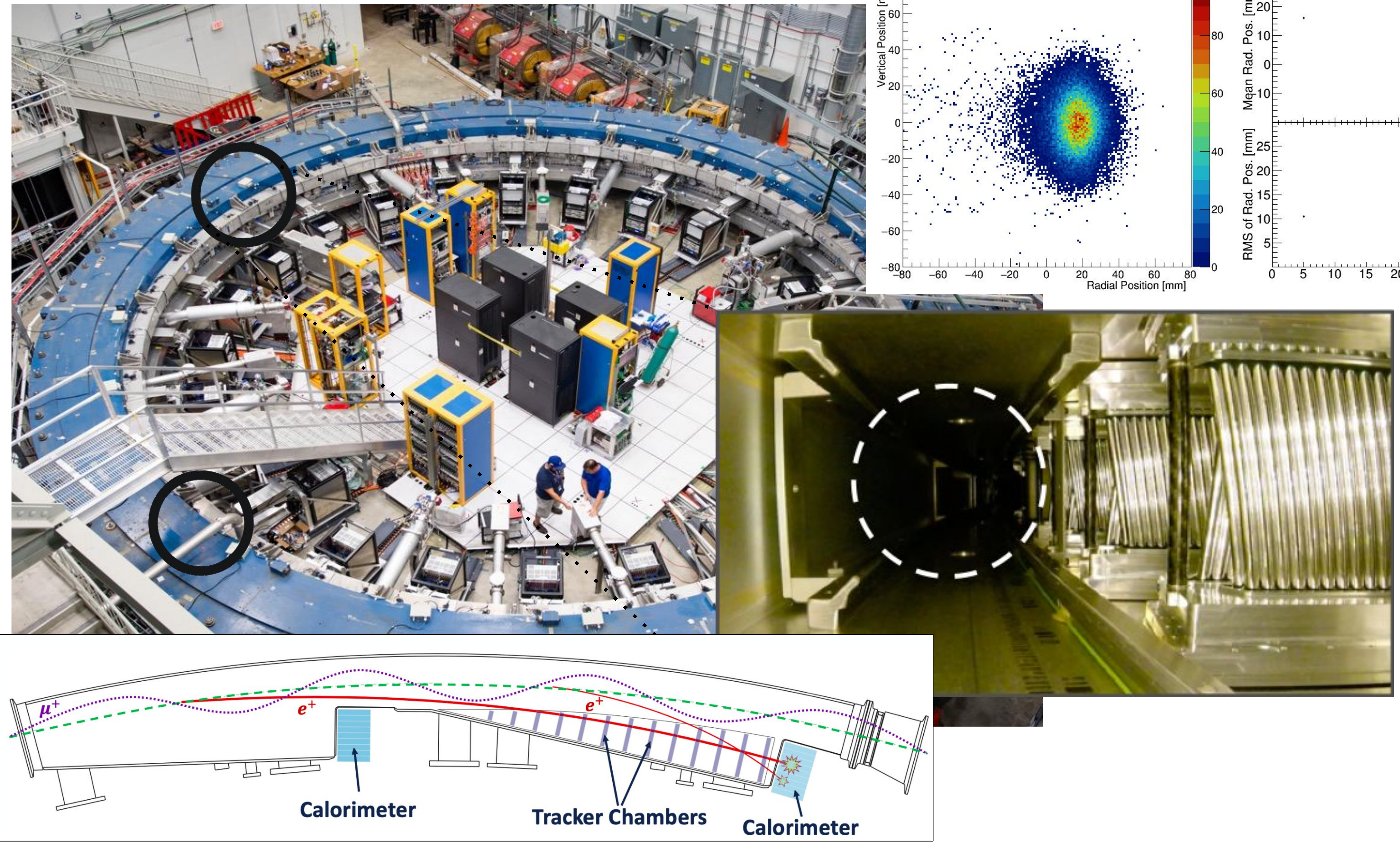

2 Straw Tracker Stations

- 8 modules/station, 128 straws/module
- Reconstruct muon decay positions from e^+ hits to obtain spatial beam profile

Measure Positrons with Calorimeters

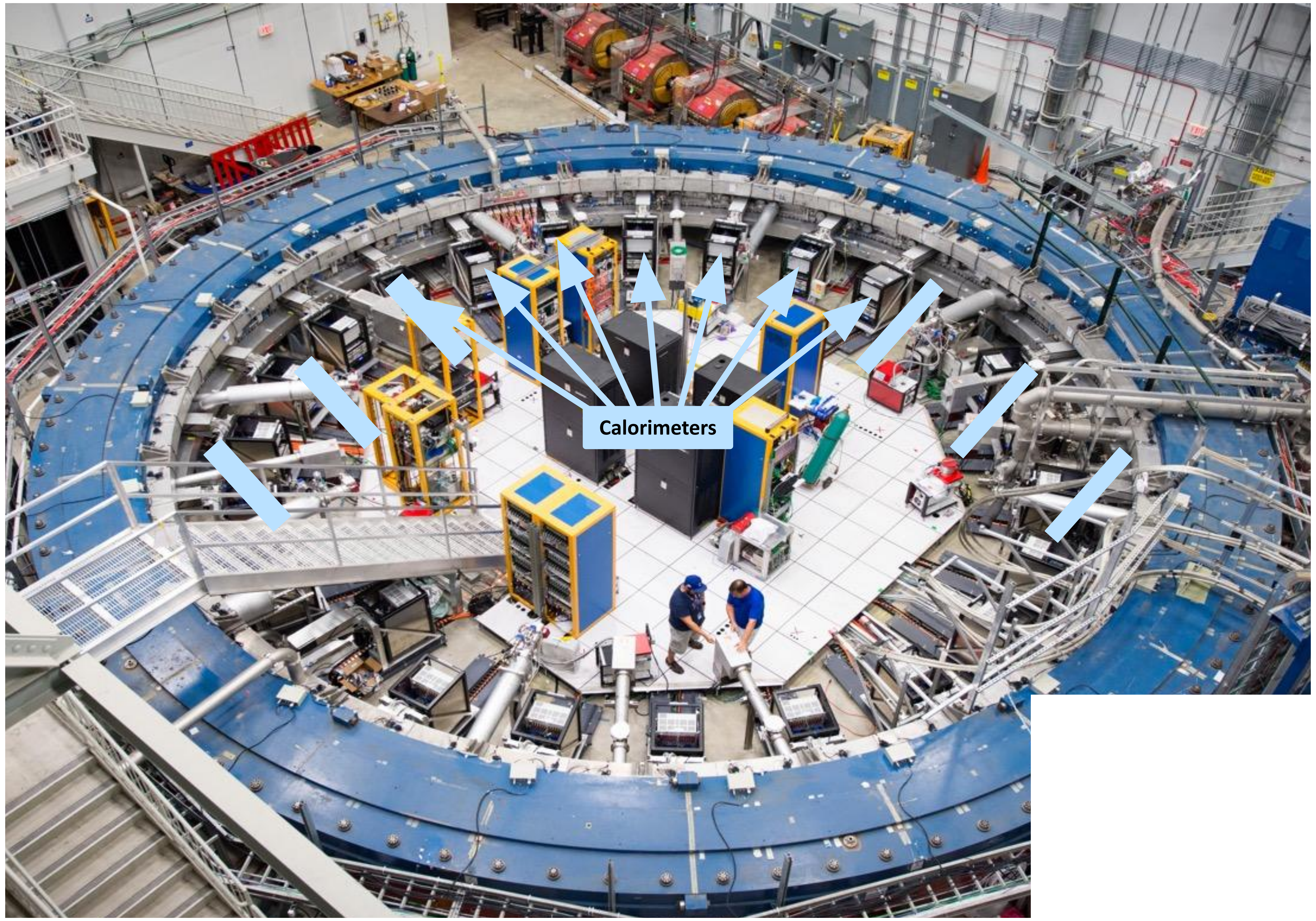

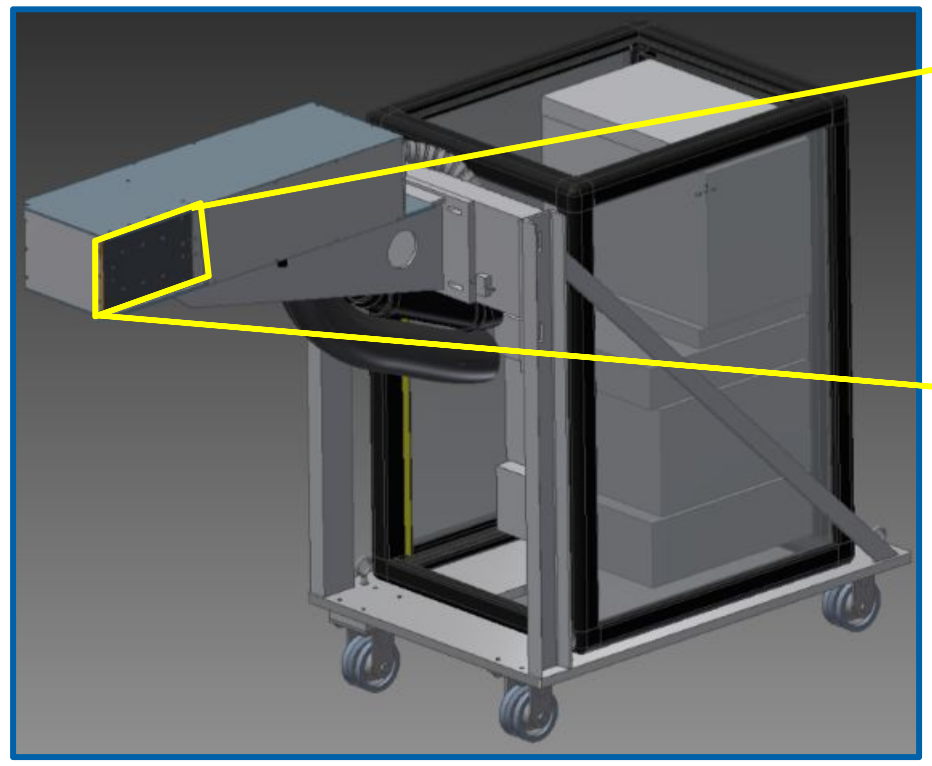

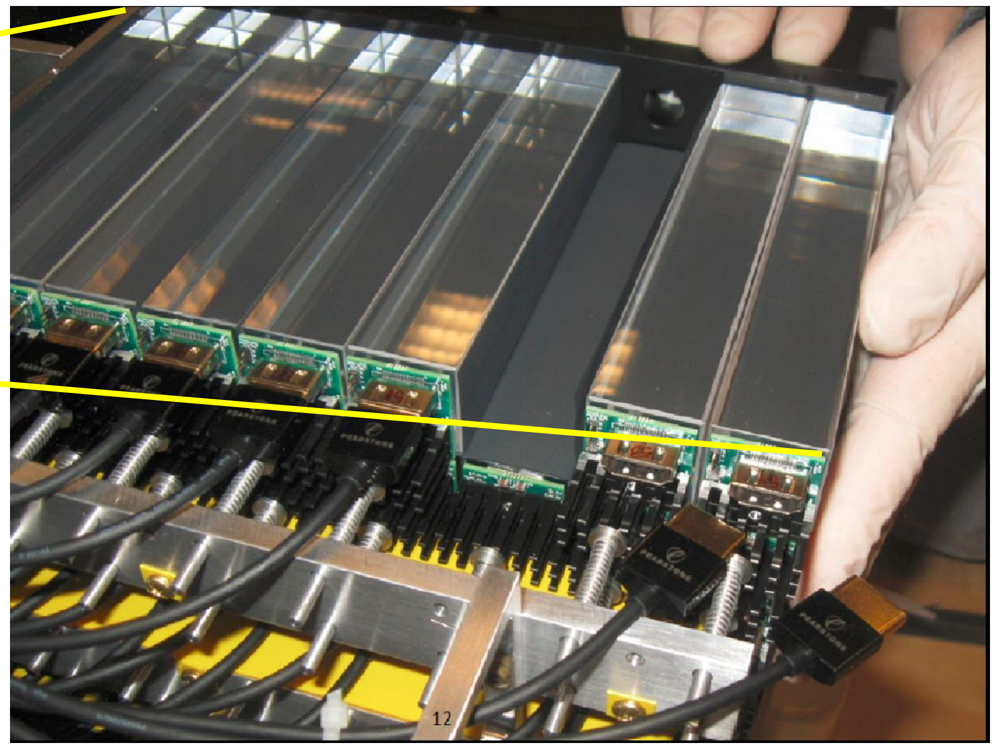

24 Electromagnetic Calorimeters

- 9x6 arrays of PbF_2 crystals
- Fast SiPM readout
- Measure arrival time & energy of the decay e^+

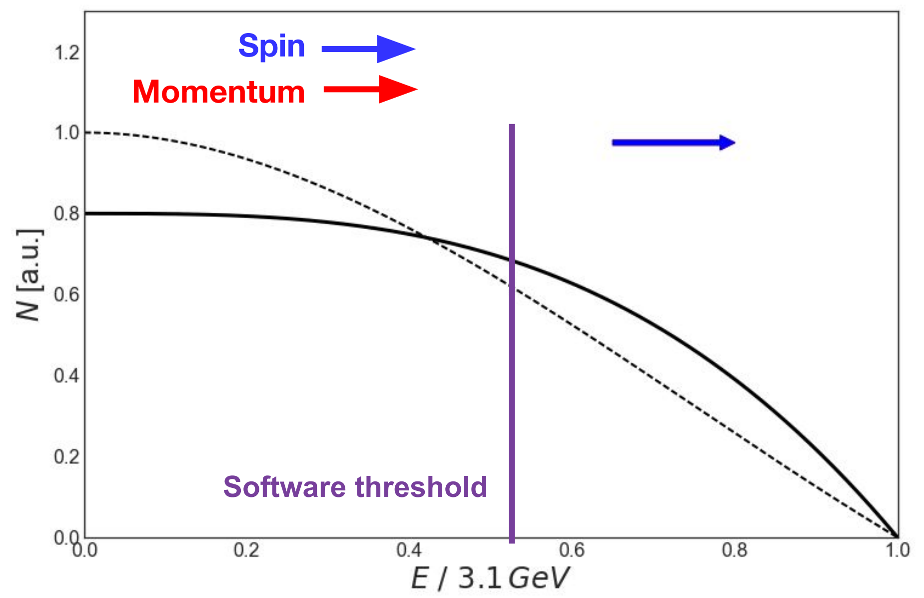

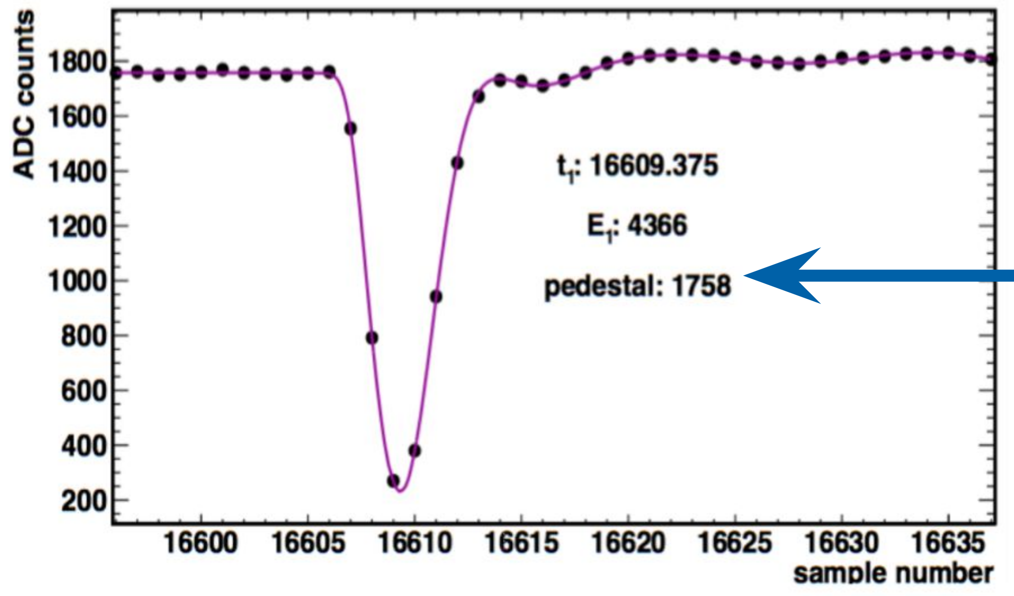

Collected statistics from Muon $g-2$: x21.9 BNL datasets

On 27 February 2023: proposal Goal of x21 BNL datasets!

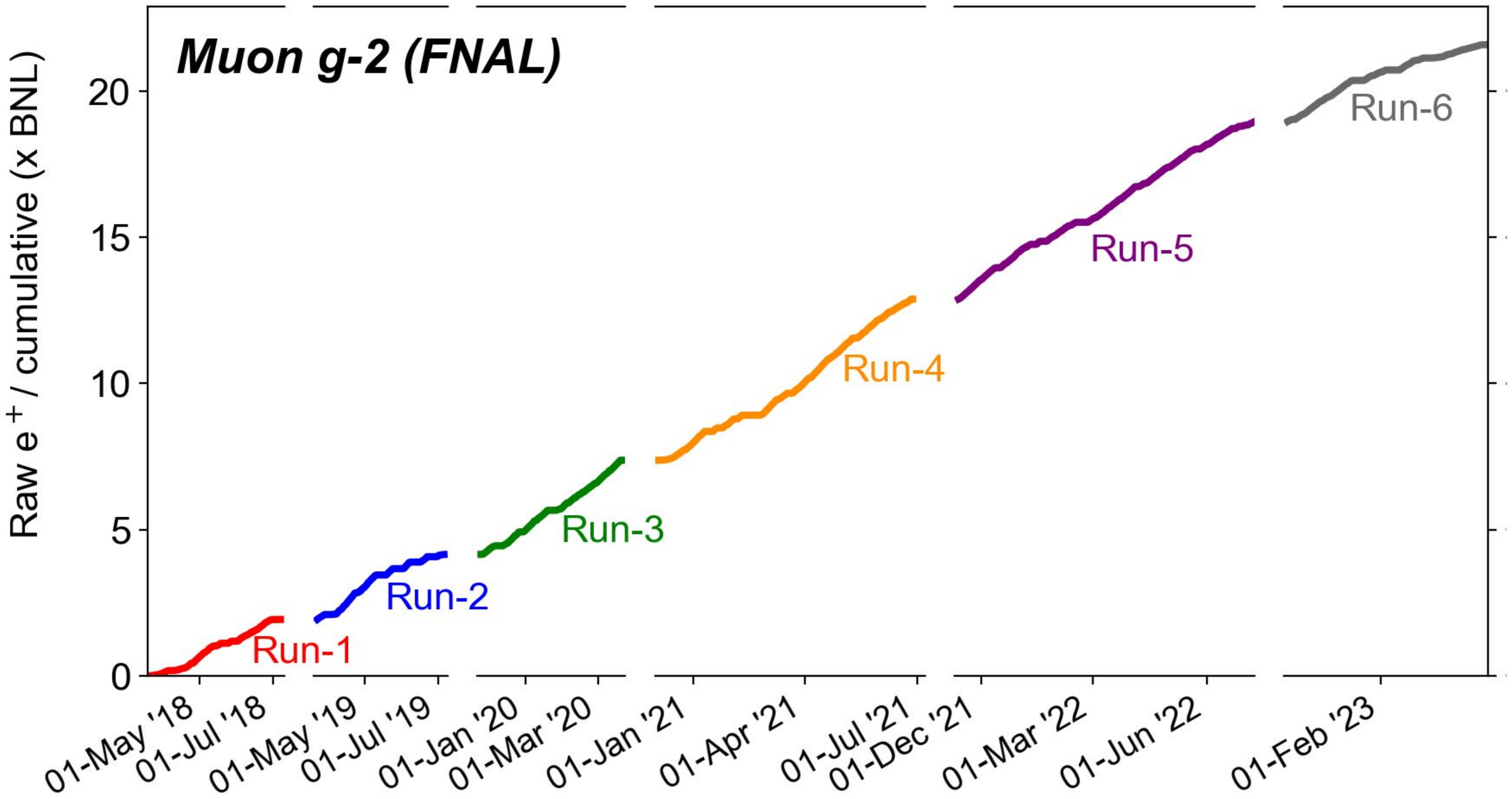

Measuring Muon g-2

- **Only measure frequencies!**

$$\vec{\omega}_a = \vec{\omega}_S - \vec{\omega}_C = \left(\frac{g-2}{2}\right)\frac{e}{\gamma m}\vec{B} = a_\mu \frac{e}{\gamma m}\vec{B}$$

  - With $\hbar\omega_p = 2\mu_p|\vec{B}|$ (*B* measured in terms of proton Larmor precession frequency)

We measure | From literature

$$a_\mu = \frac{\omega_a}{\tilde{\omega}_p'(T_r)} \frac{\mu_p'(T_r)}{\mu_e(H)} \frac{\mu_e(H)}{\mu_e} \frac{m_\mu}{m_e} \frac{g_e}{2}$$

3 ppb

22 ppb

0.3 ppt

$$\frac{\omega_a}{\tilde{\omega}_p'} = \frac{f_{\text{clock}}\, \omega_a^{meas}\left(1 + C_e + C_p + C_{ml} + C_{pa} + C_{dd}\right)}{f_{\text{calib}} \left\langle \omega_p'(x,y,\phi) \times M(x,y,\phi) \right\rangle \left(1 + B_k + B_q\right)}$$

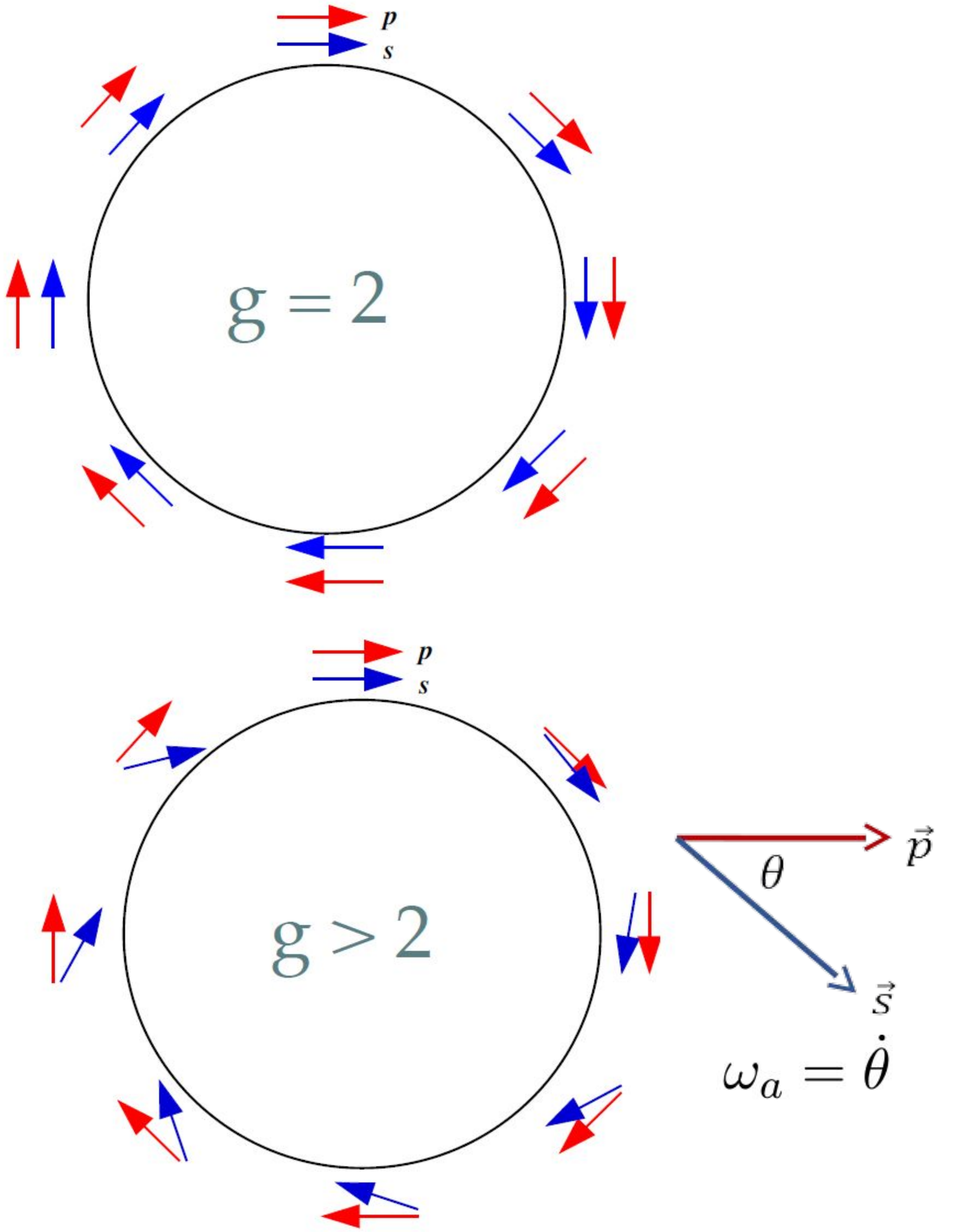

Measurement of precession frequency, ω_a, with positrons:

Fitting the time spectrum

- Simple 5-parameter fit to extract ω_a^{meas}.
- This model captures exponential decay and $g-2$ oscillation.
- $N(t) = N_0 e^{-t/\tau_\mu}\left[1 + A\cos(\omega_a t + \phi_0)\right]$

The "wiggle plot"

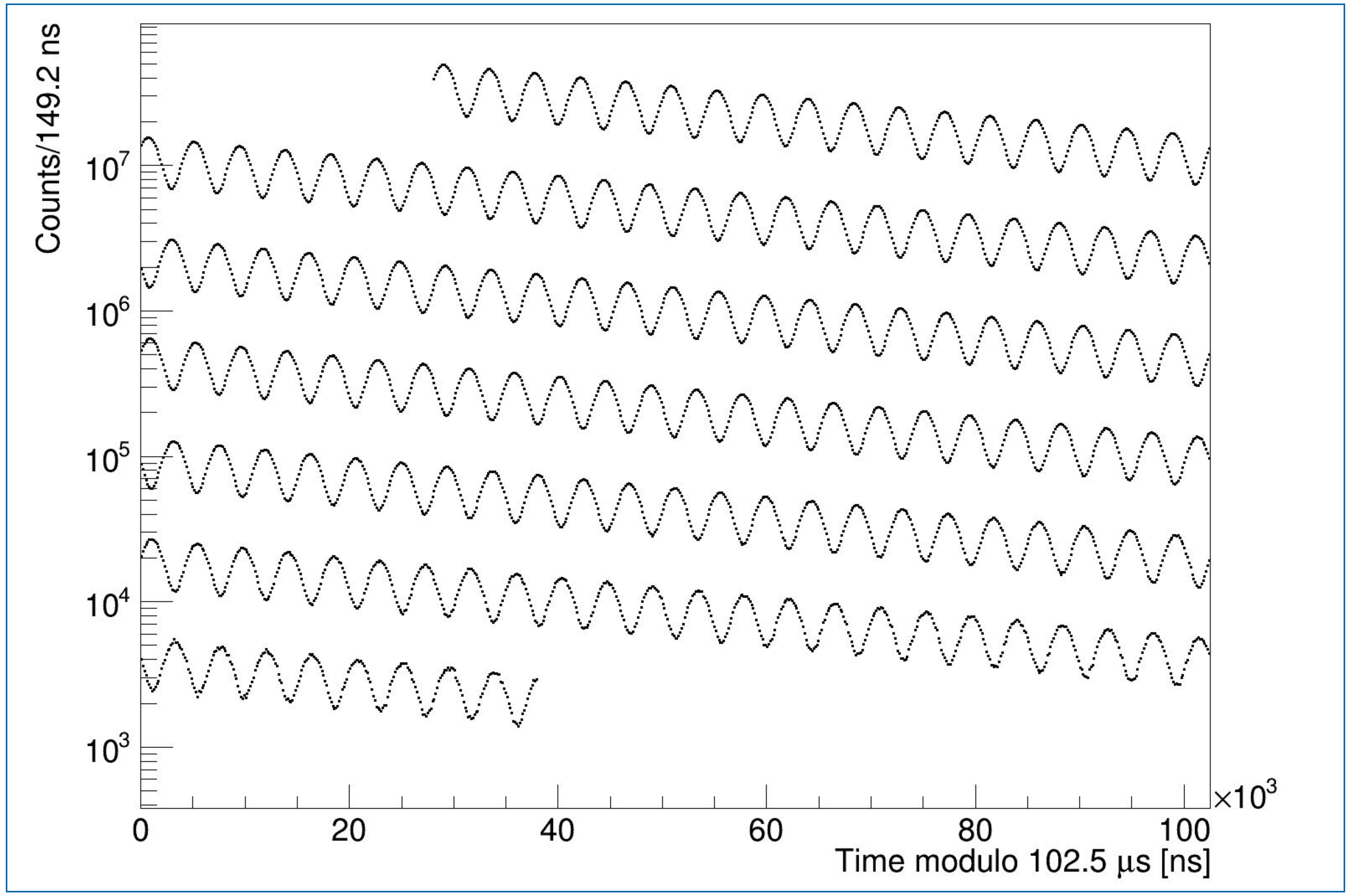

Measurement of precession frequency, ω_a, with positrons:
Fitting the time spectrum

- A simple 5-parameter fit is not sufficient due to complex beam dynamics effects.
  - The most significant one is due to Coherent Betatron Oscillation (CBO)

- Each beam dynamic effect contributes an additional frequency component to the wiggle plot

- Need to account for beam oscillations that couple to detector acceptance, muons lost before decay to positron, and detector effects such as pileup, gain.

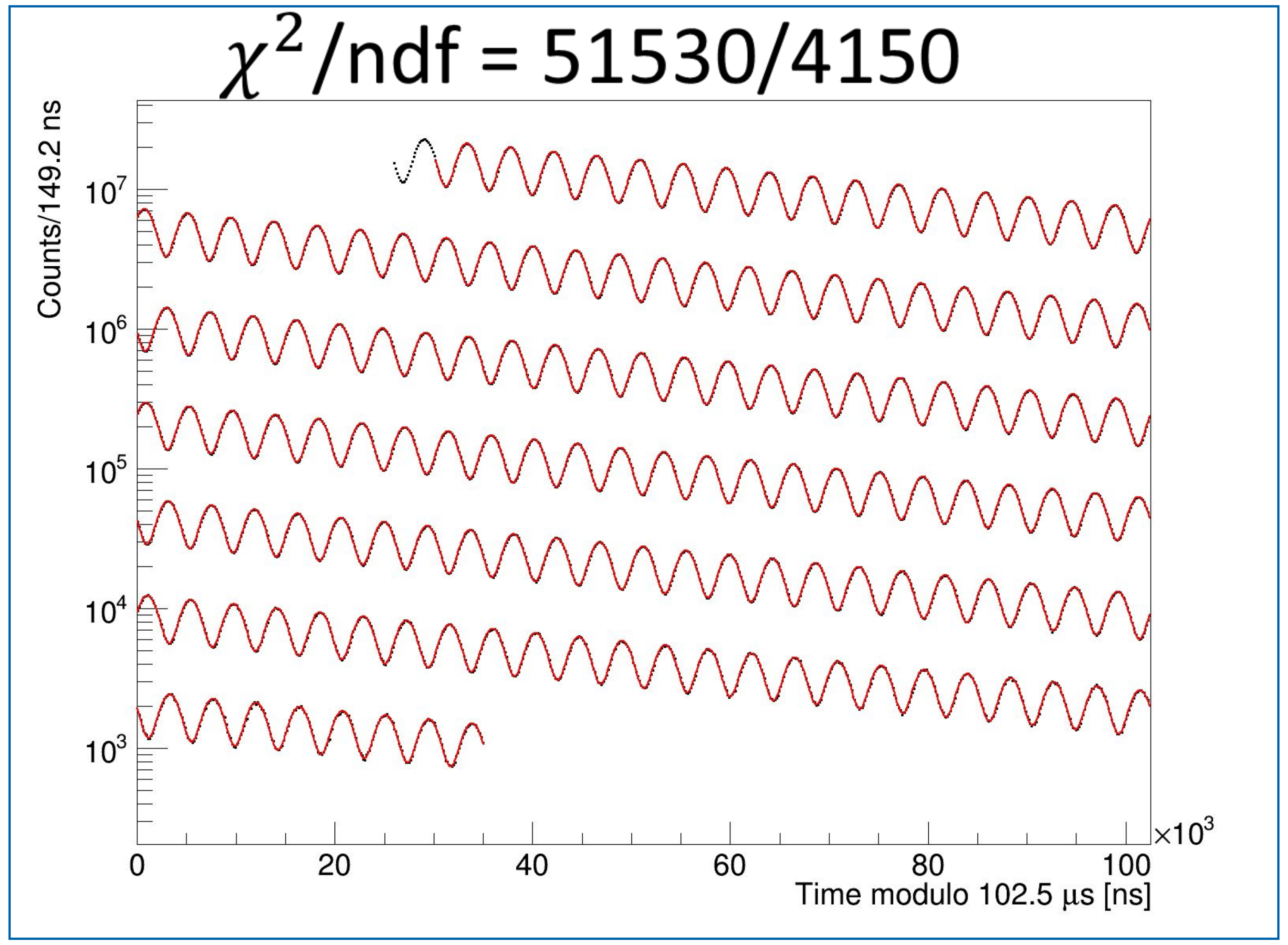

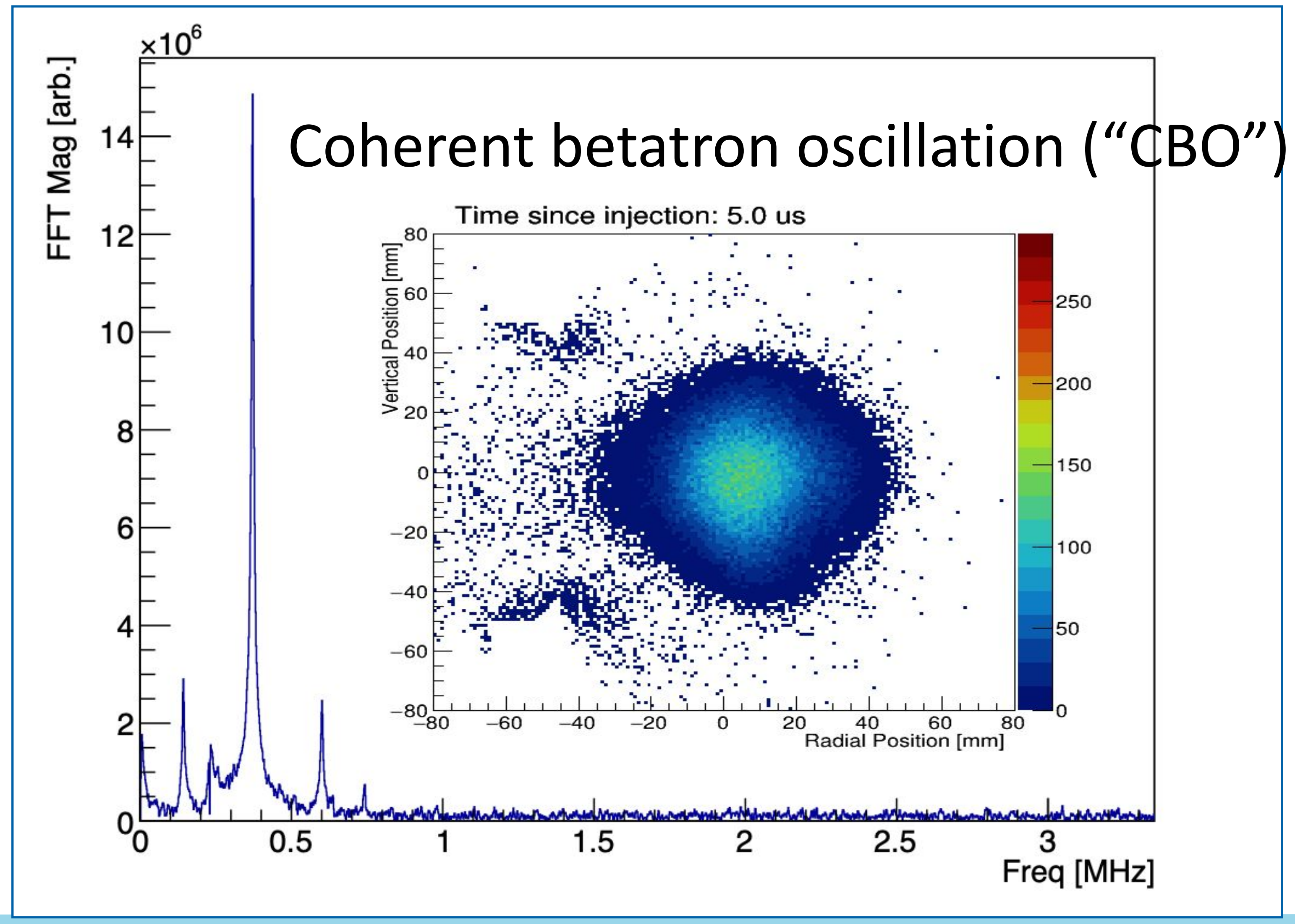

Measurement of precession frequency, ω_a, with positrons:
Fitting the time spectrum

- FFT of fit residual shows several peaks representing beam dynamics effect components.
- Modification of fit function required to incorporate beam dynamics effects.
- The full model (31-parameter fit) gives good fit quality, significantly reducing fit residuals.

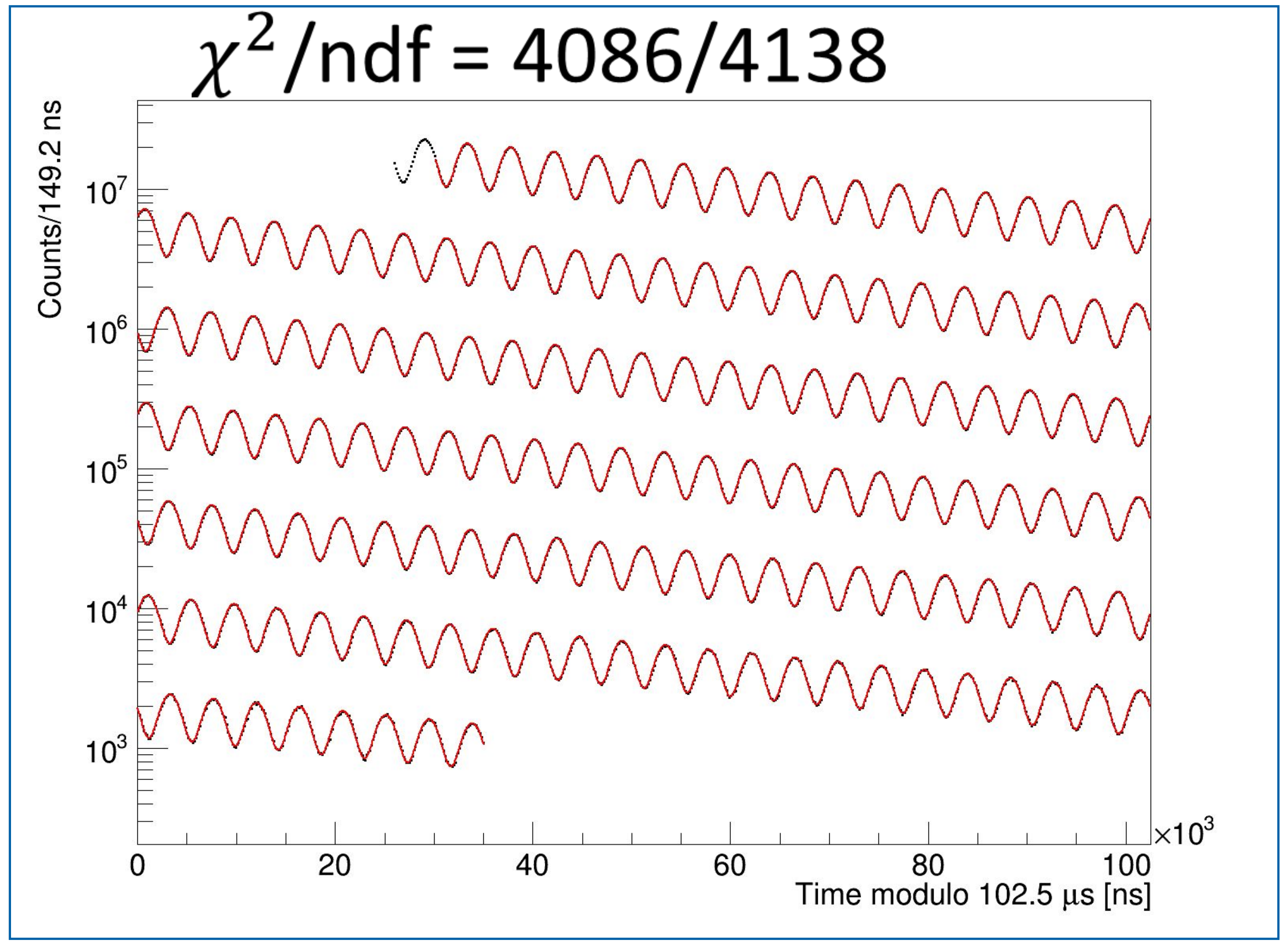

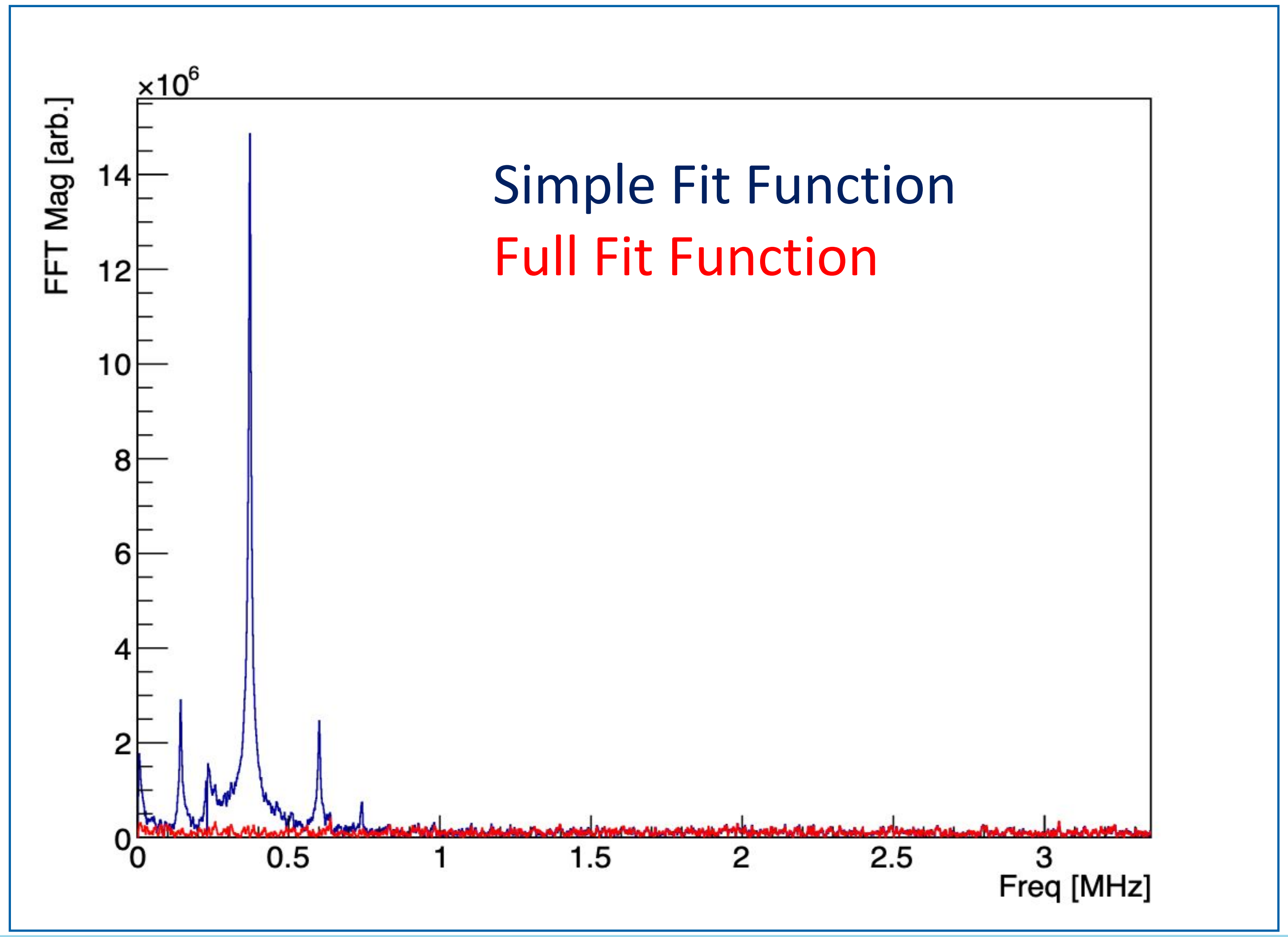

The anomalous precession frequency correction

$$\frac{\omega_a}{\tilde{\omega}'_p} = \frac{f_{\text{clock}}\ \omega_a^{meas}\ (1+C_e+C_p+C_{ml}+C_{pa}+C_{dd})}{f_{\text{calib}}\ \langle\ \omega'_p(x,y,\phi)\times M(x,y,\phi)\ \rangle\ (1+B_k+B_q)}$$

- **Electric field correction (C_e): Due to spread in injected muons momenta.**
- **Pitch correction (C_p): Due to vertical oscillation of muons.**
- Muon loss correction (C_{ml}): It comes from the initial phase-momentum correlation in muons. As muons are lost in time, time-dependent change in phase is observed.
- Phase acceptance correction (C_{pa}) : It is caused by decay-position and energy dependence of the positron phase. Early-to-late beam motion modulation leads to a time-dependent phase.
- Differential decay correction (C_{dd}): It accounts for high-momentum muons having a longer lifetime.

Measurement of electric field corrections C_e

$$\frac{\omega_a}{\tilde{\omega}'_p} = \frac{f_{\text{clock}}\, \omega_a^{meas}\, (1+C_e+C_p+C_{ml}+C_{pa}+C_{dd})}{f_{\text{calib}}\, \langle\, \omega'_p(x,y,\phi)\times M(x,y,\phi)\,\rangle\, (1+B_k+B_q)}$$

- Muons off the magic momentum ($\gamma = 29.3, p = 3.09\ \mathrm{GeV/c}$) will produce a motional magnetic field contribution to ω_a.

$$C_e = 2n(1-n)\beta^2 \frac{\langle x_e^2 \rangle}{R_0^2}$$

- n is the weak focusing field index ($n = \frac{\partial E}{\partial x}\frac{r_0}{vB_0}$)

- x_e is radial equilibrium position which is proportional to the momentum offset.

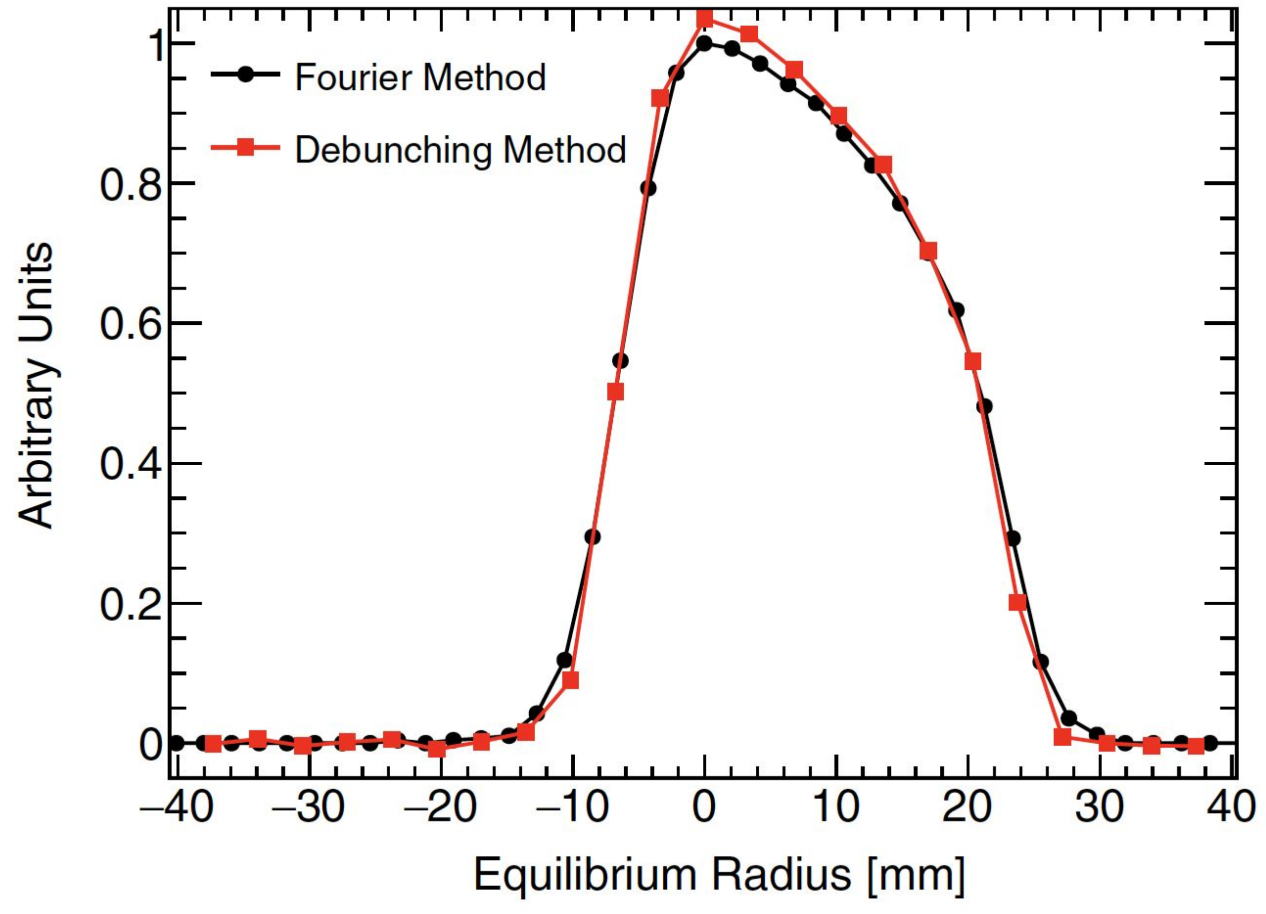

Measurement of pitch corrections C_p

$$\frac{\omega_a}{\tilde{\omega}'_p} = \frac{f_{\text{clock}}\,\omega_a^{meas}\,(1+C_e+C_p+C_{ml}+C_{pa}+C_{dd})}{f_{\text{calib}}\,\langle\,\omega'_p(x,y,\phi)\times M(x,y,\phi)\,\rangle\,(1+B_k+B_q)}$$

- The vertical motion of the muon causes the vertical spin precession.
- The horizontal precession (ω_a) is affected by coupled in-plane and out-of-plane precessions due to the vertical motion.

$$C_p = \frac{n}{2}\frac{\langle y^2\rangle}{R_0^2} = \frac{n}{4}\frac{\langle A^2\rangle}{R_0^2}$$

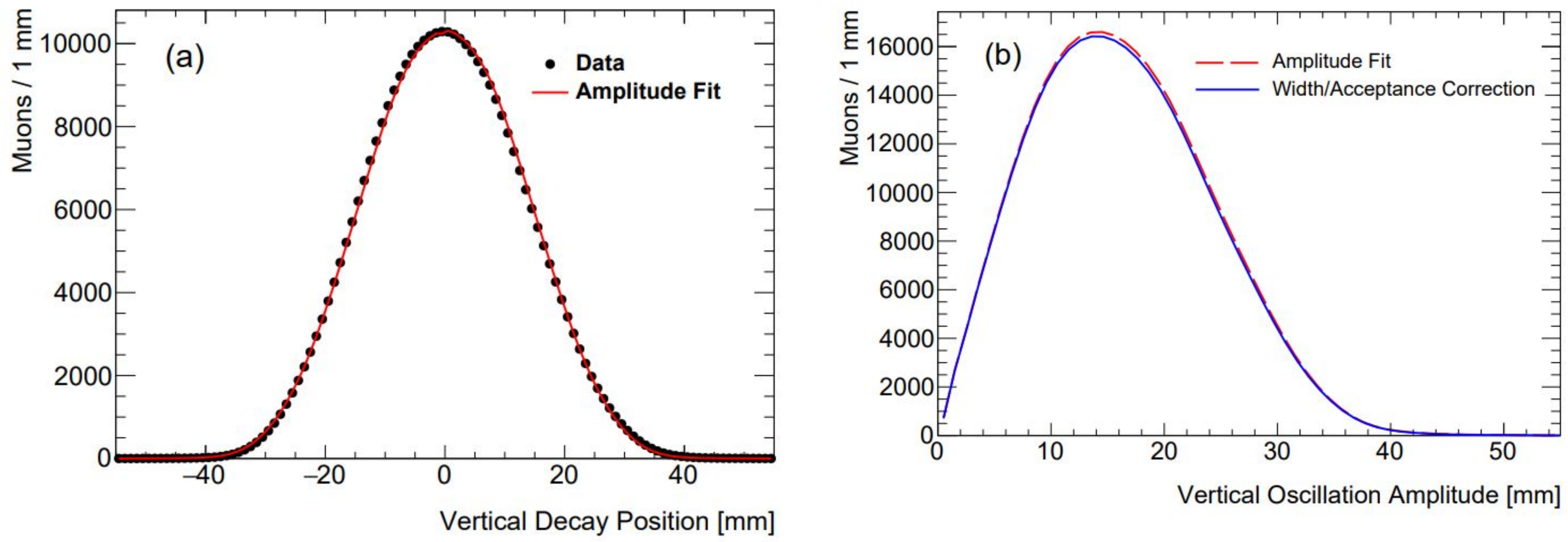

The magnetic field corrections

$$\frac{\omega_a}{\tilde{\omega}'_p} = \frac{f_{\text{clock}}\, \omega_a^{meas}\left(1+C_e+C_p+C_{ml}+C_{pa}+C_{dd}\right)}{f_{\text{calib}}\, \langle\, \omega'_p(x,y,\phi)\times M(x,y,\phi)\, \rangle \left(1+B_k+B_q\right)}$$

- Muon weighted magnetic field: $\langle\, \omega'_p(x,y,\phi) \times M(x,y,\phi)\, \rangle$
- Kicker transient (B_k): Magnetic field change caused by residual field after kicker pulse.
- Quad transient (B_q) : It is caused by vibration of ESQ plates, that perturbs the magnetic field.
- f_{calib} is calibration factor related to the magnetic field measurement.

Run 2/3 : Total Uncertainties (Statistical + Systematics)

Quantity	Correction [ppb]	Uncertainty [ppb]
ω_a^m (statistical)	–	201
ω_a^m (systematic)	–	25
C_e	451	32
C_p	170	10
C_{pa}	-27	13
C_{dd}	-15	17
C_{ml}	0	3
$f_{\text{calib}} \langle \omega'_p(\vec{r}) \times M(\vec{r}) \rangle$	–	46
B_k	-21	13
B_q	-21	20
$\mu'_p(34.7°)/\mu_e$	–	11
m_μ/m_e	–	22
$g_e/2$	–	0
Total systematic	–	70
Total external parameters	–	25
Totals	622	215

arXiv:2402.15410 [hep-ex]

- The total uncertainty is still dominated by statistical uncertainty.
- $C_e, C_p, \langle\, \omega'_p(x,y,\phi) \times M(x,y,\phi)\, \rangle$: important for CPT and Lorentz Invariance analysis.

FNAL Muon g-2 Run 1: Biggest SM Crack So Far!

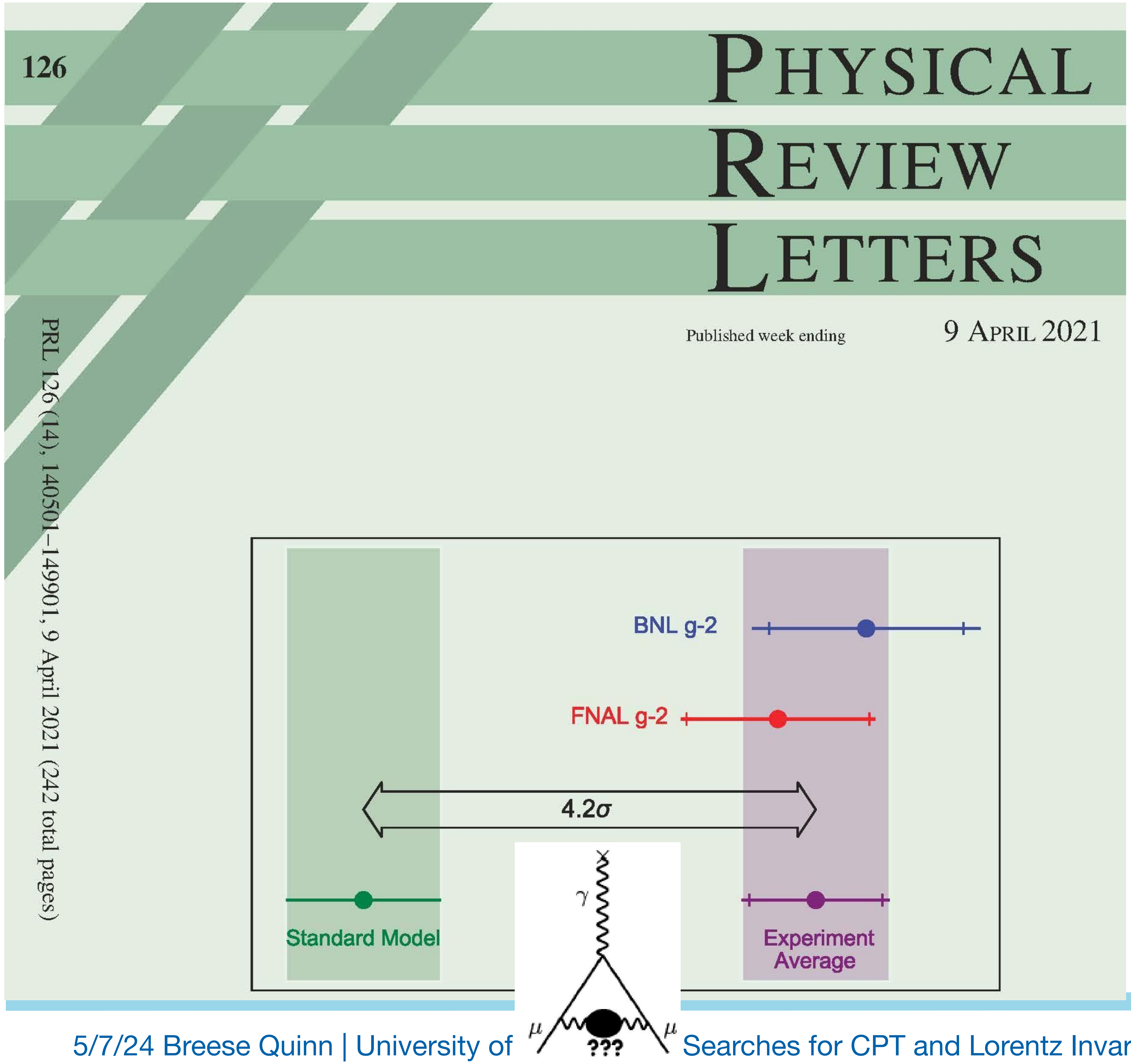

$a_\mu(\text{BNL}) = 116\,592\,089(63) \times 10^{-11}$ (540 ppb)

- Current analysis found no issues with BNL result

$a_\mu(\text{FNAL}) = 116\,592\,040(54) \times 10^{-11}$ (460 ppb)

- Consistent with BNL, 15% smaller uncertainty
  Phys. Rev. Lett. **126**, 141801 (2021)

$a_\mu(\text{Exp} - SM) = 251(59) \times 10^{-11}$

- Tension stood at 4.2σ

$a_\mu(\text{Exp}) = 116\,592\,061(41) \times 10^{-11}$ (350 ppb)

- Uncertainty comparable with 370 ppb WP20 SM
  Phys. Rept. **887**,1 (2020)

FNAL Muon g-2 Run 2/3: Is the crack sealed back up?

a_μ(FNAL) = 116 592 055(24) x 10^{-11} [203 ppb] Phys. Rev. Lett. **131**, 161802 (2023)

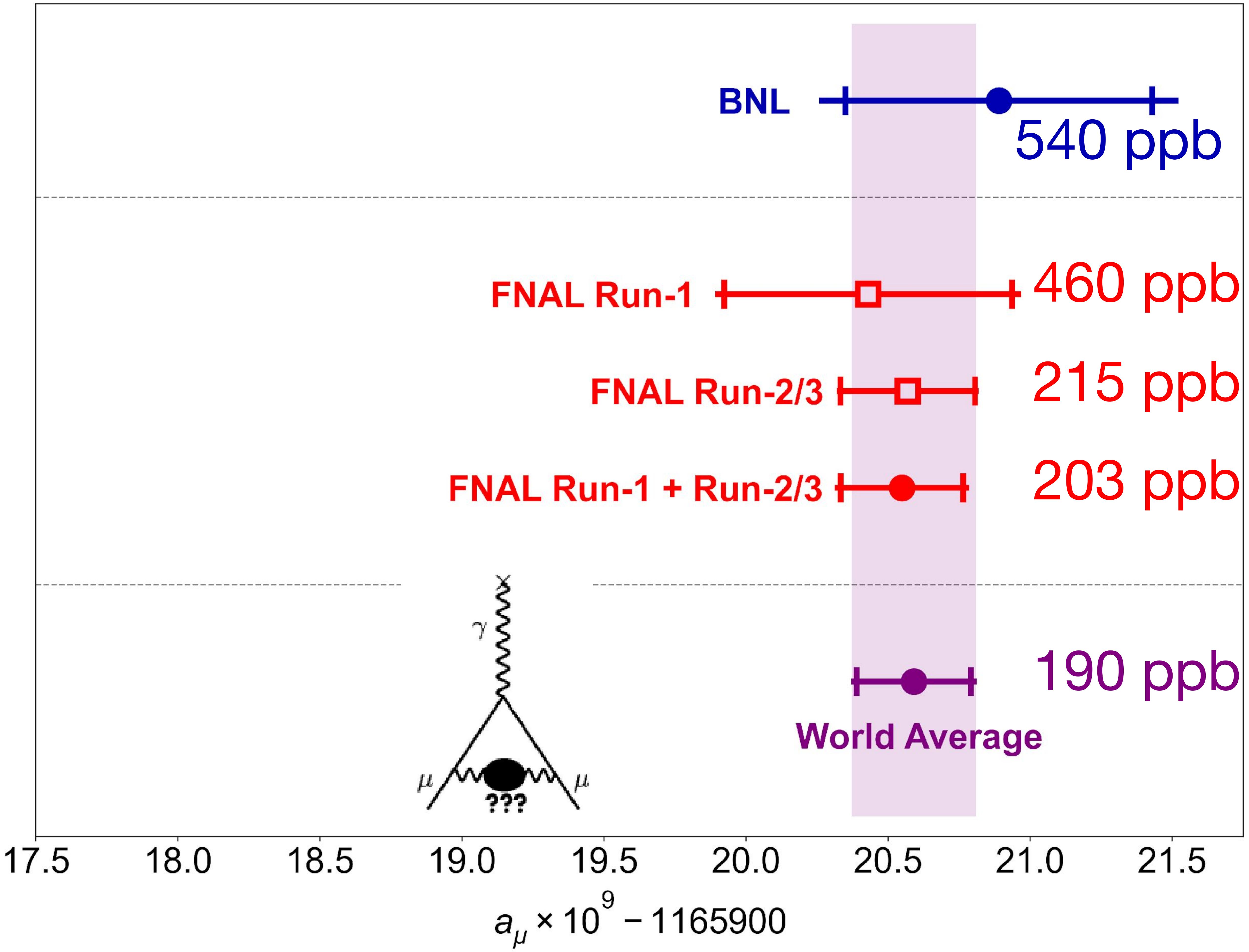

a_μ(Exp) = 116 592 059(22) x 10^{-11} [190 ppb]

- All measurements and combinations still dominated by statistical error
- World average is almost completely determined by ultra-precise FNAL result
- Theory value now up in the air

Why Frequencies? → Clocks

- We're checking if ω_a measurements show any evidence of CPTLIV
- But are our clocks sensitive to CPTLIV?

Muon g-2 Clock(Time) Reference

- How do you make a high precision measurement?
  - Compare to instruments/values that are more precise
- What values do we reference (what rulers)?
  - Magnetic moments, masses: μ_p/μ_e: 3 ppb, m_μ/m_e: 22 ppb
  - Time/frequency: Rb-87 hyperfine transition
- Rb clock: secondary standard
  - Based on atomic trans, but..
  - Inherent inaccuracies due to e.g. gas cell ΔP, ΔT
  - Disciplines crystal osc.: gas cells reduce intensity by ~0.1% when exposed to μwave near trans. f; osc. stabilzed by detecting dip while sweeping RF synthesizer through f

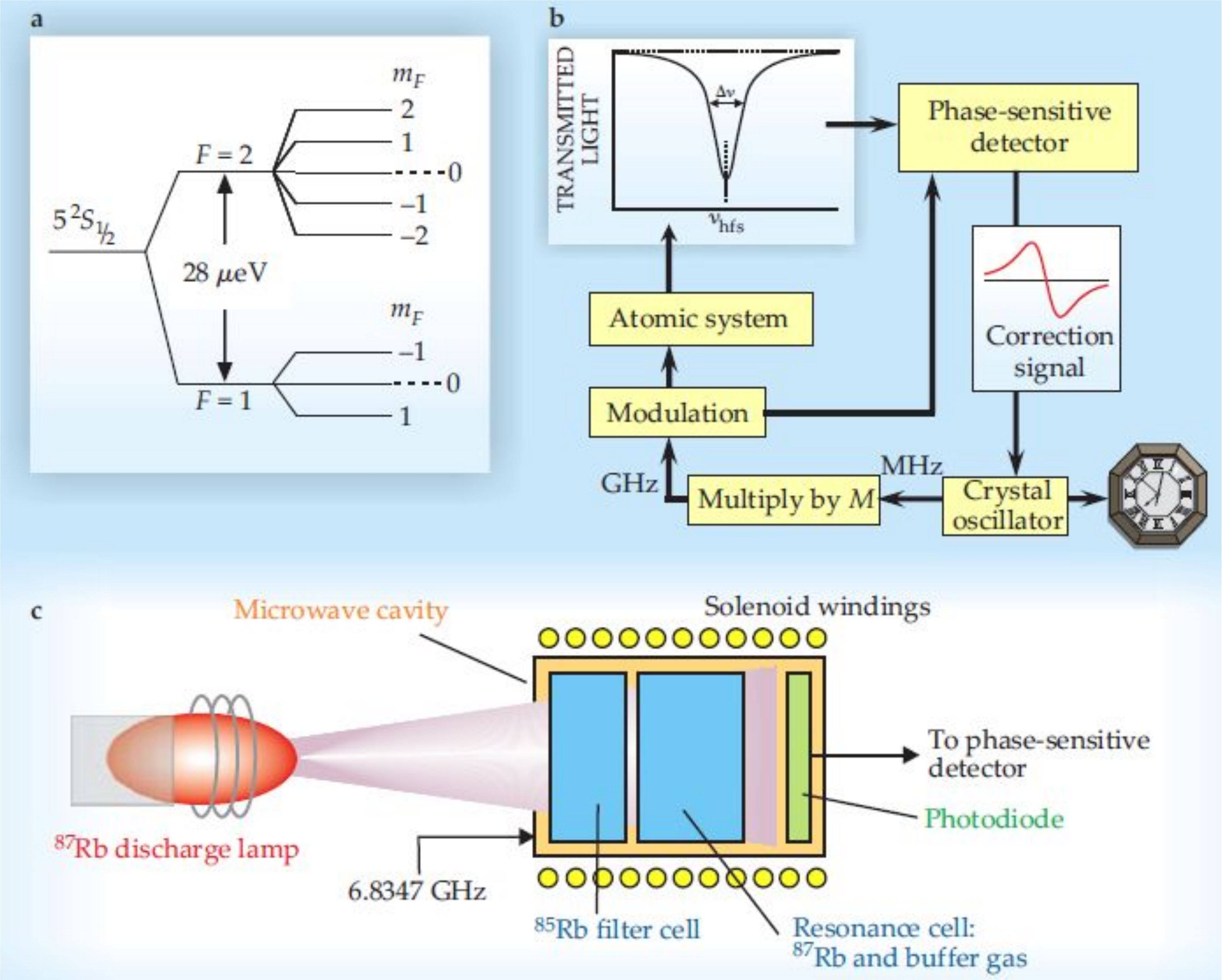

Muon g-2 Clock(Time) Reference

- Rb good enough?
  - Precision of ~1 ppb, but issues with long-term stability, therefore…
- GPS-disciplined Rb oscillator
  - GPS uses Cs and Rb. Cs: more precise (defines 1 s), but $$$

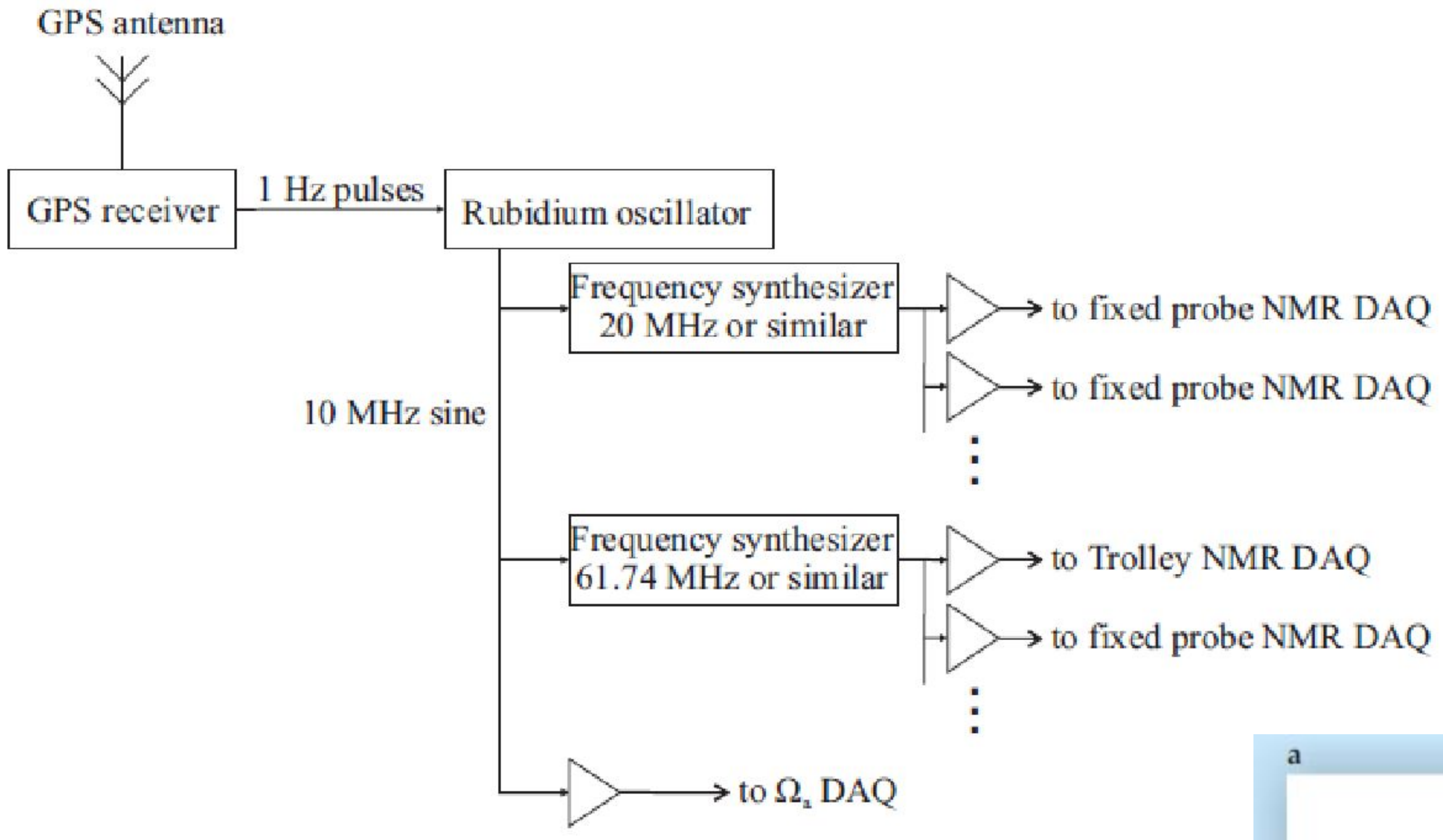

Figure 15.6: Scheme for common master-clock.

- Why do we need that particular m_F=0→0 transition?
  - Does not depend on orientation
  - CPTLV invariant! (Brillet and Hall, 1979 : due to earth's rotation <10^{-14}, negligible for us)

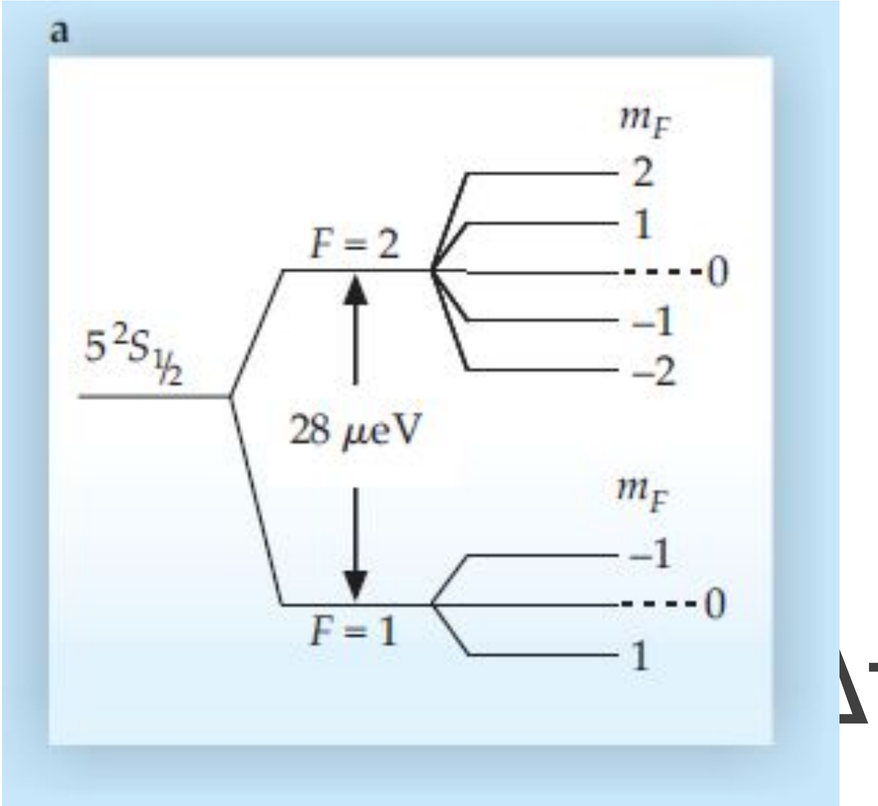

Muon g-2 Clock(Time) Reference

- What did E821 use (GPS wasn't ready at the time)?
  - **- LORAN-C system**
    - LOngRangeNavigation-Cyclan
    - Hyperbolic radio navigation: timing difference between two radio signals (i.e. GPS, but with land-based radio stations)
    - Based on Cs atomic clocks

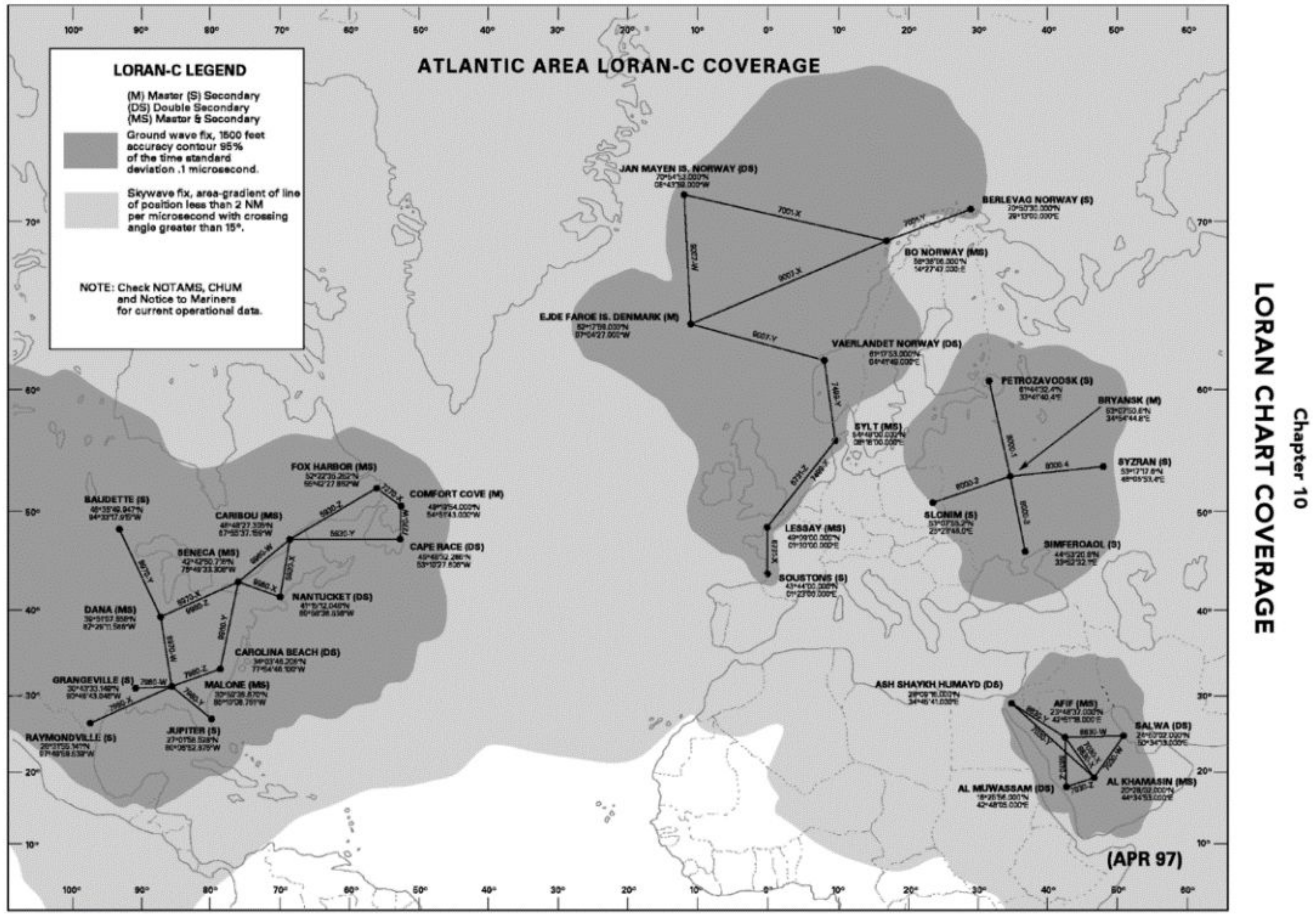

- Thanks to L. Roberts, S. Baessler

CPTLV: SME

- SME Lagrangian:

$$\mathcal{L}' = -a_\kappa \bar{\psi}\gamma^\kappa\psi - b_\kappa \bar{\psi}\gamma_5\gamma^\kappa\psi - \frac{1}{2}H_{\kappa\lambda}\bar{\psi}\sigma^{\kappa\lambda}\psi + \frac{1}{2}ic_{\kappa\lambda}\bar{\psi}\gamma^\kappa \overleftrightarrow{D}^\lambda \psi + \frac{1}{2}id_{\kappa\lambda}\bar{\psi}\gamma_5\gamma^\kappa \overleftrightarrow{D}^\lambda \psi$$

  - All terms violate Lorentz invariance
  - a_κ, b_κ are CPT-odd; others are CPT-even
- Does not assume anything specific about the nature of the violating physics
- Don't know what particles it might or might not couple to
  - Have to check all sectors!
  - But there is ***one*** sector in which we have very strong evidence for new physics – ***muons***!

SME Experimental Tests

Table D6. Electron sector, $d = 3, 4$ (part 1 of 3)

Combination	Result	System	Ref.
$\lvert \mathrm{Re}\, H_{011}^{\mathrm{NR}(0B)}\rvert$, $\lvert \mathrm{Im}\, H_{011}^{\mathrm{NR}(0B)}\rvert$, $\lvert \mathrm{Re}\, g_{011}^{\mathrm{NR}(0B)}\rvert$, $\lvert \mathrm{Im}\, g_{011}^{\mathrm{NR}(0B)}\rvert$	$< 9 \times 10^{-27}$ GeV	H maser	[36]*
$\lvert \mathrm{Re}\, H_{011}^{\mathrm{NR}(1B)}\rvert$, $\lvert \mathrm{Im}\, H_{011}^{\mathrm{NR}(1B)}\rvert$, $\lvert \mathrm{Re}\, g_{011}^{\mathrm{NR}(1B)}\rvert$, $\lvert \mathrm{Im}\, g_{011}^{\mathrm{NR}(1B)}\rvert$	$< 5 \times 10^{-27}$ GeV	"	[36]*
$\lvert \tilde{b}_X \rvert$	$< 6 \times 10^{-25}$ GeV	Penning trap	[32]*
$\lvert \tilde{b}_Y \rvert$	$< 6 \times 10^{-25}$ GeV	"	[32]*
$\lvert \tilde{b}_Z \rvert$	$< 7 \times 10^{-24}$ GeV	"	[32]*
$\lvert \tilde{b}^*_Z \rvert$	$< 7 \times 10^{-24}$ GeV	"	[32]*
$\lvert b_0 \rvert$	$< 2 \times 10^{-14}$ GeV	Cs spectroscopy	[37]*, [38]*
"	$< 2 \times 10^{-12}$ GeV	Tl spectroscopy	[37]*, [38]*
"	$< 7 \times 10^{-15}$ GeV	Dy spectroscopy	[37]*, [38]*
"	$< 2 \times 10^{-12}$ GeV	Yb spectroscopy	[38]*
$\tilde{b}_X$	$(-0.9 \pm 1.4) \times 10^{-31}$ GeV	Torsion pendulum	[39]
$\tilde{b}_Y$	$(-0.9 \pm 1.4) \times 10^{-31}$ GeV	"	[39]
$\tilde{b}_Z$	$(-0.3 \pm 4.4) \times 10^{-30}$ GeV	"	[39]
$\frac{1}{2}(\tilde{b}_T + \tilde{d}_- - 2\tilde{g}_c - 3\tilde{g}_T + 4\tilde{d}_+ - \tilde{d}_Q)$	$(0.9 \pm 2.2) \times 10^{-27}$ GeV	"	[39]
$\frac{1}{2}(2\tilde{g}_c - \tilde{g}_T - \tilde{b}_T + 4\tilde{d}_+ - \tilde{d}_- - \tilde{d}_Q) + \tan\eta(\tilde{d}_{YZ} - \tilde{H}_{XT})$	$(-0.8 \pm 2.0) \times 10^{-27}$ GeV	"	[39]
$\tilde{b}_X$	$(2.8 \pm 6.1) \times 10^{-29}$ GeV	K/He magnetometer	[40]
$\tilde{b}_Y$	$(6.8 \pm 6.1) \times 10^{-29}$ GeV	"	[40]
$\tilde{b}_X$	$(0.1 \pm 2.4) \times 10^{-31}$ GeV	Torsion pendulum	[41]
$\tilde{b}_Y$	$(-1.7 \pm 2.5) \times 10^{-31}$ GeV	"	[41]
$\tilde{b}_Z$	$(-29 \pm 39) \times 10^{-31}$ GeV	"	[41]
$\tilde{b}_\perp$	$< 3.1 \times 10^{-29}$ GeV	"	[42]
$\lvert \tilde{b}_Z \rvert$	$< 7.1 \times 10^{-28}$ GeV	"	[42]

UW Adelberger group

SME Experimental Tests

Table D9. Proton sector, $d = 3$

Combination	Result	System	Ref.
$\lvert\mathrm{Re}\, H_{011}^{\mathrm{NR}(0B)}\rvert$, $\lvert\mathrm{Im}\, H_{011}^{\mathrm{NR}(0B)}\rvert$, $\lvert\mathrm{Re}\, g_{011}^{\mathrm{NR}(0B)}\rvert$, $\lvert\mathrm{Im}\, g_{011}^{\mathrm{NR}(0B)}\rvert$	$< 9 \times 10^{-27}$ GeV	H maser	[36]*
$\lvert\mathrm{Re}\, H_{011}^{\mathrm{NR}(1B)}\rvert$, $\lvert\mathrm{Im}\, H_{011}^{\mathrm{NR}(1B)}\rvert$, $\lvert\mathrm{Re}\, g_{011}^{\mathrm{NR}(1B)}\rvert$, $\lvert\mathrm{Im}\, g_{011}^{\mathrm{NR}(1B)}\rvert$	$< 5 \times 10^{-27}$ GeV	"	[36]*
$\lvert\tilde{b}_Z\rvert$	$< 1.8 \times 10^{-24}$ GeV	Penning trap	[76]
$\lvert\tilde{b}^*_Z\rvert$	$< 3.5 \times 10^{-24}$ GeV	"	[76]
$\lvert\tilde{b}_Z\rvert$	$< 2.1 \times 10^{-22}$ GeV	"	[77]
$\lvert\tilde{b}^*_Z\rvert$	$< 2.6 \times 10^{-22}$ GeV	"	[77]
$\lvert\tilde{b}_Z\rvert$	$< 2 \times 10^{-21}$ GeV	"	[32]*
$\lvert\tilde{b}^*_Z\rvert$	$< 6 \times 10^{-21}$ GeV	"	[32]*
$\lvert\tilde{b}_\perp\rvert$	$< 7.6 \times 10^{-33}$ GeV	He/Xe magnetometer	[78]*
$\lvert b_0\rvert$	$< 3 \times 10^{-8}$ GeV	Cs spectroscopy	[37]*
"	$< 7 \times 10^{-8}$ GeV	"	[78]*
"	$< 4 \times 10^{-8}$ GeV	"	[38]*
"	$< 8 \times 10^{-8}$ GeV	Tl spectroscopy	[37]*, [38]*
$\tilde{b}_Z$	$< 7 \times 10^{-29}$ GeV	Hg/Cs comparison	[79]
$\tilde{b}_\perp$	$< 4 \times 10^{-30}$ GeV	"	[79]

- Similar for neutron sector

SME Experimental Tests

Table D21. Muon sector, $d = 3$

Combination	Result	System	Ref.
$\lvert\mathrm{Re}\, H_{011}^{\mathrm{NR}(0B)}\rvert,\ \lvert\mathrm{Im}\, H_{011}^{\mathrm{NR}(0B)}\rvert,\ \lvert\mathrm{Re}\, g_{011}^{\mathrm{NR}(0B)}\rvert,\ \lvert\mathrm{Im}\, g_{011}^{\mathrm{NR}(0B)}\rvert$	$< 2 \times 10^{-22}$ GeV	Muonium spectroscopy	[20]*
$\lvert\mathrm{Re}\, H_{011}^{\mathrm{NR}(1B)}\rvert,\ \lvert\mathrm{Im}\, H_{011}^{\mathrm{NR}(1B)}\rvert,\ \lvert\mathrm{Re}\, g_{011}^{\mathrm{NR}(1B)}\rvert,\ \lvert\mathrm{Im}\, g_{011}^{\mathrm{NR}(1B)}\rvert$	$< 7 \times 10^{-23}$ GeV	"	[20]*
b^T/m_μ	$(7.3 \pm 5.0) \times 10^{-7}$	Muon decay	[184]*
b_Z	$-(1.0 \pm 1.1) \times 10^{-23}$ GeV	BNL $g_\mu - 2$	[185]
$\sqrt{(\check{b}_X^{\mu^+})^2 + (\check{b}_Y^{\mu^+})^2}$	$< 1.4 \times 10^{-24}$ GeV	"	[185]
$\sqrt{(\check{b}_X^{\mu^-})^2 + (\check{b}_Y^{\mu^-})^2}$	$< 2.6 \times 10^{-24}$ GeV	"	[185]
$\sqrt{(\tilde{b}_X)^2 + (\tilde{b}_Y)^2}$	$< 2 \times 10^{-23}$ GeV	Muonium spectroscopy	[186]
$b_Z - 1.19(m_\mu d_{Z0} + H_{XY})$	$(-1.4 \pm 1.0) \times 10^{-22}$ GeV	BNL, CERN $g_\mu - 2$ data	[187]
b_Z	$(-2.3 \pm 1.4) \times 10^{-22}$ GeV	CERN $g_\mu - 2$ data	[187], [188]*
$\lvert\mathrm{Re}\, H_{011}^{(3)(0B)}\rvert,\ \lvert\mathrm{Im}\, H_{011}^{(3)(0B)}\rvert$	$< 5 \times 10^{-23}$ GeV	"	[20]*
$\check{H}_{010}^{(3)}$	$(-1.6 \pm 1.7) \times 10^{-22}$ GeV	BNL, CERN $g_\mu - 2$ data	[20]*
$\lvert\mathrm{Re}\, \check{H}_{011}^{(3)}\rvert,\ \lvert\mathrm{Im}\, \check{H}_{011}^{(3)}\rvert$	$< 2.0 \times 10^{-24}$ GeV	BNL $g_\mu - 2$	[20]*
$m_\mu d_{Z0} + H_{XY}$	$(1.8 \pm 6.0) \times 10^{-23}$ GeV	"	[185]

CPTLV: SME and Muon g-2

- SME Lagrangian:

$$\mathcal{L}' = -a_\kappa \bar{\psi}\gamma^\kappa\psi - b_\kappa\bar{\psi}\gamma_5\gamma^\kappa\psi - \frac{1}{2}H_{\kappa\lambda}\bar{\psi}\sigma^{\kappa\lambda}\psi + \frac{1}{2}ic_{\kappa\lambda}\bar{\psi}\gamma^\kappa \overleftrightarrow{D}^\lambda \psi + \frac{1}{2}id_{\kappa\lambda}\bar{\psi}\gamma_5\gamma^\kappa \overleftrightarrow{D}^\lambda \psi$$

  - All terms violate Lorentz invariance
  - a_κ, b_κ are CPT-odd; others are CPT-even
- Predicts two CPT/Lorentz Violating signatures for muon g-2:
  - Gomes, Kostelecky, Vargas, Phys.Rev.D90:076009,2014
  - **Sidereal (or annual) variation in ω_a**
  - **Difference in ω_a between μ^+ / μ^-**
  - Use frame where Z is the orientation of the earth's axis relative to the fixed, distant stars, and χ is the colatitude (earth's precession negligible in our case)

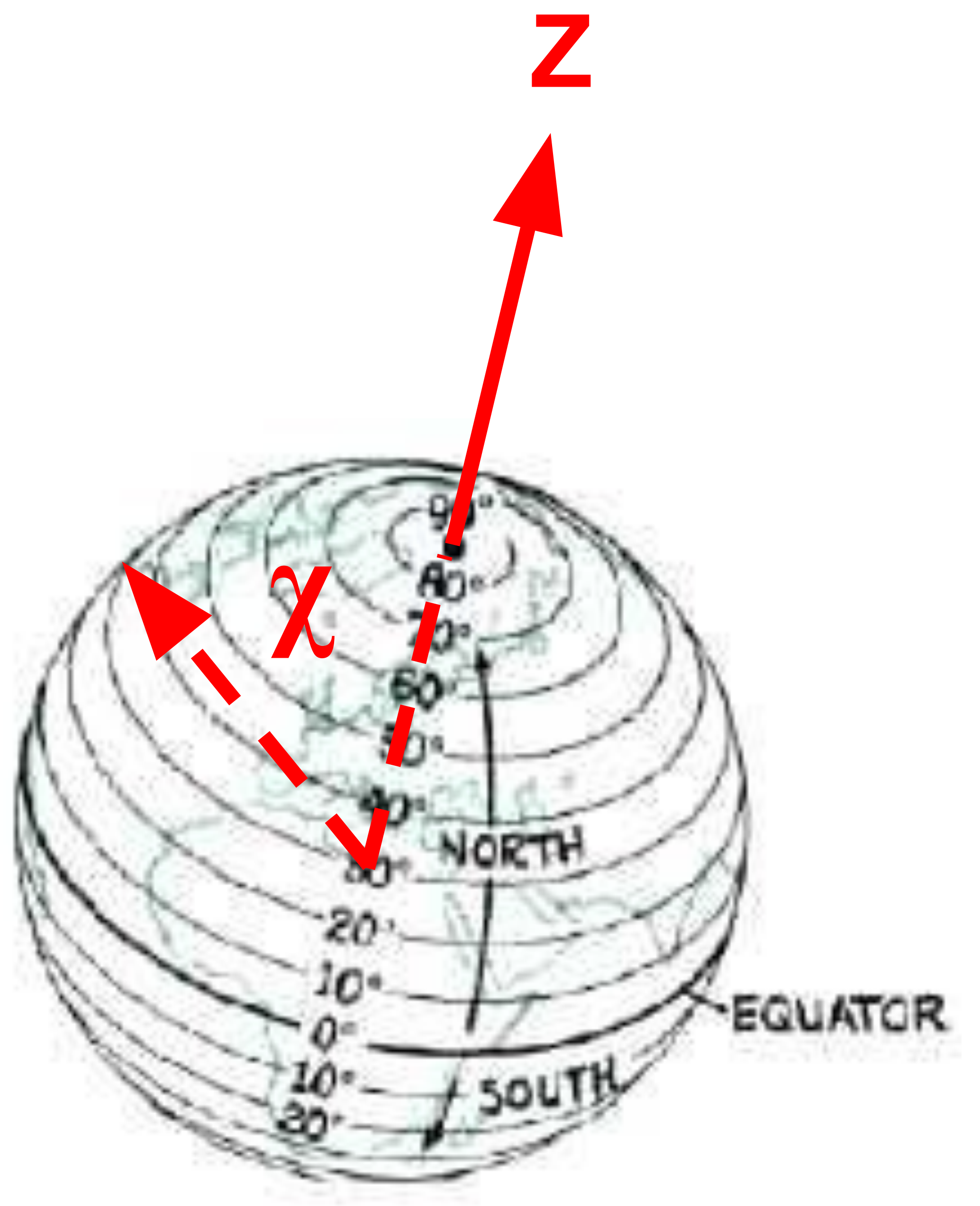

CPTLV: μ^+/μ^- ω_a Difference

$$\Delta\omega_a \equiv \langle\omega_a^{\mu^+}\rangle - \langle\omega_a^{\mu^-}\rangle = \frac{4b_Z}{\gamma}\cos\chi$$

- However, the magnetic field can vary, so when comparing frequencies, instead of ω_a, we use $\mathcal{R} = \omega_a / \omega_p$

- BNL E821 Results (2008)

$$\Delta\mathcal{R} = -(3.6 \pm 3.7) \times 10^{-9}$$

$$b_Z = -(1.0 \pm 1.1) \times 10^{-23}\ \text{GeV}$$

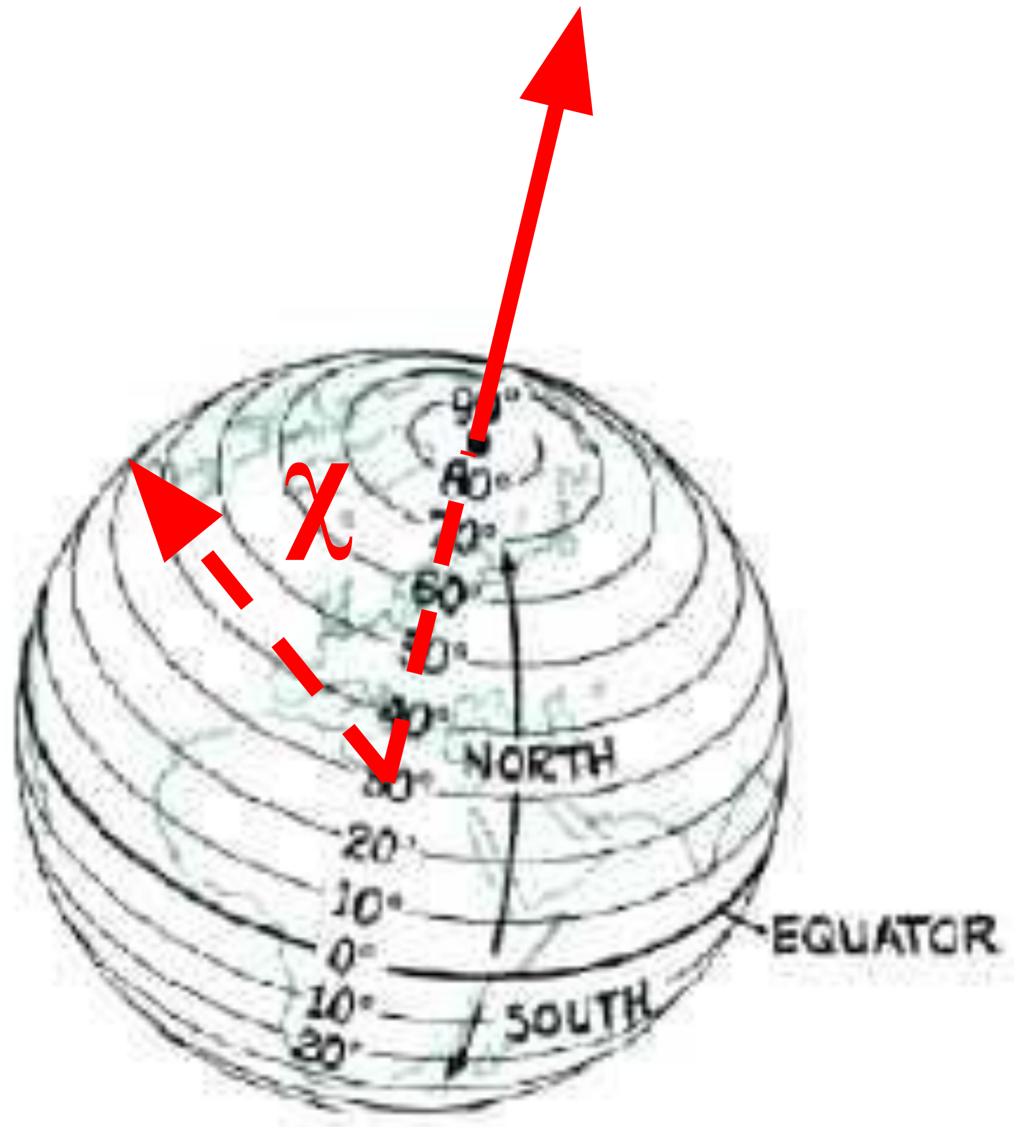

CPTLV: μ^+/μ^- ω_a Difference

- For two experiments at different colatitudes:
  - e.g. BNL & CERN, ***FNAL & J-PARC***

$$\Delta\mathcal{R} = \frac{2b_Z}{\gamma}\left(\frac{\cos\chi_1}{\omega_{p1}} + \frac{\cos\chi_2}{\omega_{p2}}\right) + 2(m_\mu d_{Z0} + H_{XY})\left(\frac{\cos\chi_1}{\omega_{p1}} - \frac{\cos\chi_2}{\omega_{p2}}\right)$$

But J-PARC can't do μ^-…
FNAL E989 was the only and last shot at improving this!

- BNL E821 Results (2008)
  - BNL & CERN

$$(m_\mu d_{Z0} + H_{XY}) = (1.6 \pm 5.6 \times 10^{-23})\ \text{GeV}$$

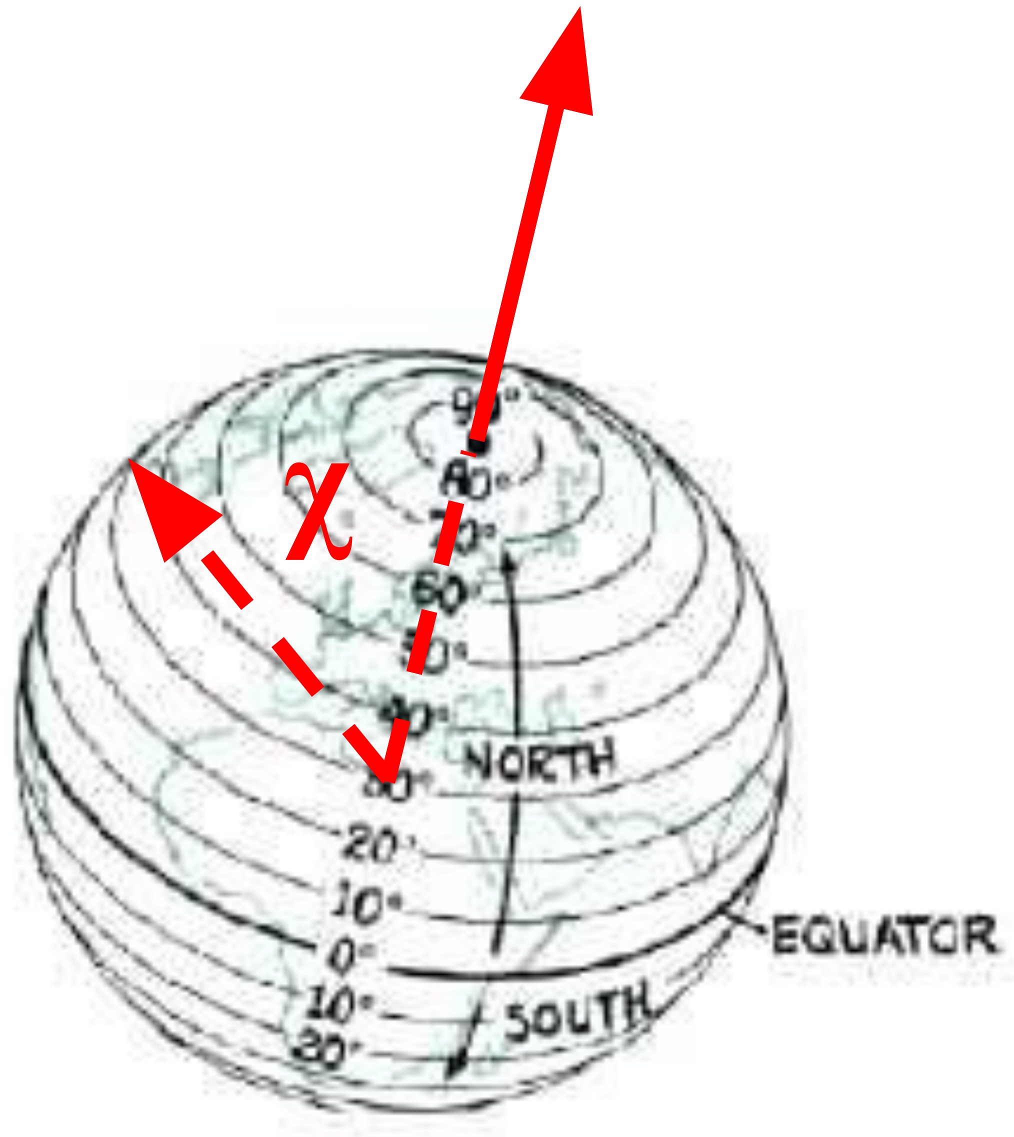

CPTLV: Sidereal oscillation of ω_a

E989 Run 2 Data

M. Bhattacharya Dissertation

- $$b_{\perp}^{\mu^\pm} = \frac{\hat{\omega}_a^{\mu^\pm}}{2|sin\chi|}$$

- $\widehat{\omega}_a{}^{\mu^\pm}$: amplitude of sidereal ω_a oscillation
- Calculate $\mathcal{R}$ = ω_a / ω_p on a Run-by-Run basis
  - A run is ~1 hour of data
- Approaches to search for oscillation
  - Multi-parameter fit: good for all data
  - Lomb-Scargle test: designed for unequally spaced data
- Previous results:
  - BNL E821

    $$A < 2.2 \text{ ppm } b_T^{\mu^+} \leq 1.4 \times 10^{-24} \text{ GeV}$$
  - FNAL E989 (PRELIMINARY)

    $$A < 2.0 \text{ ppm}, b_T^{\mu^+} \leq 1.3 \times 10^{-24} \text{ GeV}$$

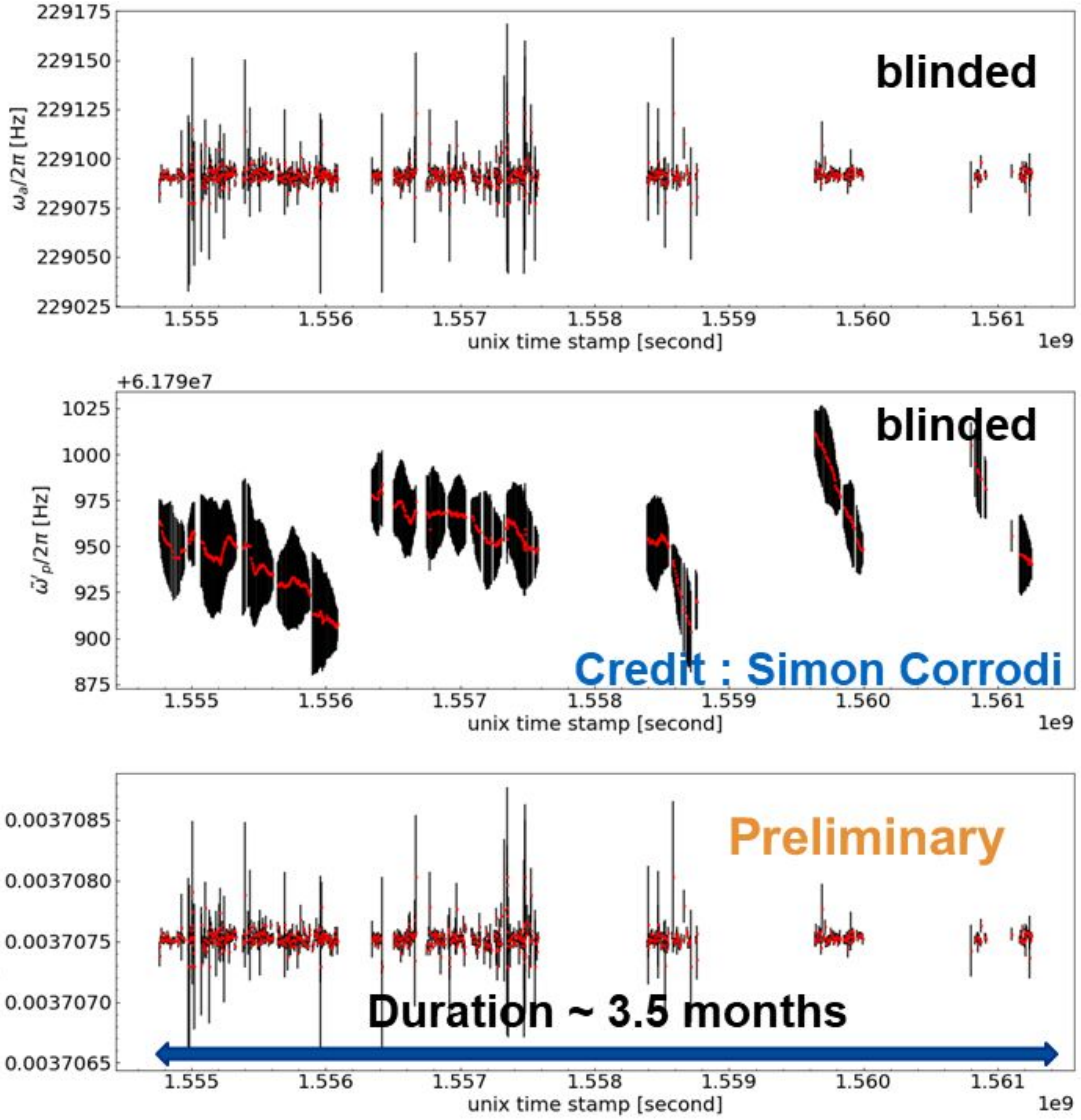

SME Muon Sector Current Limits (Kostelecký et.al.)

Table D21. Muon sector, $d = 3$

Combination	Result	System	Ref.
$\lvert\text{Re}\,H_{011}^{NR(0B)}\rvert$, $\lvert\text{Im}\,H_{011}^{NR(0B)}\rvert$, $\lvert\text{Re}\,g_{011}^{NR(0B)}\rvert$, $\lvert\text{Im}\,g_{011}^{NR(0B)}\rvert$	$< 2 \times 10^{-22}$ GeV	Muonium spectroscopy	[20]*
$\lvert\text{Re}\,H_{011}^{NR(1B)}\rvert$, $\lvert\text{Im}\,H_{011}^{NR(1B)}\rvert$, $\lvert\text{Re}\,g_{011}^{NR(1B)}\rvert$, $\lvert\text{Im}\,g_{011}^{NR(1B)}\rvert$	$< 7 \times 10^{-23}$ GeV	"	[20]*
b^T/m_μ	$(7.3 \pm 5.0) \times 10^{-7}$	Muon decay	[184]*
b_Z	$-(1.0 \pm 1.1) \times 10^{-23}$ GeV	BNL $g_\mu - 2$	[185]
$\sqrt{(\check{b}_X^{\mu^+})^2 + (\check{b}_Y^{\mu^+})^2}$	$< 1.4 \times 10^{-24}$ GeV	"	[185]
$\sqrt{(\check{b}_X^{\mu^-})^2 + (\check{b}_Y^{\mu^-})^2}$	$< 2.6 \times 10^{-24}$ GeV	"	[185]
$\sqrt{(\tilde{b}_X)^2 + (\tilde{b}_Y)^2}$	$< 2 \times 10^{-23}$ GeV	Muonium spectroscopy	[186]
$b_Z - 1.19(m_\mu d_{Z0} + H_{XY})$	$(-1.4 \pm 1.0) \times 10^{-22}$ GeV	BNL, CERN $g_\mu - 2$ data	[187]
b_Z	$(-2.3 \pm 1.4) \times 10^{-22}$ GeV	CERN $g_\mu - 2$ data	[187], [188]*
$\lvert\text{Re}\,H_{011}^{(3)(0B)}\rvert$, $\lvert\text{Im}\,H_{011}^{(3)(0B)}\rvert$	$< 5 \times 10^{-23}$ GeV	"	[20]*
$\check{H}_{010}^{(3)}$	$(-1.6 \pm 1.7) \times 10^{-22}$ GeV	BNL, CERN $g_\mu - 2$ data	[20]*
$\lvert\text{Re}\,\check{H}_{011}^{(3)}\rvert$, $\lvert\text{Im}\,\check{H}_{011}^{(3)}\rvert$	$< 2.0 \times 10^{-24}$ GeV	BNL $g_\mu - 2$	[20]*
$m_\mu d_{Z0} + H_{XY}$	$(1.8 \pm 6.0) \times 10^{-23}$ GeV	"	[185]

SME Muon Sector Current Limits

Table D21. Muon sector, $d = 3$

Combination	Result	System	Ref.
$\lvert\mathrm{Re}\,H_{011}^{\mathrm{NR}(0B)}\rvert$, $\lvert\mathrm{Im}\,H_{011}^{\mathrm{NR}(0B)}\rvert$, $\lvert\mathrm{Re}\,g_{011}^{\mathrm{NR}(0B)}\rvert$, $\lvert\mathrm{Im}\,g_{011}^{\mathrm{NR}(0B)}\rvert$	$< 2 \times 10^{-22}$ GeV	Muonium spectroscopy	[20]*
$\lvert\mathrm{Re}\,H_{011}^{\mathrm{NR}(1B)}\rvert$, $\lvert\mathrm{Im}\,H_{011}^{\mathrm{NR}(1B)}\rvert$, $\lvert\mathrm{Re}\,g_{011}^{\mathrm{NR}(1B)}\rvert$, $\lvert\mathrm{Im}\,g_{011}^{\mathrm{NR}(1B)}\rvert$	$< 7 \times 10^{-23}$ GeV	"	[20]*
b^T/m_μ	$(7.3 \pm 5.0) \times 10^{-7}$	Muon decay	[184]*
b_Z	$-(1.0 \pm 1.1) \times 10^{-23}$ GeV	BNL $g_\mu - 2$	[185]
$\sqrt{(\check{b}_X^{\mu^+})^2 + (\check{b}_Y^{\mu^+})^2}$	$< 1.4 \times 10^{-24}$ GeV	"	[185]
$\sqrt{(\check{b}_X^{\mu^-})^2 + (\check{b}_Y^{\mu^-})^2}$	$< 2.6 \times 10^{-24}$ GeV	"	[185]
$\sqrt{(\tilde{b}_X)^2 + (\tilde{b}_Y)^2}$	$< 2 \times 10^{-23}$ GeV	Muonium spectroscopy	[186]
$b_Z - 1.19(m_\mu d_{Z0} + H_{XY})$	$(-1.4 \pm 1.0) \times 10^{-22}$ GeV	BNL, CERN $g_\mu - 2$ data	[187]
b_Z	$(-2.3 \pm 1.4) \times 10^{-22}$ GeV	CERN $g_\mu - 2$ data	[187], [188]*
$\lvert\mathrm{Re}\,H_{011}^{(3)(0B)}\rvert$, $\lvert\mathrm{Im}\,H_{011}^{(3)(0B)}\rvert$	$< 5 \times 10^{-23}$ GeV	"	[20]*
$\check{H}_{010}^{(3)}$	$(-1.6 \pm 1.7) \times 10^{-22}$ GeV	BNL, CERN $g_\mu - 2$ data	[20]*
$\lvert\mathrm{Re}\,\check{H}_{011}^{(3)}\rvert$, $\lvert\mathrm{Im}\,\check{H}_{011}^{(3)}\rvert$	$< 2.0 \times 10^{-24}$ GeV	BNL $g_\mu - 2$	[20]*
$m_\mu d_{Z0} + H_{XY}$	$(1.8 \pm 6.0) \times 10^{-23}$ GeV	"	[185]

SME Muon Sector Current Limits

Table D22. Muon sector, $d = 4$

Combination	Result	System	Ref.
$c_{TT} + 0.35(c_{XX} + c_{YY}) + 0.28c_{ZZ}$	$< 8.5 \times 10^{-11}$	BNL $g_\mu - 2$	[189]*
$\lvert c_\mu - c_\gamma \rvert$	$< 3 \times 10^{-11}$	Astrophysics	[48]*
$c^{TT} - 0.05c^{ZZ}$	$(4.9 \pm 1.1) \times 10^{-8}$	Muon decay	[184]*
$\lvert c \rvert$	$< 10^{-11}$	Astrophysics	[68]*
$\lvert \mathrm{Re}\, g_{011}^{(4)(0B)} \rvert, \ \lvert \mathrm{Im}\, g_{011}^{(4)(0B)} \rvert$	$< 5 \times 10^{-22}$	Muonium spectroscopy	[20]*
$\lvert \mathrm{Re}\, \check{g}_{011}^{(4)} \rvert, \ \lvert \mathrm{Im}\, \check{g}_{011}^{(4)} \rvert$	$< 6.6 \times 10^{-25}$	BNL $g_\mu - 2$	[20]*
$\check{g}_{010}^{(4)}$	$(-2.3 \pm 2.4) \times 10^{-25}$	"	[20]*
$m_\mu g_{XYT}^{(M)}$	$-(7.8 \pm 8.5) \times 10^{-27}$ GeV	"	[20]*
$m_\mu \sqrt{(g_{XZT}^{(M)})^2 + (g_{YZT}^{(M)})^2}$	$< 1.1 \times 10^{-27}$ GeV	"	[20]*

SME Muon Sector Current Limits

Table D23. Nonminimal muon sector, $d \geq 5$

Combination	Result	System	Ref.
$\lvert\mathring{a}_2^{\rm NR}\rvert$	$< 8 \times 10^{-6}$ GeV^{-1}	Muonium spectroscopy	[20]*
$\lvert\mathring{c}_2^{\rm NR}\rvert$	$< 8 \times 10^{-6}$ GeV^{-1}	"	[20]*
$\lvert{\rm Re}\, H_{211}^{{\rm NR}(0B)}\rvert$, $\lvert{\rm Im}\, H_{211}^{{\rm NR}(0B)}\rvert$, $\lvert{\rm Re}\, g_{211}^{{\rm NR}(0B)}\rvert$, $\lvert{\rm Im}\, g_{211}^{{\rm NR}(0B)}\rvert$	$< 1 \times 10^{-11}$ GeV^{-1}	"	[20]*
$\lvert{\rm Re}\, H_{211}^{{\rm NR}(1B)}\rvert$, $\lvert{\rm Im}\, H_{211}^{{\rm NR}(1B)}\rvert$, $\lvert{\rm Re}\, g_{211}^{{\rm NR}(1B)}\rvert$, $\lvert{\rm Im}\, g_{211}^{{\rm NR}(1B)}\rvert$	$< 6 \times 10^{-12}$ GeV^{-1}	"	[20]*
$\mathring{a}^{{\rm UR}(5)} - m_\mu \mathring{g}^{{\rm UR}(6)}$	$(-1$ to $1) \times 10^{-34}$ GeV^{-1}	Astrophysics	[73]*, [18]*
$\lvert{\rm Re}\, H_{011}^{(5)(0B)}\rvert$, $\lvert{\rm Im}\, H_{011}^{(5)(0B)}\rvert$	$< 5 \times 10^{-21}$ GeV^{-1}	Muonium spectroscopy	[20]*
$\lvert{\rm Re}\, \check{H}_{011}^{(5)}\rvert$, $\lvert{\rm Im}\, \check{H}_{011}^{(5)}\rvert$, $\lvert{\rm Re}\, \check{H}_{211}^{(5)}\rvert$, $\lvert{\rm Im}\, \check{H}_{211}^{(5)}\rvert$	$< 2.1 \times 10^{-25}$ GeV^{-1}	BNL $g_\mu - 2$	[20]*
$\lvert{\rm Re}\, \check{H}_{221}^{(5)}\rvert$, $\lvert{\rm Im}\, \check{H}_{221}^{(5)}\rvert$	$< 1.3 \times 10^{-25}$ GeV^{-1}	"	[20]*
$\check{H}_{010}^{(5)}$, $\check{H}_{210}^{(5)}$	$(-1.7 \pm 1.7) \times 10^{-23}$ GeV^{-1}	BNL, CERN $g_\mu - 2$ data	[20]*
$\check{H}_{230}^{(5)}$	$(2.9 \pm 3.0) \times 10^{-24}$ GeV^{-1}	"	[20]*
$\mathring{c}^{{\rm UR}(6)}$	$(-8.5$ to $0.0025) \times 10^{-20}$ GeV^{-2}	Astrophysics	[73]*, [18]*
$\lvert{\rm Re}\, g_{011}^{(6)(0B)}\rvert$, $\lvert{\rm Im}\, g_{011}^{(6)(0B)}\rvert$	$< 5 \times 10^{-20}$ GeV^{-2}	Muonium spectroscopy	[20]*
$\lvert{\rm Re}\, \check{g}_{011}^{(6)}\rvert$, $\lvert{\rm Im}\, \check{g}_{011}^{(6)}\rvert$, $\lvert{\rm Re}\, \check{g}_{211}^{(6)}\rvert$, $\lvert{\rm Im}\, \check{g}_{211}^{(6)}\rvert$	$< 6.8 \times 10^{-26}$ GeV^{-2}	BNL $g_\mu - 2$	[20]*
$\lvert{\rm Re}\, \check{g}_{221}^{(6)}\rvert$, $\lvert{\rm Im}\, \check{g}_{221}^{(6)}\rvert$	$< 4.3 \times 10^{-26}$ GeV^{-2}	"	[20]*
$\check{g}_{010}^{(6)}$, $\check{g}_{210}^{(6)}$	$(-2.4 \pm 2.5) \times 10^{-26}$ GeV^{-2}	"	[20]*
$\check{g}_{230}^{(6)}$	$(-2.5 \pm 2.5) \times 10^{-26}$ GeV^{-2}	"	[20]*
$\lvert\mathring{a}_4^{\rm NR}\rvert$	$< 1 \times 10^{5}$ GeV^{-3}	Muonium spectroscopy	[20]*
$\lvert\mathring{a}_4^{\rm NR}\rvert$	$< 1 \times 10^{6}$ GeV^{-3}	"	[20]*
$\lvert\mathring{c}_4^{\rm NR}\rvert$	$< 1 \times 10^{5}$ GeV^{-3}	"	[20]*
$\lvert\mathring{c}_4^{\rm NR}\rvert$	$< 1 \times 10^{6}$ GeV^{-3}	"	[20]*
$\lvert{\rm Re}\, H_{411}^{{\rm NR}(0B)}\rvert$, $\lvert{\rm Im}\, H_{411}^{{\rm NR}(0B)}\rvert$, $\lvert{\rm Re}\, g_{411}^{{\rm NR}(0B)}\rvert$, $\lvert{\rm Im}\, g_{411}^{{\rm NR}(0B)}\rvert$	$< 2 \times 10^{-1}$ GeV^{-3}	"	[20]*
$\lvert{\rm Re}\, H_{411}^{{\rm NR}(1B)}\rvert$, $\lvert{\rm Im}\, H_{411}^{{\rm NR}(1B)}\rvert$, $\lvert{\rm Re}\, g_{411}^{{\rm NR}(1B)}\rvert$, $\lvert{\rm Im}\, g_{411}^{{\rm NR}(1B)}\rvert$	$< 8 \times 10^{-2}$ GeV^{-3}	"	[20]*

SME Muon Sector Current Limits

$\lvert \mathrm{Re}\, H^{(7)(0B)}_{011} \rvert$, $\lvert \mathrm{Im}\, H^{(7)(0B)}_{011} \rvert$	$< 4 \times 10^{-19}$ GeV^{-3}	Muonium spectroscopy	[20]*
$\check{H}^{(7)}_{010}$, $\check{H}^{(7)}_{210}$, $\check{H}^{(7)}_{410}$	$(-1.7 \pm 1.8) \times 10^{-24}$ GeV^{-3}	BNL, CERN $g_\mu - 2$ data	[20]*
$\check{H}^{(7)}_{230}$, $\check{H}^{(7)}_{430}$	$(3.0 \pm 3.1) \times 10^{-25}$ GeV^{-3}	"	[20]*
$\check{H}^{(7)}_{450}$	$(2.6 \pm 2.6) \times 10^{-25}$ GeV^{-3}	"	[20]*
$\lvert \mathrm{Re}\, \check{H}^{(7)}_{011} \rvert$, $\lvert \mathrm{Im}\, \check{H}^{(7)}_{011} \rvert$, $\lvert \mathrm{Re}\, \check{H}^{(7)}_{211} \rvert$, $\lvert \mathrm{Im}\, \check{H}^{(7)}_{211} \rvert$	$< 2.2 \times 10^{-26}$ GeV^{-3}	BNL $g_\mu - 2$	[20]*
$\lvert \mathrm{Re}\, \check{H}^{(7)}_{411} \rvert$, $\lvert \mathrm{Im}\, \check{H}^{(7)}_{411} \rvert$	$< 2.2 \times 10^{-26}$ GeV^{-3}	"	[20]*
$\lvert \mathrm{Re}\, \check{H}^{(7)}_{231} \rvert$, $\lvert \mathrm{Im}\, \check{H}^{(7)}_{231} \rvert$, $\lvert \mathrm{Re}\, \check{H}^{(7)}_{431} \rvert$, $\lvert \mathrm{Im}\, \check{H}^{(7)}_{431} \rvert$	$< 1.4 \times 10^{-26}$ GeV^{-3}	"	[20]*
$\lvert \mathrm{Re}\, \check{H}^{(7)}_{451} \rvert$, $\lvert \mathrm{Im}\, \check{H}^{(7)}_{451} \rvert$	$< 1.1 \times 10^{-26}$ GeV^{-3}	"	[20]*
$\lvert \mathrm{Re}\, g^{(8)(0B)}_{011} \rvert$, $\lvert \mathrm{Im}\, g^{(8)(0B)}_{011} \rvert$	$< 4 \times 10^{-18}$ GeV^{-4}	Muonium spectroscopy	[20]*
$\check{g}^{(8)}_{010}$, $\check{g}^{(8)}_{210}$, $\check{g}^{(8)}_{410}$	$(2.5 \pm 2.6) \times 10^{-27}$ GeV^{-4}	BNL $g_\mu - 2$	[20]*
$\check{g}^{(8)}_{230}$, $\check{g}^{(8)}_{430}$	$(2.6 \pm 2.6) \times 10^{-27}$ GeV^{-4}	"	[20]*
$\check{g}^{(8)}_{450}$	$(1.6 \pm 1.7) \times 10^{-27}$ GeV^{-4}	"	[20]*
$\lvert \mathrm{Re}\, \check{g}^{(8)}_{011} \rvert$, $\lvert \mathrm{Im}\, \check{g}^{(8)}_{011} \rvert$, $\lvert \mathrm{Re}\, \check{g}^{(8)}_{211} \rvert$, $\lvert \mathrm{Im}\, \check{g}^{(8)}_{211} \rvert$	$< 7.1 \times 10^{-27}$ GeV^{-4}	"	[20]*
$\lvert \mathrm{Re}\, \check{g}^{(8)}_{411} \rvert$, $\lvert \mathrm{Im}\, \check{g}^{(8)}_{411} \rvert$	$< 7.1 \times 10^{-27}$ GeV^{-4}	"	[20]*
$\lvert \mathrm{Re}\, \check{g}^{(8)}_{231} \rvert$, $\lvert \mathrm{Im}\, \check{g}^{(8)}_{231} \rvert$, $\lvert \mathrm{Re}\, \check{g}^{(8)}_{431} \rvert$, $\lvert \mathrm{Im}\, \check{g}^{(8)}_{431} \rvert$	$< 4.5 \times 10^{-27}$ GeV^{-4}	"	[20]*
$\lvert \mathrm{Re}\, \check{g}^{(8)}_{451} \rvert$, $\lvert \mathrm{Im}\, \check{g}^{(8)}_{451} \rvert$	$< 3.6 \times 10^{-27}$ GeV^{-4}	"	[20]*
$\check{H}^{(9)}_{010}$, $\check{H}^{(9)}_{210}$, $\check{H}^{(9)}_{410}$, $\check{H}^{(9)}_{610}$	$(-1.8 \pm 1.9) \times 10^{-25}$ GeV^{-5}	BNL, CERN $g_\mu - 2$ data	[20]*
$\check{H}^{(9)}_{230}$, $\check{H}^{(9)}_{430}$, $\check{H}^{(9)}_{630}$	$(3.2 \pm 3.3) \times 10^{-26}$ GeV^{-5}	"	[20]*
$\check{H}^{(9)}_{450}$, $\check{H}^{(9)}_{650}$	$(2.7 \pm 2.7) \times 10^{-26}$ GeV^{-5}	"	[20]*
$\check{H}^{(9)}_{670}$	$(-1.1 \pm 1.1) \times 10^{-26}$ GeV^{-5}	"	[20]*
$\check{g}^{(10)}_{010}$, $\check{g}^{(10)}_{210}$, $\check{g}^{(10)}_{410}$, $\check{g}^{(10)}_{610}$	$(-2.6 \pm 2.7) \times 10^{-28}$ GeV^{-6}	BNL $g_\mu - 2$	[20]*
$\check{g}^{(10)}_{230}$, $\check{g}^{(10)}_{430}$, $\check{g}^{(10)}_{630}$	$(-2.7 \pm 2.7) \times 10^{-28}$ GeV^{-6}	"	[20]*
$\check{g}^{(10)}_{450}$, $\check{g}^{(10)}_{650}$	$(1.7 \pm 1.7) \times 10^{-28}$ GeV^{-6}	"	[20]*
$\check{g}^{(10)}_{670}$	$(1.3 \pm 1.4) \times 10^{-28}$ GeV^{-6}	"	[20]*

SME and CPTLV in Muon $g-2$

$$\mathcal{L} = -a_{\kappa\,AB}\,\bar{l}_A\gamma^\kappa l_B - b_{\kappa\,AB}\,\bar{l}_A\gamma_5\gamma^\kappa l_B - \tfrac{1}{2}H_{\kappa\lambda\,AB}\,\bar{l}_A\sigma^{\kappa\lambda}l_B + \tfrac{1}{2}ic_{\kappa\lambda\,AB}\,\bar{l}_A\gamma^\kappa \overleftrightarrow{D}^\lambda l_B + \tfrac{1}{2}id_{\kappa\lambda\,AB}\,\bar{l}_A\gamma_5\gamma^\kappa \overleftrightarrow{D}^\lambda l_B \quad .$$

$$b_\perp^{\mu^\pm} = \frac{\overset{\wedge}{\omega}{}_a^{\mu^\pm}}{2|sin\chi|}$$

- CPTLV effects with the signal at sidereal frequency:
  - In cartesian coordinate $c_{X\ or\ Y\ or\ antisymm\ XY\ pair}$
  - In spherical coordinate c_{kl1} (i.e. azimuthal index $m = 1$)
- CPTLV effects with the signal at sidereal frequency harmonics:
  - In cartesian coordinate $c_{symm\ XY\ pair}$
  - In spherical coordinate c_{klm} (i.e. azimuthal index $m > 1$)

No search for signal at sidereal harmonics has ever been conducted!

Muon g-2 Run 2/3 CPTLV Analysis

- The rest of the talk is basically copied from Dr. Baisakhi Mitra's 28 May 2024 dissertation defense!

SME and CPTLV in Muon $g-2$

$$A_m^{\pm} = \left| 4 \sum_{dnj} E_0^{d-3} G_{jm}(\chi) \left[\check{H}_{njm}^{(d)} \pm E_0 \, \check{g}_{njm}^{(d+1)} \right] \right|, \quad m \neq 0$$

- A_m : Total amplitude of m^{th}harmonic. This term is energy dependent.
- E_0 : unperturbed muon energy.
- G_{jm} : Dimensionless factor. $G_{jm}(\chi) \equiv \sqrt{j(j+1)}\,{}_1Y_{j0}(\pi/2,0) d_{0m}^{(j)}(-\chi)$
- $d \leq 4$: Minimal SME, $d > 4$: Nonminimal SME.
- Nonminimal terms produce effects that grow with energy.
- d : mass dimension of the SME coefficient. odd d : $m_{max} = d - 2$; even d : $m_{max} = d - 3$.

SME and CPTLV in Muon $g-2$

TABLE IX: Constraints on the moduli of the real and imaginary parts of spherical coefficients determined from sidereal variations of the antimuon anomaly frequency in the BNL experiment. Units are GeV^{4-d}.

d	Coefficient $\check{\mathcal{K}}$	Constraint on $\lvert\text{Re}\,\check{\mathcal{K}}\rvert$, $\lvert\text{Im}\,\check{\mathcal{K}}\rvert$
3	$\check{H}^{(3)}_{011}$	$< 2.0 \times 10^{-24}$
4	$\check{g}^{(4)}_{011}$	$< 6.6 \times 10^{-25}$
5	$\check{H}^{(5)}_{011}$, $\check{H}^{(5)}_{211}$	$< 2.1 \times 10^{-25}$
	$\check{H}^{(5)}_{231}$	$< 1.3 \times 10^{-25}$
6	$\check{g}^{(6)}_{011}$, $\check{g}^{(6)}_{211}$	$< 6.8 \times 10^{-26}$
	$\check{g}^{(6)}_{231}$	$< 4.3 \times 10^{-26}$
7	$\check{H}^{(7)}_{011}$, $\check{H}^{(7)}_{211}$, $\check{H}^{(7)}_{411}$	$< 2.2 \times 10^{-26}$
	$\check{H}^{(7)}_{231}$, $\check{H}^{(7)}_{431}$	$< 1.4 \times 10^{-26}$
	$\check{H}^{(7)}_{451}$	$< 1.1 \times 10^{-26}$
8	$\check{g}^{(8)}_{011}$, $\check{g}^{(8)}_{211}$, $\check{g}^{(8)}_{411}$	$< 7.1 \times 10^{-27}$
	$\check{g}^{(8)}_{231}$, $\check{g}^{(8)}_{431}$	$< 4.5 \times 10^{-27}$
	$\check{g}^{(8)}_{451}$	$< 3.6 \times 10^{-27}$

- BNL and FNAL: maximum muon energy (3.09 GeV) is the same.
  - BNL data allowed limits up to $d = 8$
- So, E989 has reach up to $d = 8 \rightarrow m_{max} = 5$, i.e. coefficients possible up to 5th harmonic.
  - $\check{H}_{nj1}, \check{H}_{nj2}, \check{H}_{nj3}, \check{H}_{nj4}, \check{H}_{nj5}$

E989 will conduct first-ever search at sidereal harmonics

CPTLV Analysis Framework

R_μ Time Series Extraction

1. Analyzer verification on the entire dataset
2. Extraction of Unix timestamp for each run
3. Extraction of $\tilde{\omega}'_p$ for each run
4. Extraction of $R_\mu = \frac{\omega_a}{\tilde{\omega}'_p}$ for each run

CPTLV Oscillation Amplitude Blinding & Extraction

- $\mathcal{R}_\mu = \frac{\omega_a}{\tilde{\omega}'_p}$
- Blinding signal $\mathcal{R}_{blinding}$
- Blinded Signal $\mathcal{R}_{blinded}$
- Apply MPF to retrieve blinded amplitude $\mathcal{R}_{blinded}$

Unblinding

- Use blinding parameters to remove injected signals
- $\mathcal{R}_\mu = \frac{\omega_a}{\tilde{\omega}'_p}$
- Perform Lomb-Scargle Periodogram Analysis
- Calculate confidence level for the detected oscillation amplitude of $\mathcal{R}_\mu$ at sidereal harmonics

Analyzer verification on the entire dataset

- Analysis done on Run 2, Run 3a, and Run 3b datasets.
- Full-fit with 31 parameters performed on Run 2, Run 3a and Run 3b datasets.
  - $\omega_a^m = \omega_{ref} \cdot (1 + [R - \Delta R] \times 10^{-6})$, ΔR is common software blinding offset

Extraction of Unix timestamp and $\tilde{\omega}'_p$ for each run: Run 2

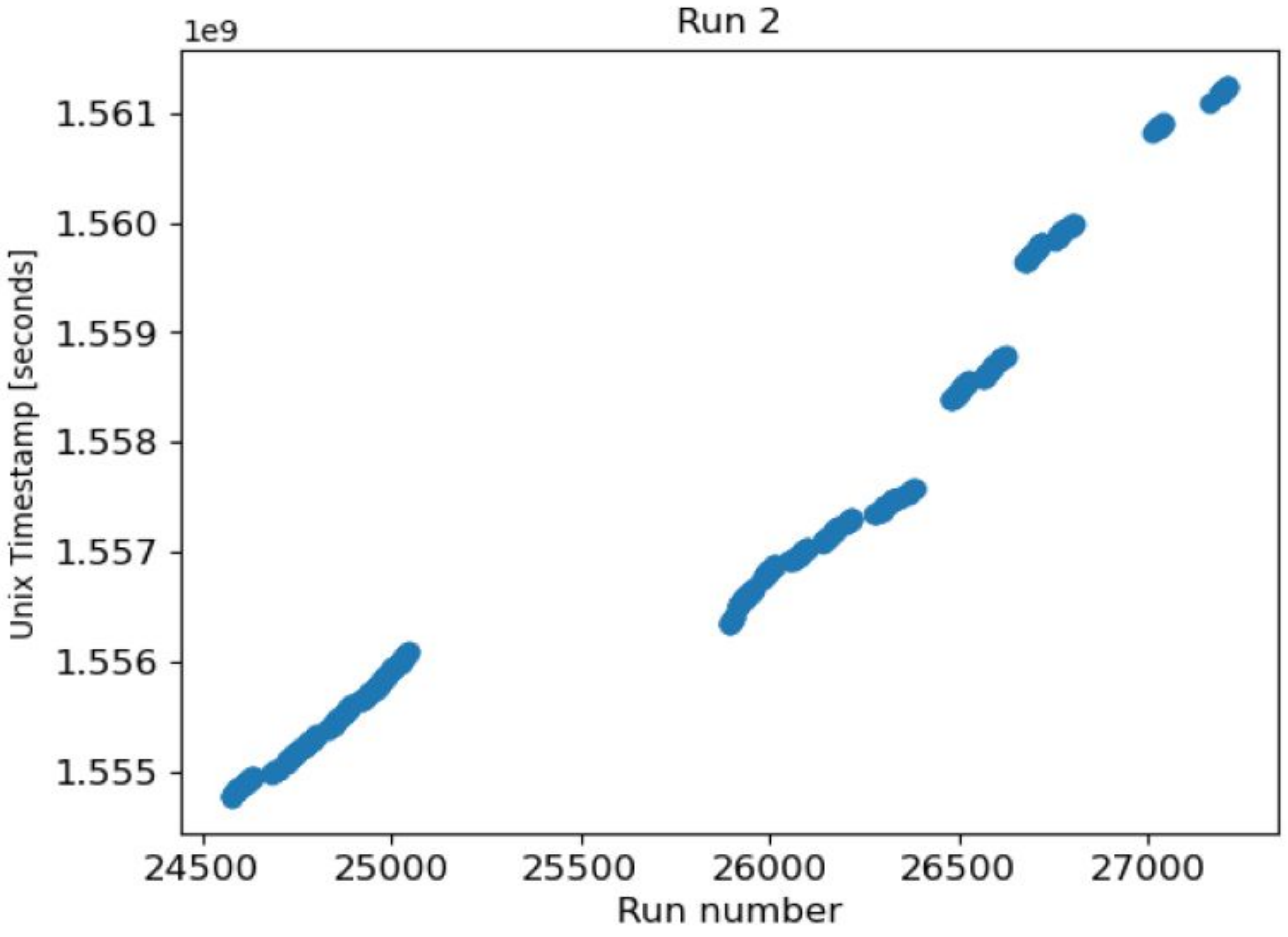

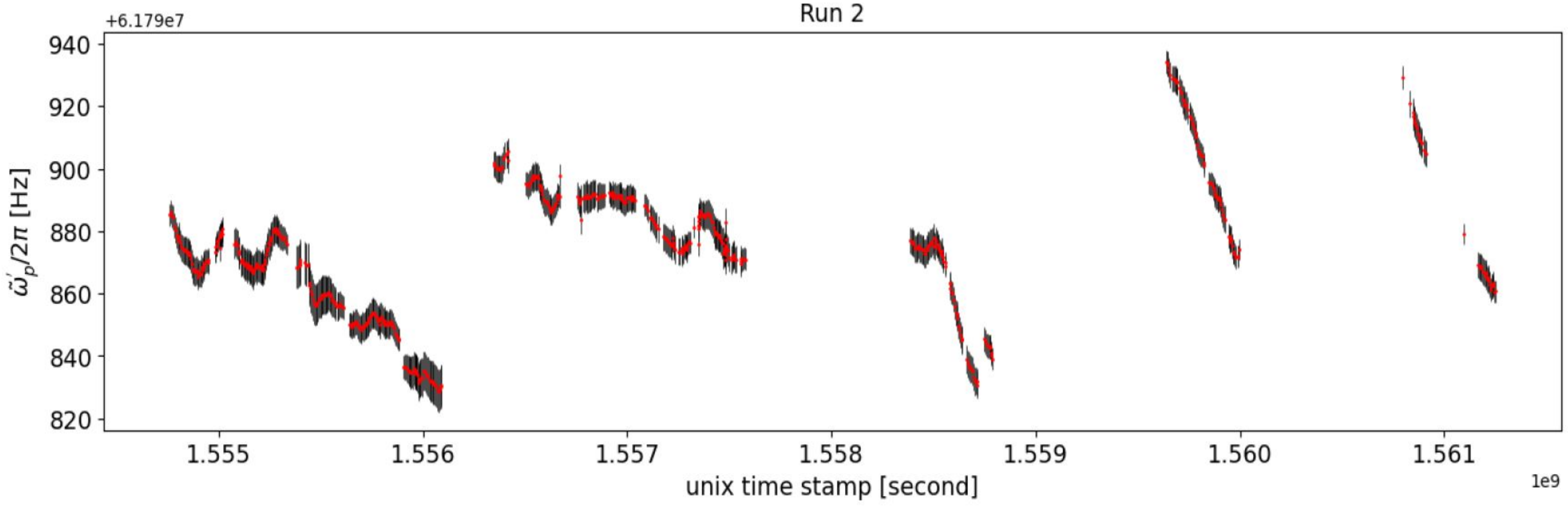

Determination of ω_a per run

- Preparation of per run wiggle plot:
  - Previous analyses: Threshold method (T)
    - Each positron above threshold equally weighted
  - Current Run 2/3 analysis: Asymmetry weighted method (A):
    - Each positron is weighted by asymmetry $A(E)$, which is a function of energy. More statistically powerful than T method.

- ω_a per run extraction : 5-parameter fit applied to per run wiggle plot.

- $N(t) = N_0 e^{-t/\tau_\mu} [1 + A\cos(\omega_a t + \phi_0)]$

ω_p

Determining ω_a per run

- Per run data suffers from poor statistics in late time bins.
- Traditional **Chi-square** fit method uses dynamic end time to cut off low statistic late time bins from the fit.
- Poisson statistics is excellent in handling low statistics. **Maximum Likelihood Estimator (MLE)** with Poisson statistics used.

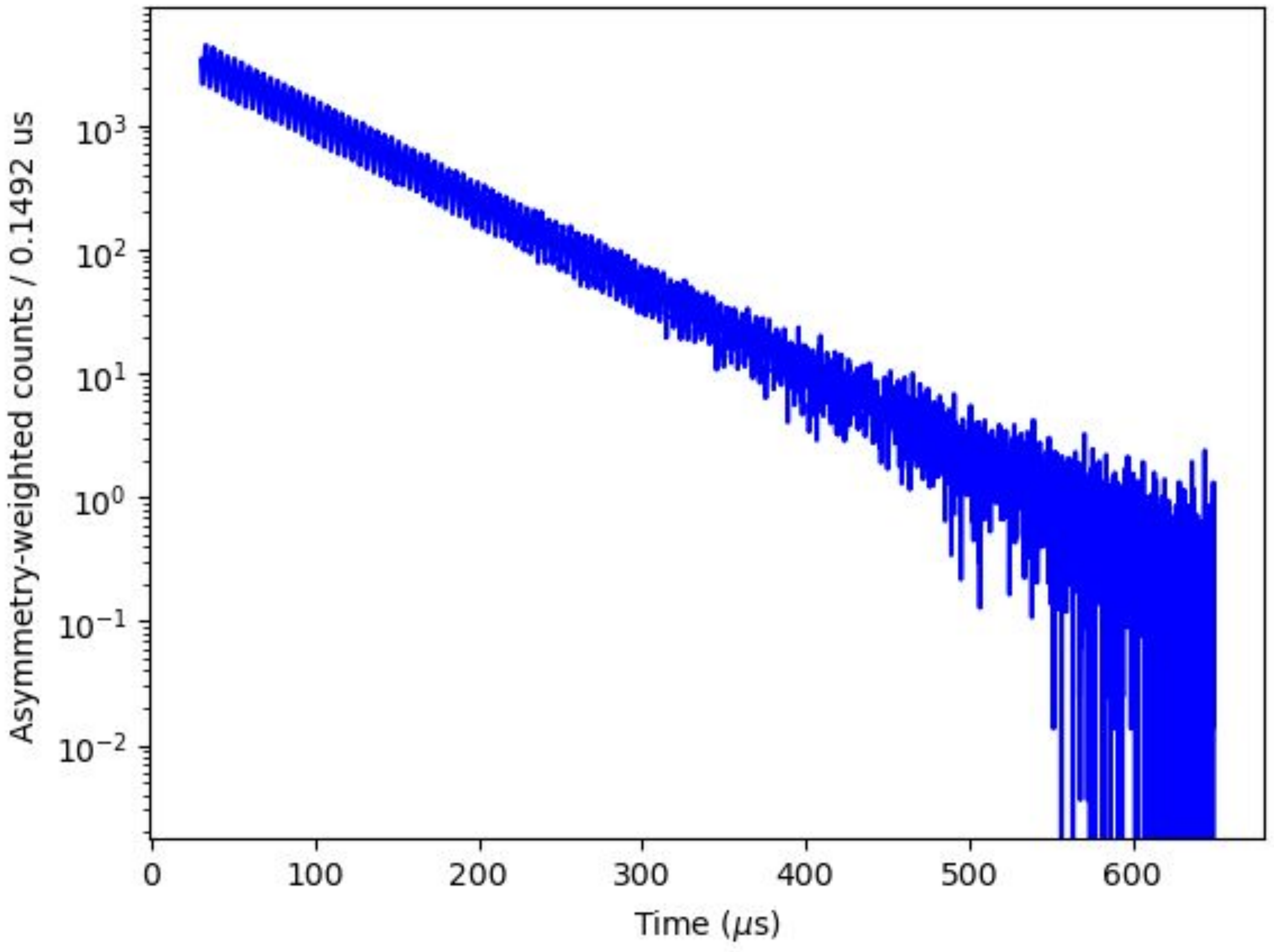

ω_p

Chi-square method and MLE method: Run 2

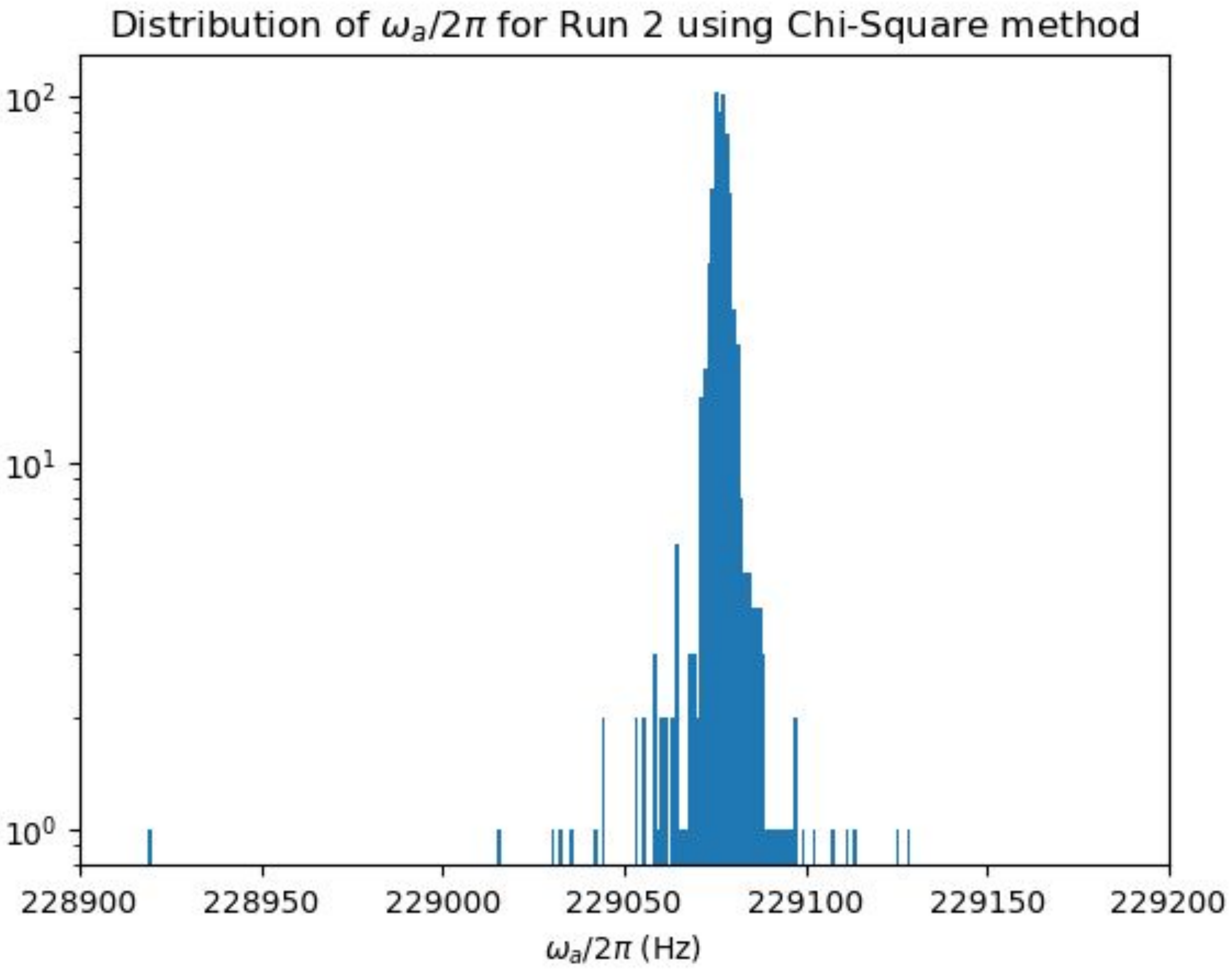

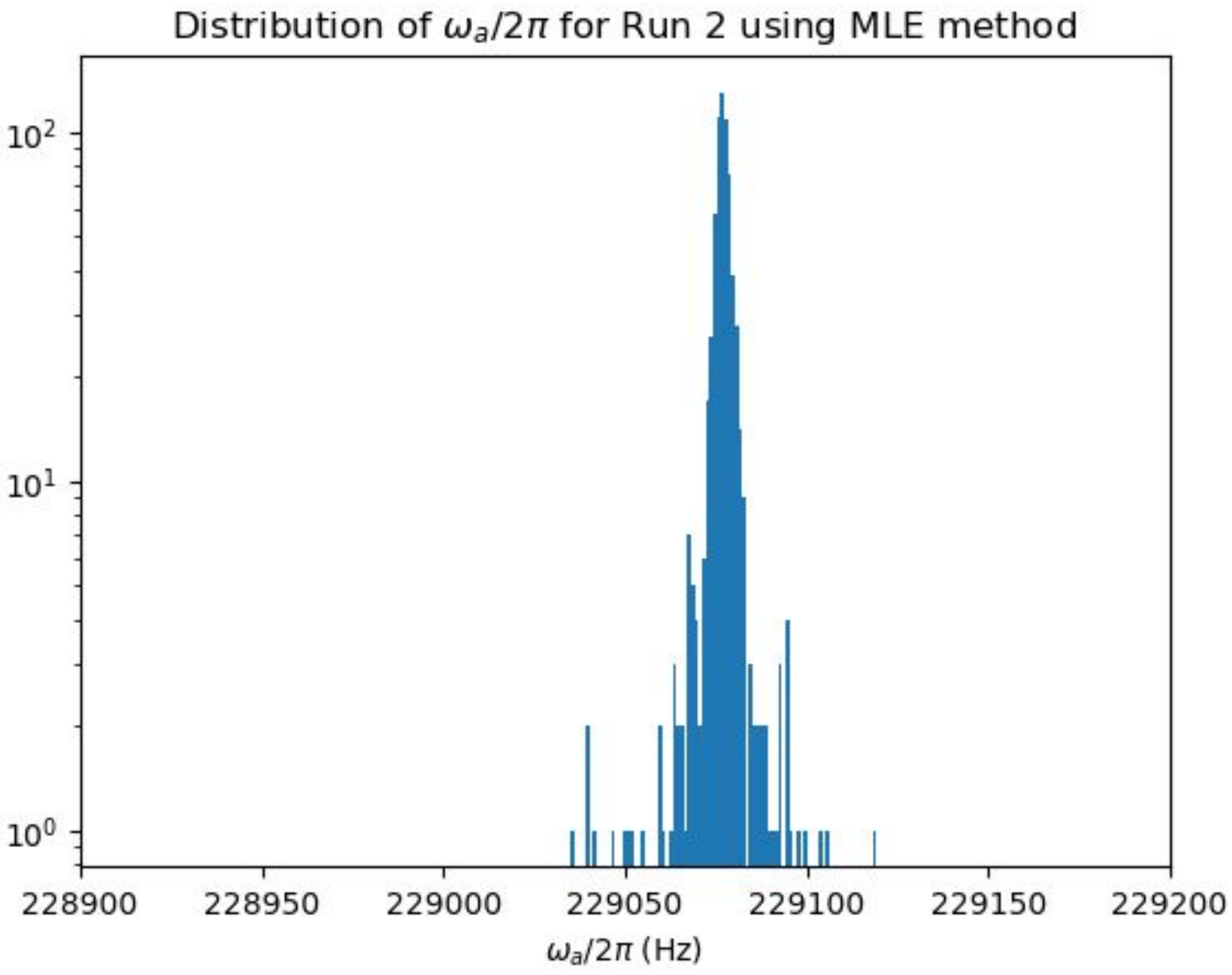

ω_p

Chi-square method and MLE method: Run 3a

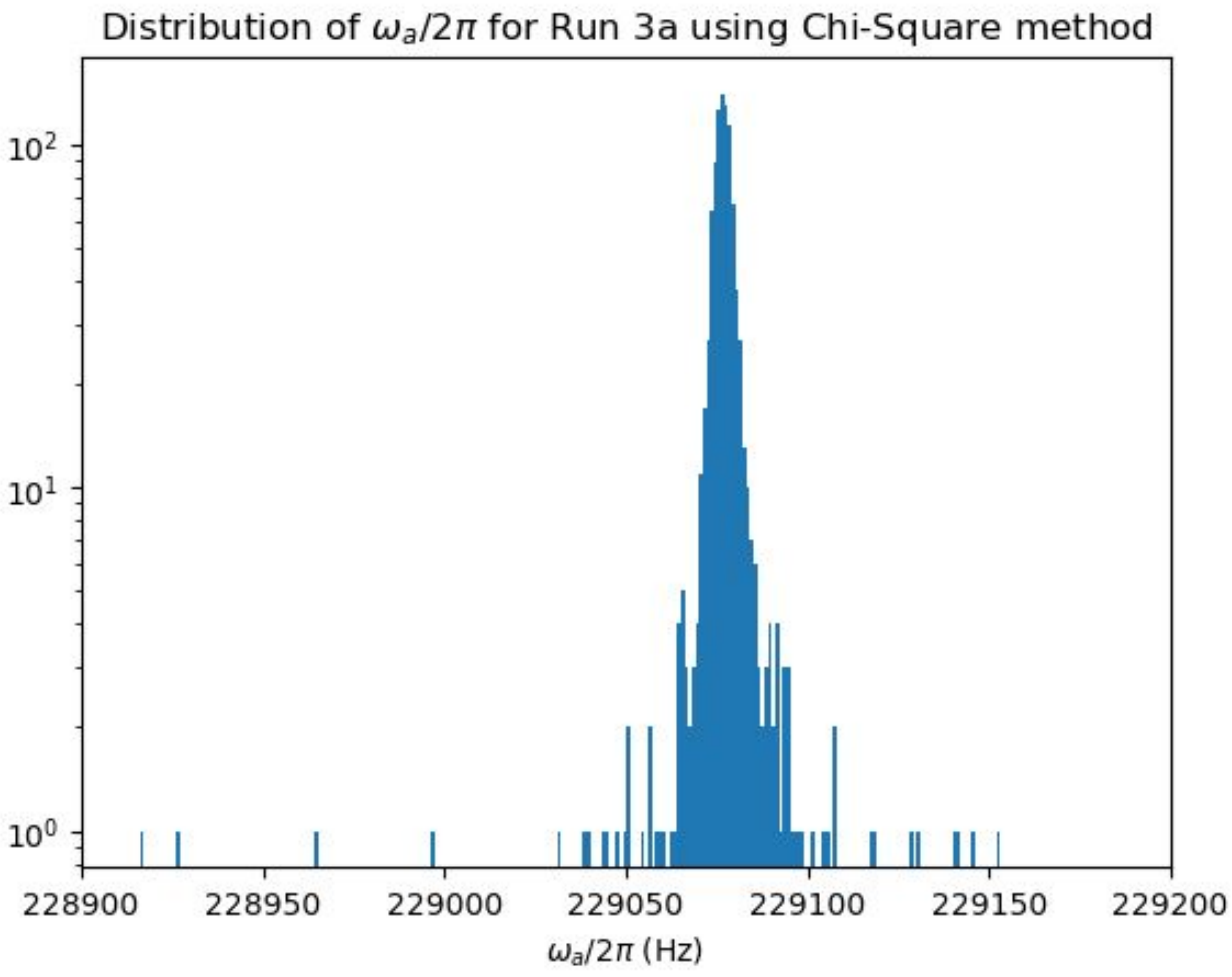

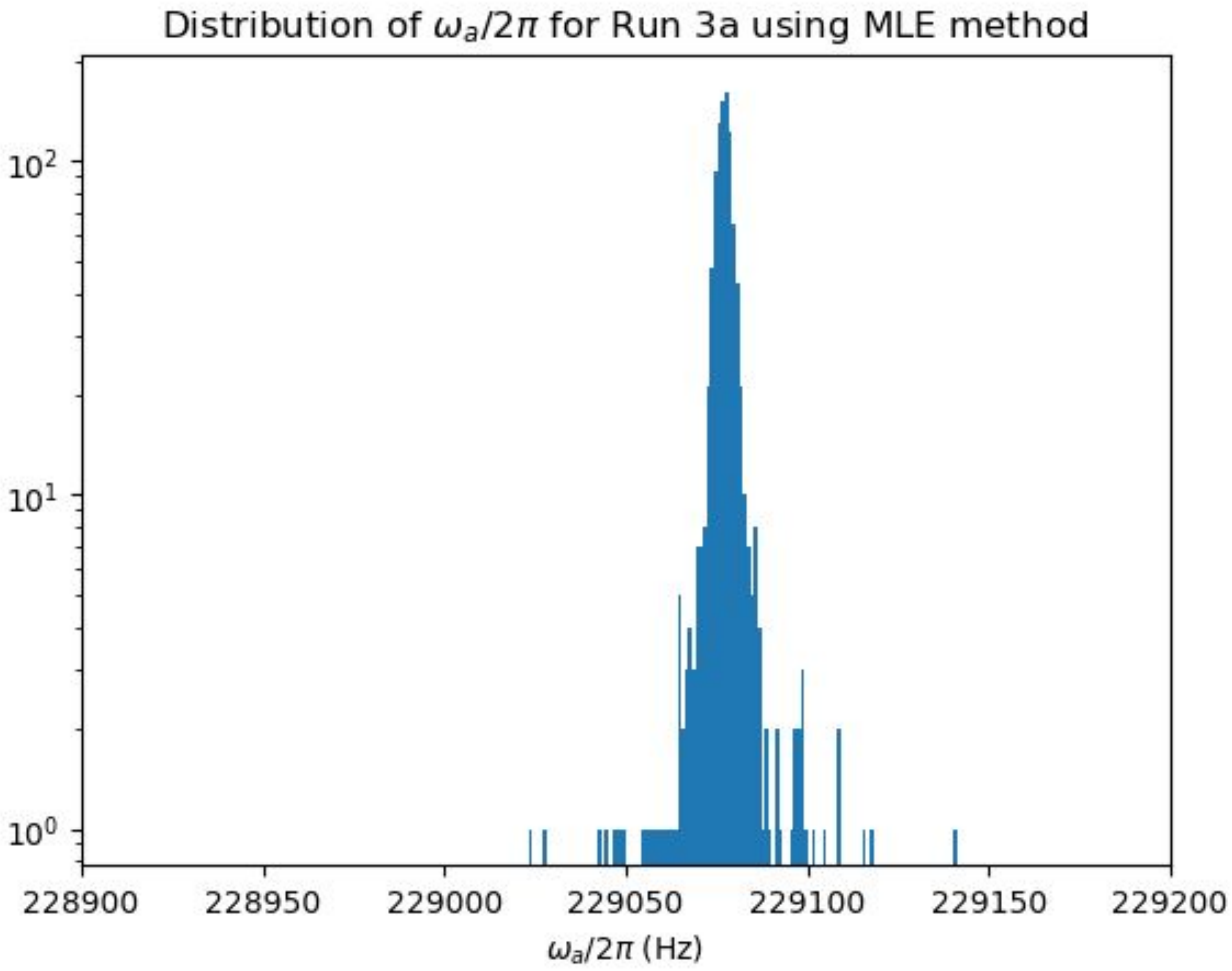

ω_p

Chi-square method and MLE method: Run 3b

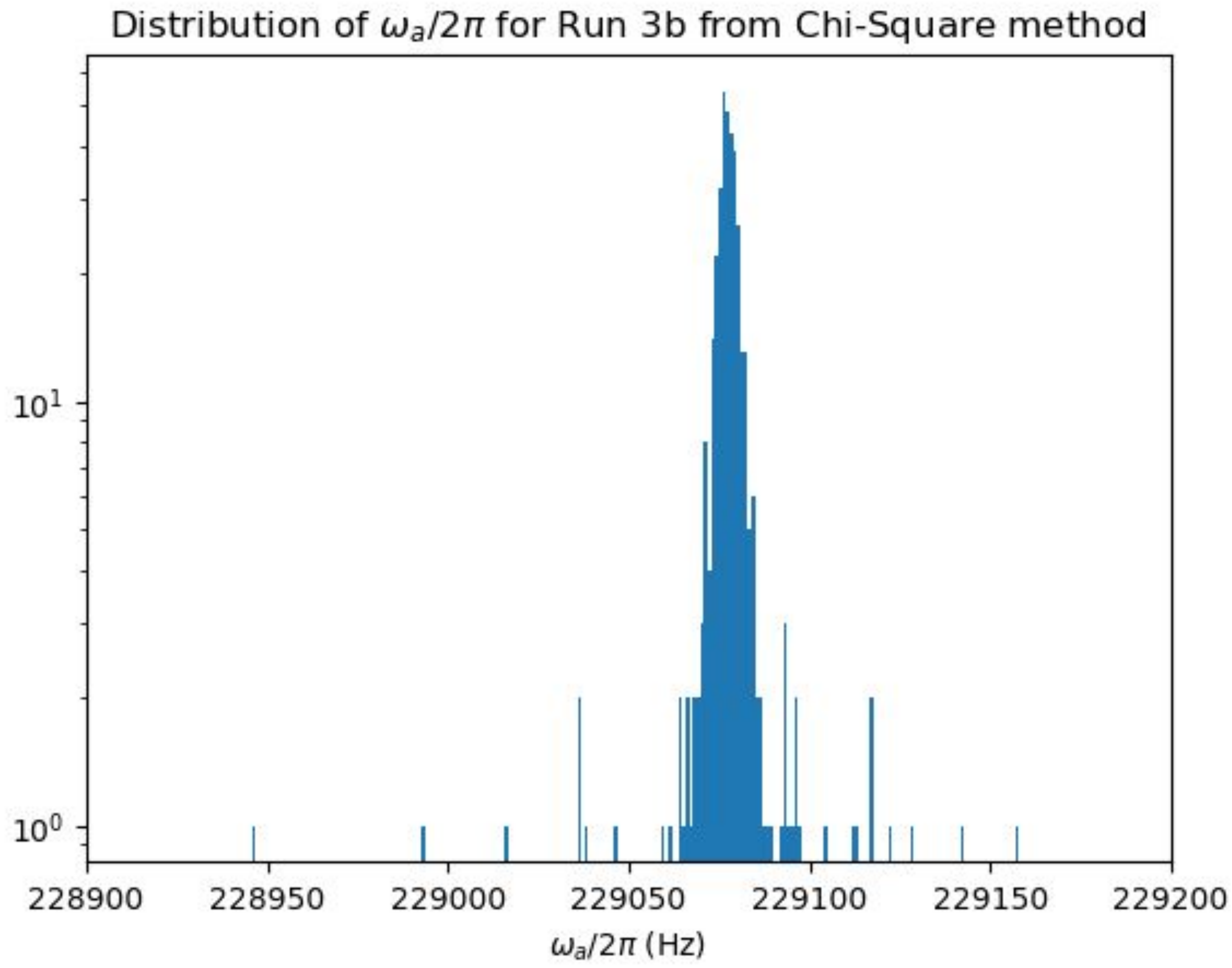

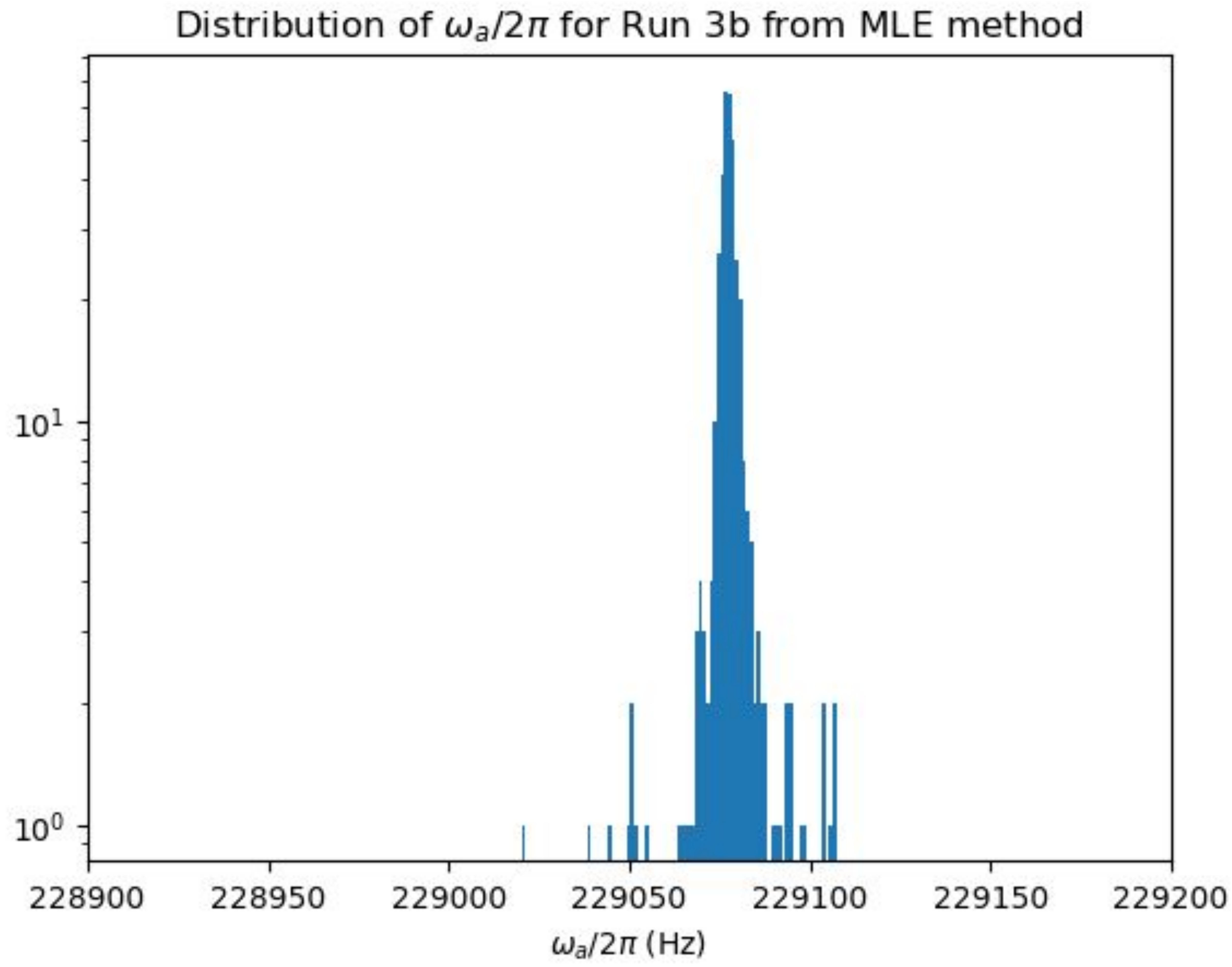

- ω_p
Comparison for Run 2

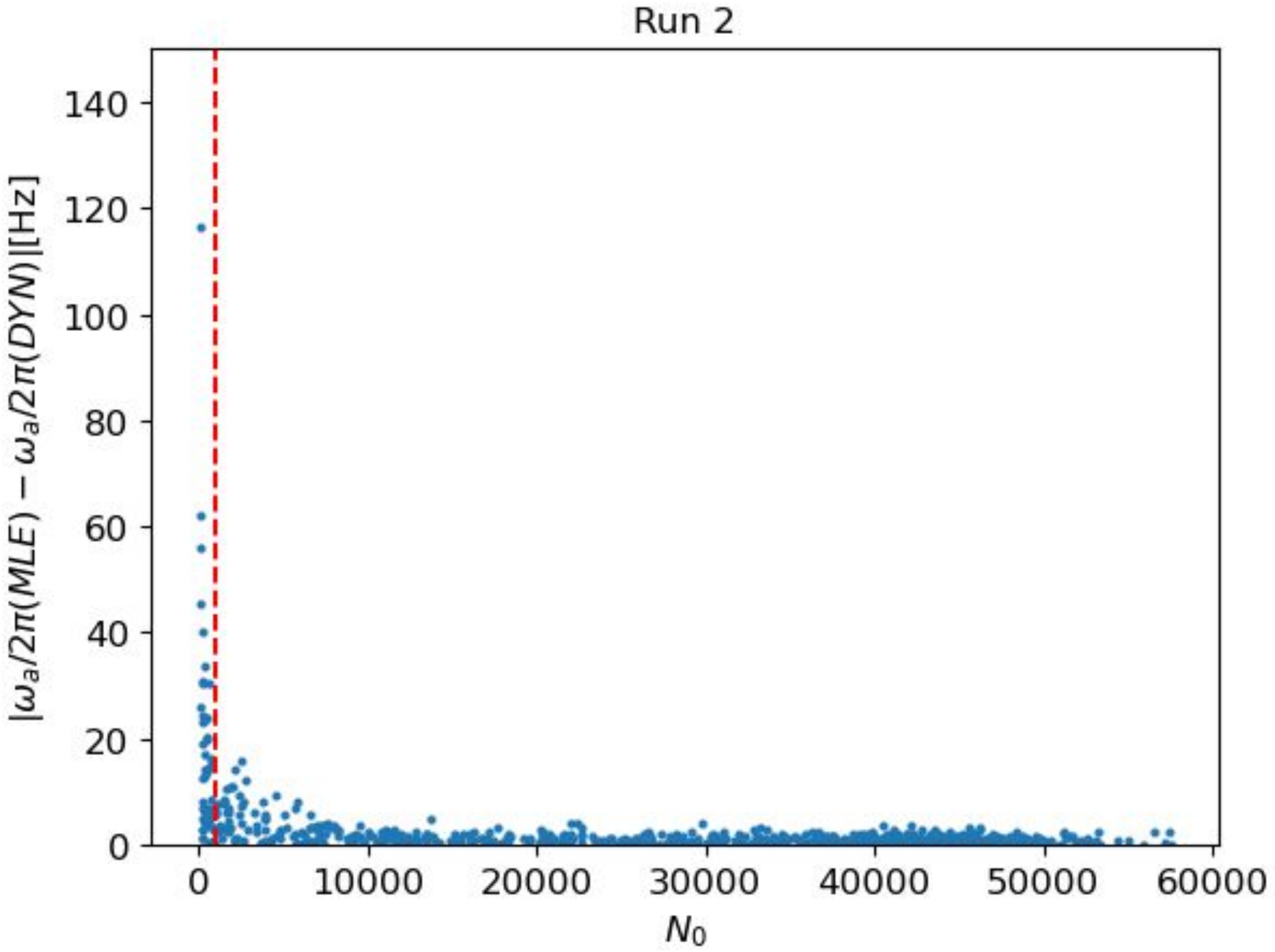

$|\omega_a/2\pi(\mathrm{MLE}) - \omega_a/2\pi(\mathrm{DYN})|$ vs N_0

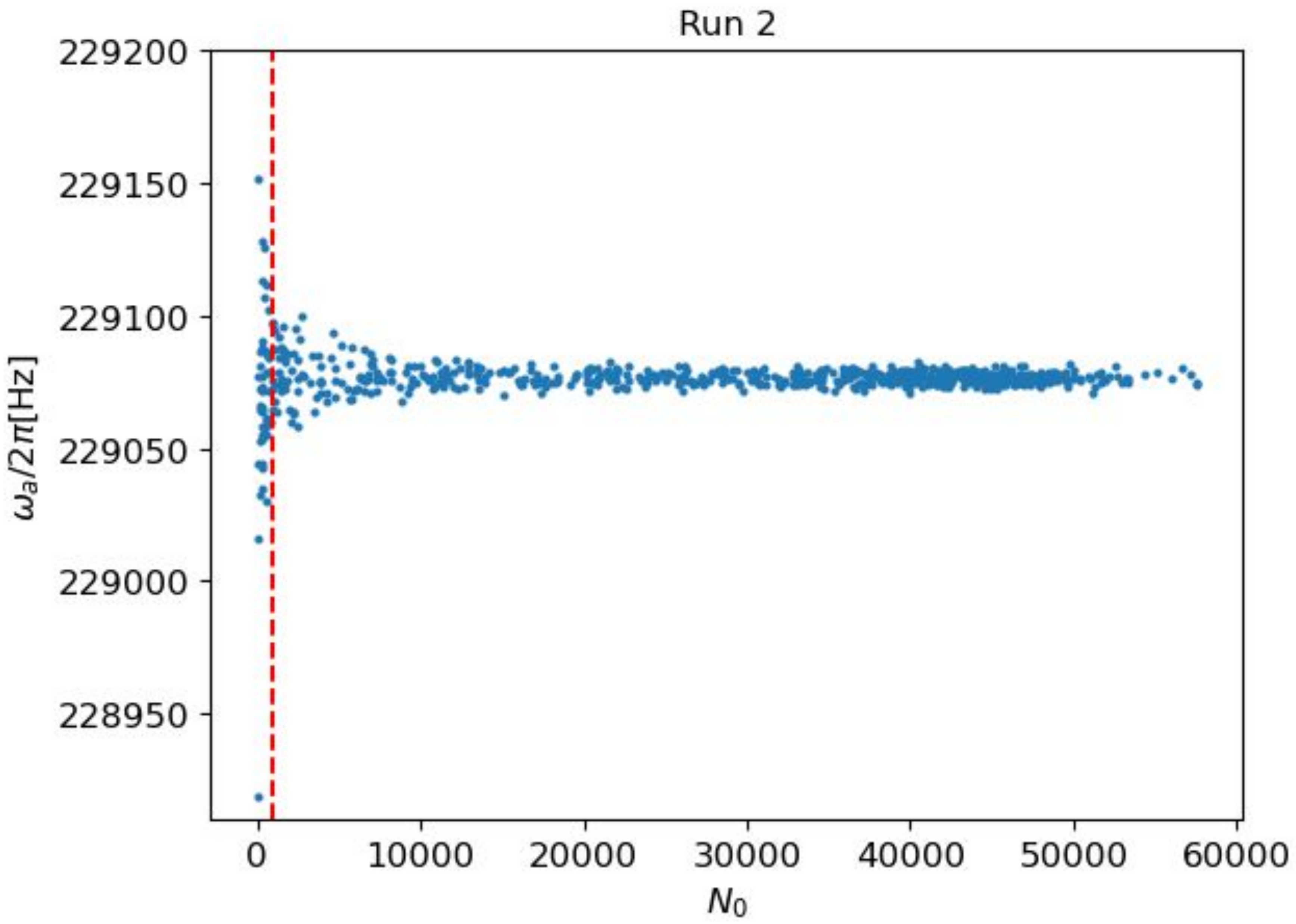

$\omega_a/2\pi$ vs N_0

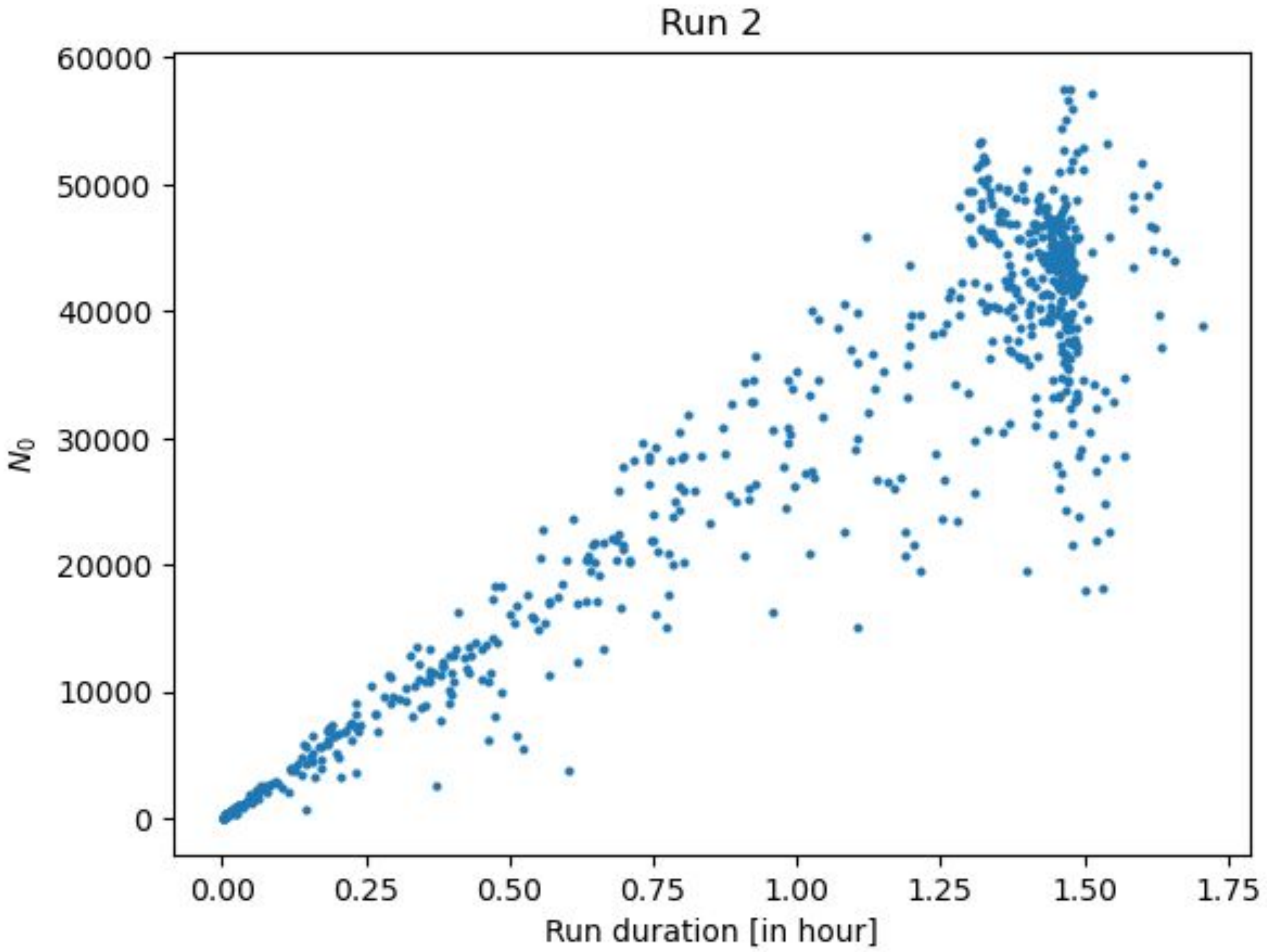

N_0 vs Run Duration

- Conclusion: Even after applying dynamic-fit end time, Chi-Square ω_a histogram has some outliers. The outlier runs have very small duration (~ minutes). Those runs excluded from the analysis.

Total run statistics used in CPTLV analysis

	Total no. of runs	Total no. of runs included in the analysis	% positrons excluded
Run 2	689	639	0.1
Run 3a	974	901	0.05
Run 3b	376	343	0.1

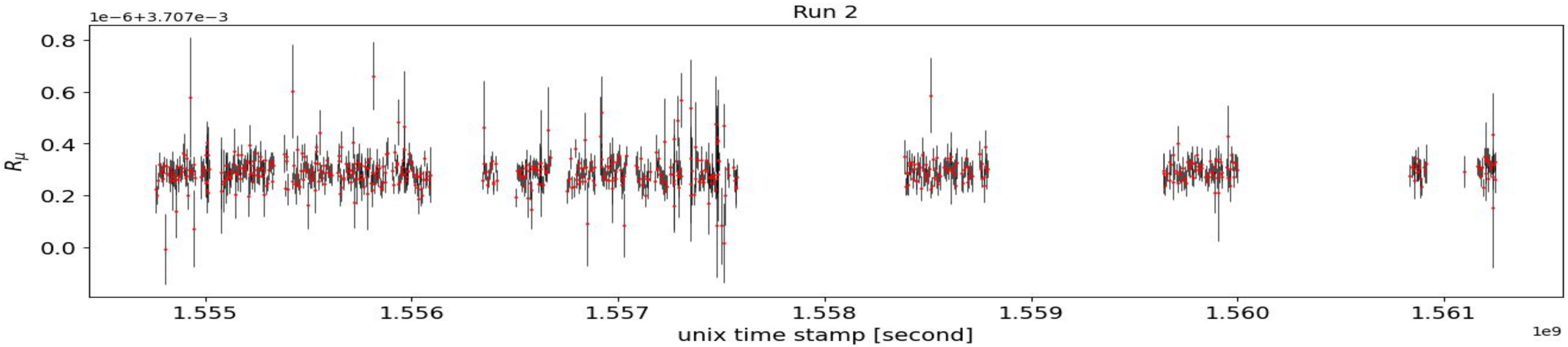

Extraction of oscillation amplitude from Run by Run x_μ: Using MPF

- Time domain extraction: Using Multi-Parameter fit (MPF)

- $R_\mu = C_0 + \frac{A}{\tilde{\omega}'_p} \sin(2\pi n f_s t + \varphi)$
  - C_0: Constant
  - A: oscillation amplitude
  - f_s: Sidereal frequency
  - n: Sidereal harmonic (1,2,3,4,5)

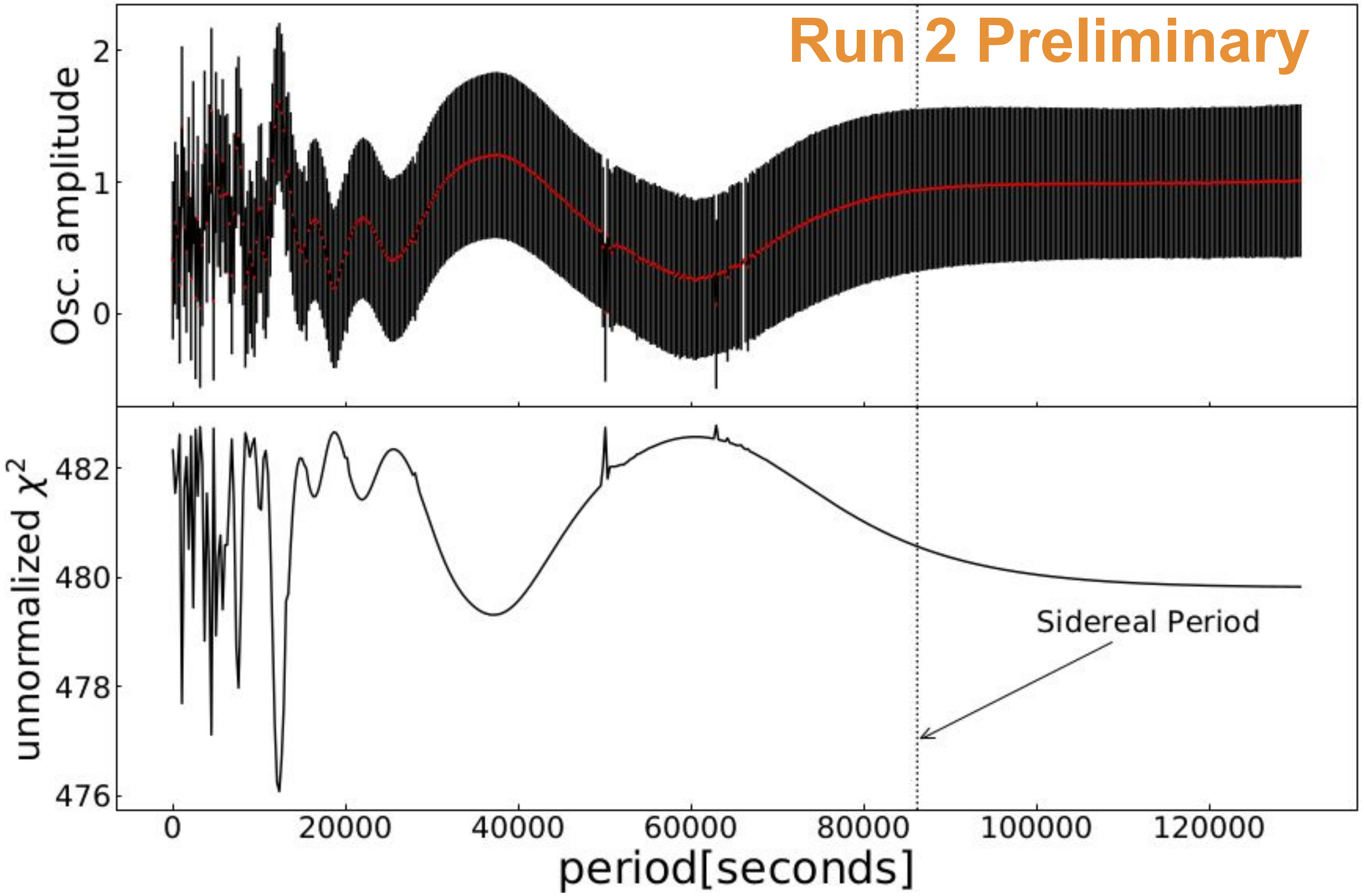

Extraction of oscillation amplitude from Run by Run χ_μ: Using GLS

- Frequency domain extraction: Using Generalized Lomb-Scargle periodogram method.
- Spectral analysis technique for unequally spaced data
- Time domain model: $g(t) = a\cos(2\pi f t) + b\sin(2\pi f t) + c$
- Minimization of χ^2 at frequency f to obtain minimum $\chi^2 = \widetilde{\chi^2}$
- Lomb Power at f: $P_S(f) = \frac{[\widetilde{\chi_0^2} - \widetilde{\chi^2}(f)]}{\widetilde{\chi_0^2}}$, where $\widetilde{\chi_0^2}$ is $\widetilde{\chi^2}$ for $g(t) = c$.

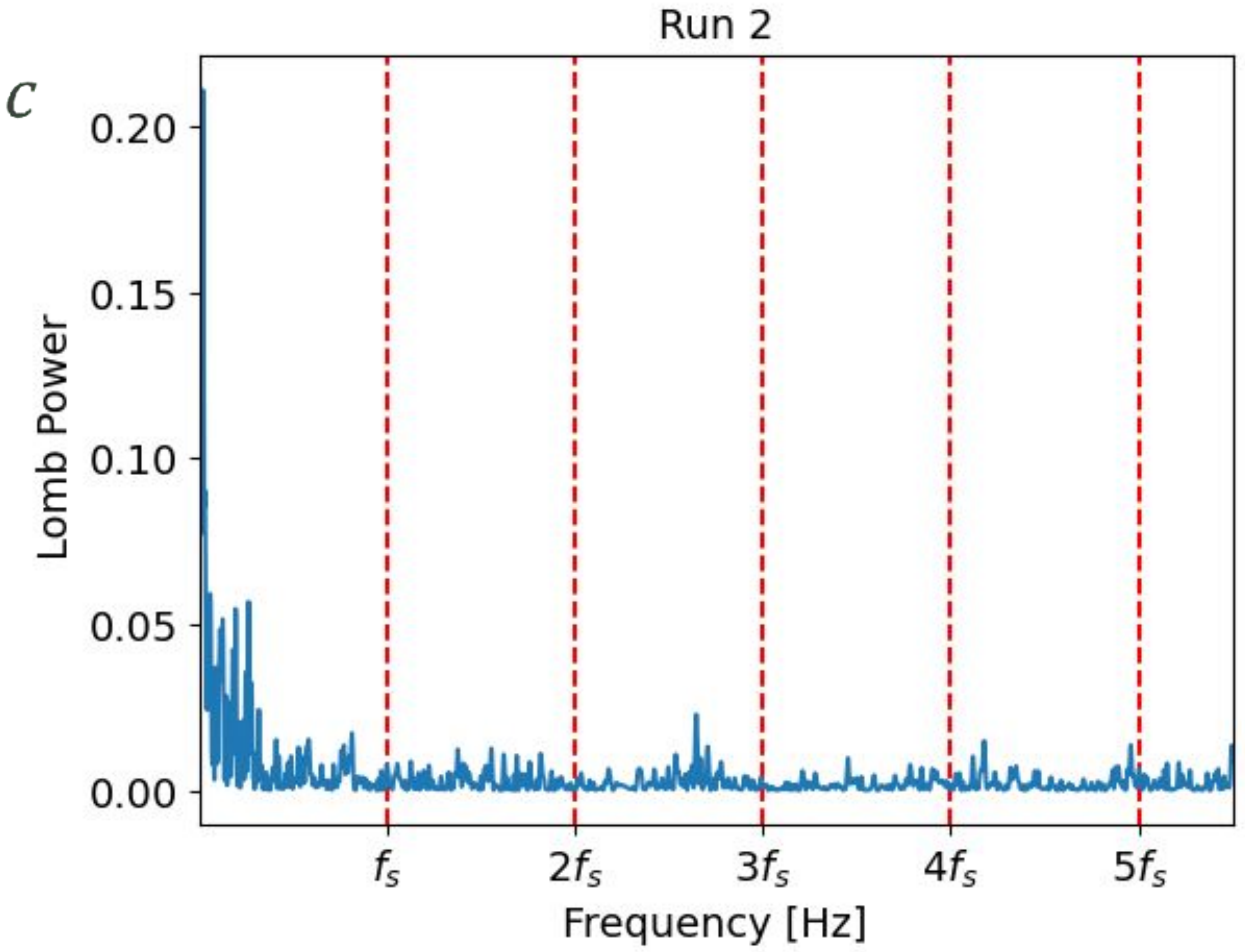

Bias Test for the Blinding procedure

- Blinding parameter: Injected amplitude $A_{blinded}$ (ppm) at sidereal frequency and harmonics. $0.5 \text{ ppm} \leq A_{blinded} \leq 5 \text{ ppm}$.

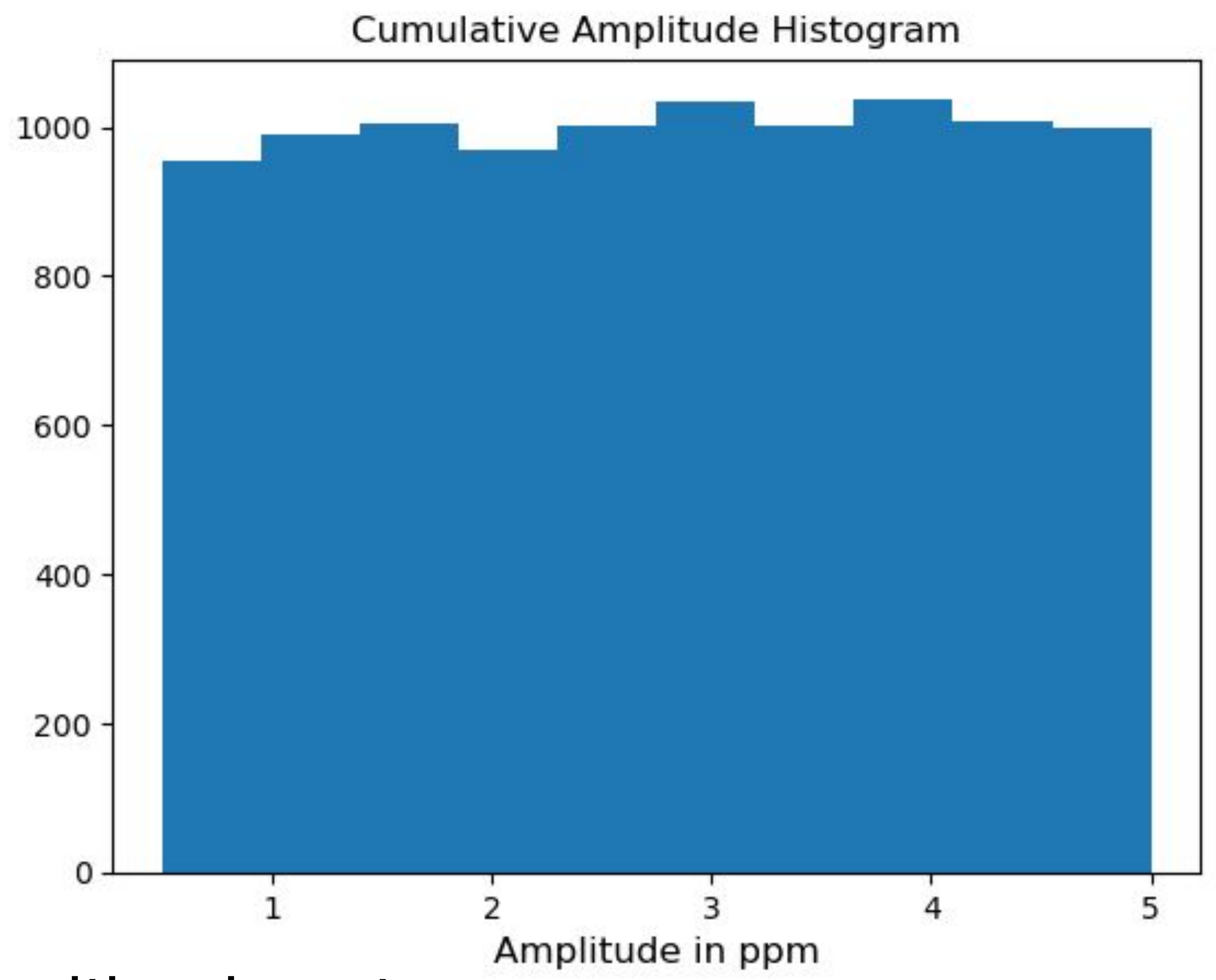

- Conclusion: Blinding algorithm is not biased.

Systematic Uncertainties

Magnetic Field related systematics

Detector gain calibration related systematics

Beam dynamics related systematics

Magnetic Field related systematics

- Search for any potential signal in $\widetilde{\omega_p'}$ at the sidereal frequency and its harmonics.
  - Set a limit on the oscillation amplitude of $\widetilde{\omega_p'}$ at the sidereal frequency and its harmonics.

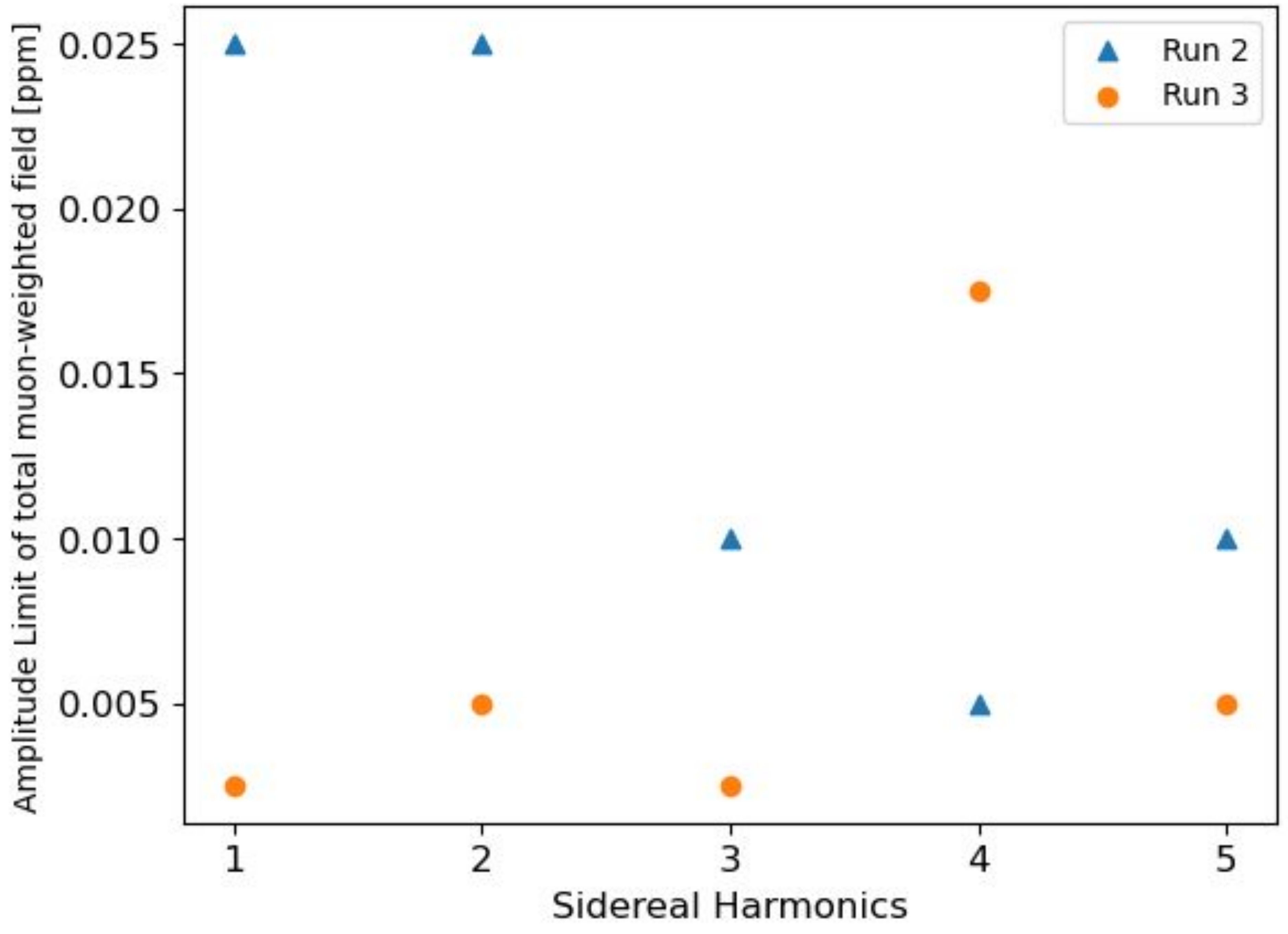

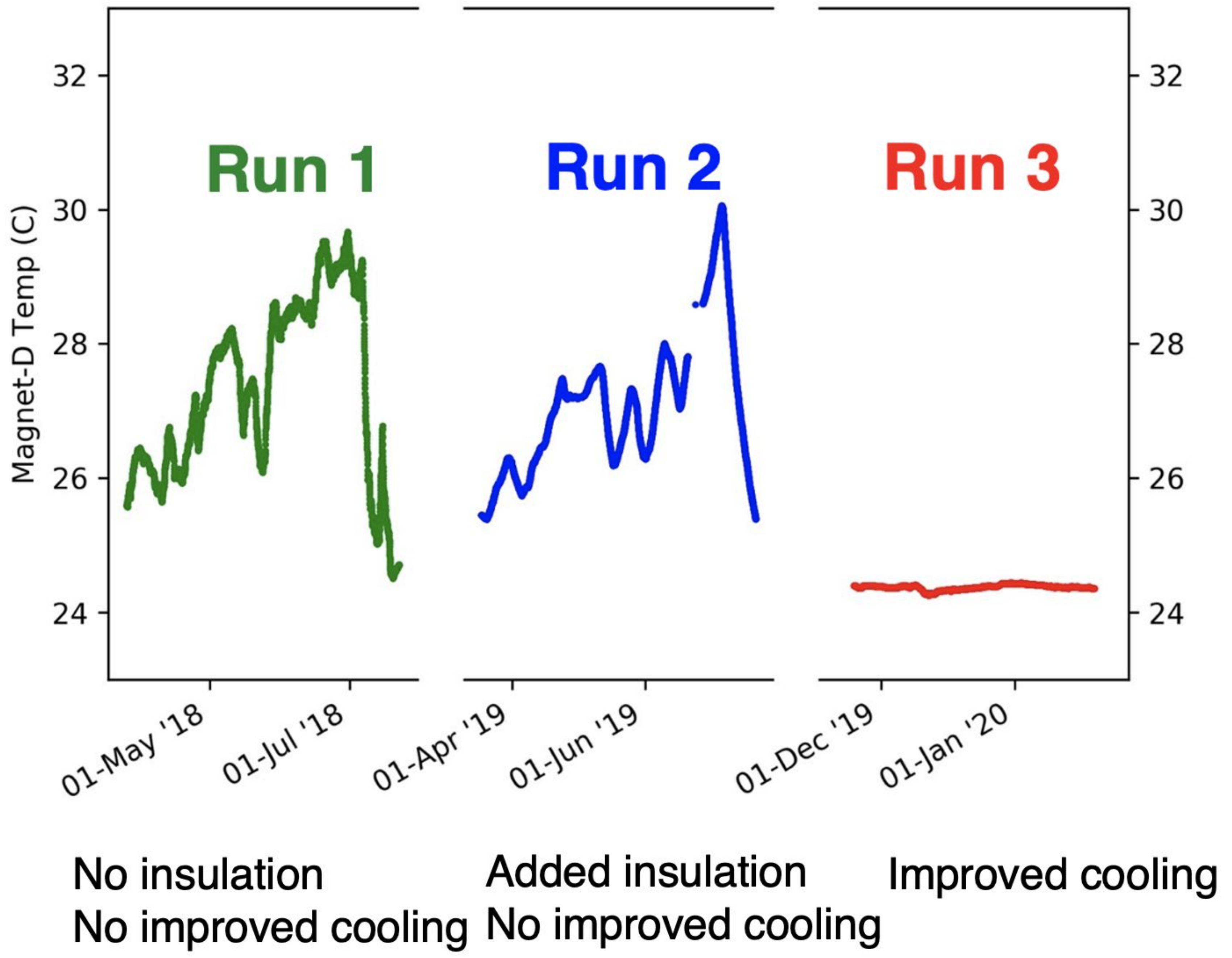

- For most of the harmonics, magnetic field oscillation amplitude is larger in Run 2 than in Run 3. It is expected because of improved hall cooling in Run 3.
- The maximum oscillation amplitude is 0.025 ppm that is less than sensitivity limit 0.5 ppm

Magnetic Field related systematics: Spectral analysis

- Generalized Lomb Scargle Periodogram (GLS): Spectral analysis technique to analyze non-uniformly spaced time series data. Spectral power or Lomb power is normalized. Maximum Lomb Power = 1.

The red dotted lines indicate sidereal frequency and its harmonics.

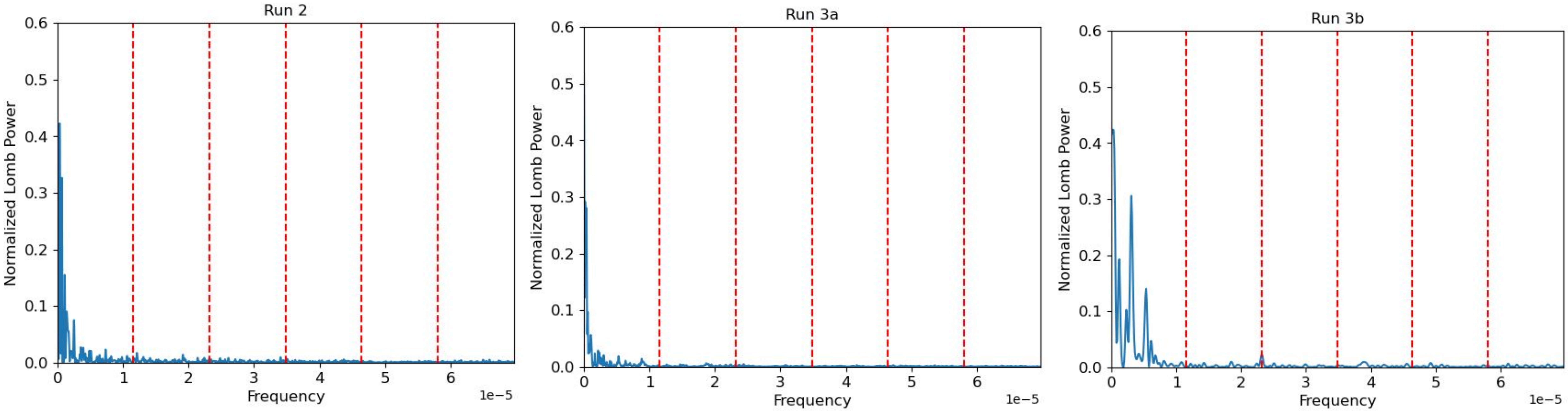

- Conclusion: Spectral analysis of $\widetilde{\omega_p'}$ vs time data shows no significant peak .

Detector gain calibration related systematics

- Gain: The ratio of a positron detectors (calorimeters) output to its input.
- Calorimeters: A positron of a certain energy generates an output signal of a certain size in the SiPM sensors.
- The output of SiPM sensors is converted to energy units by calibration procedures.
- Ideally, this ratio should remain constant in time so that the calibration remains accurate.
- The gain of the calorimeters can vary due to temperature variation.
- Long term effects (~ hours) are important for CPTLV: Out-of-fill (OOF) gain correction. This

Detector gain calibration related systematics: OOF gain correction

The red dotted lines indicate sidereal frequency and its harmonics.

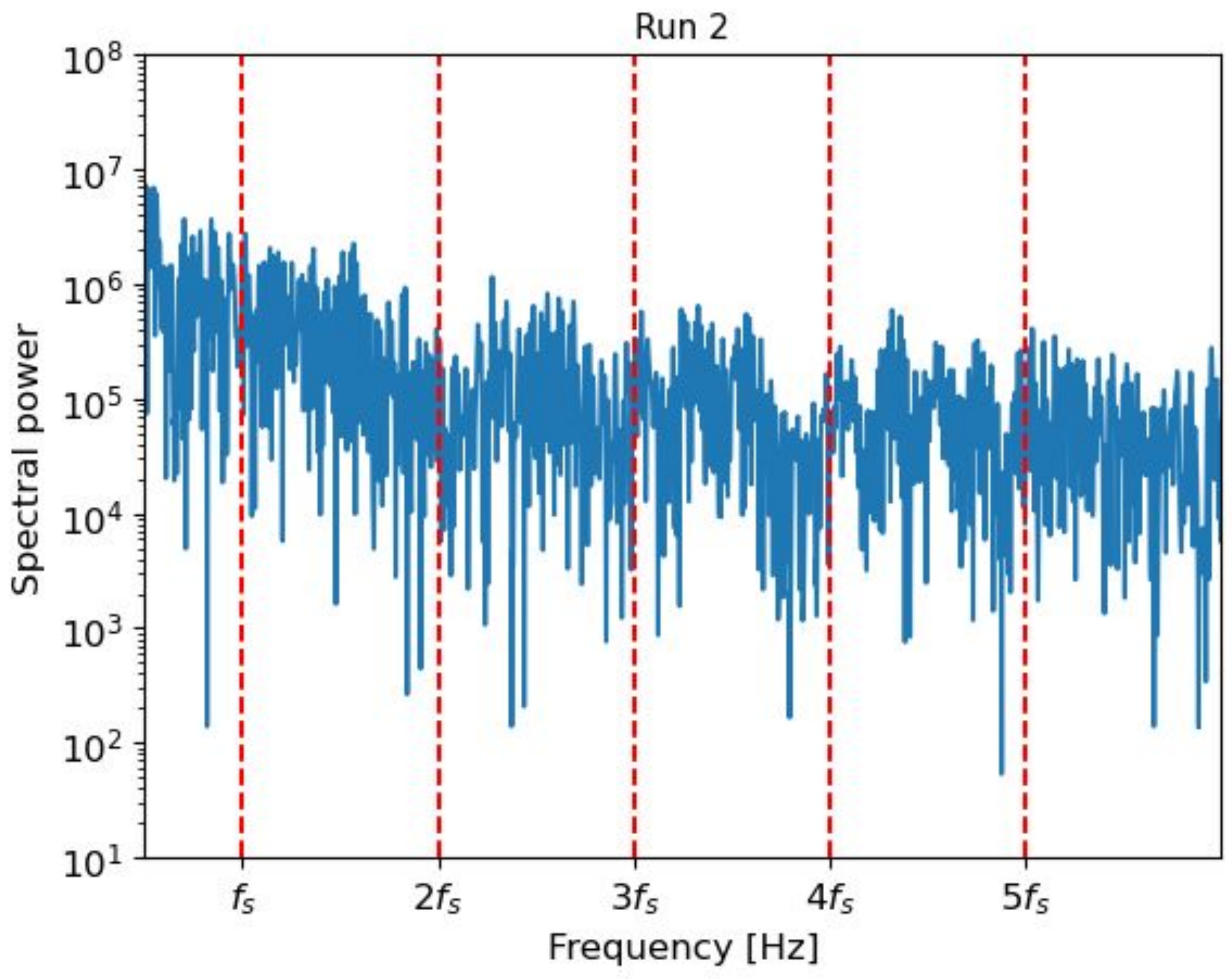

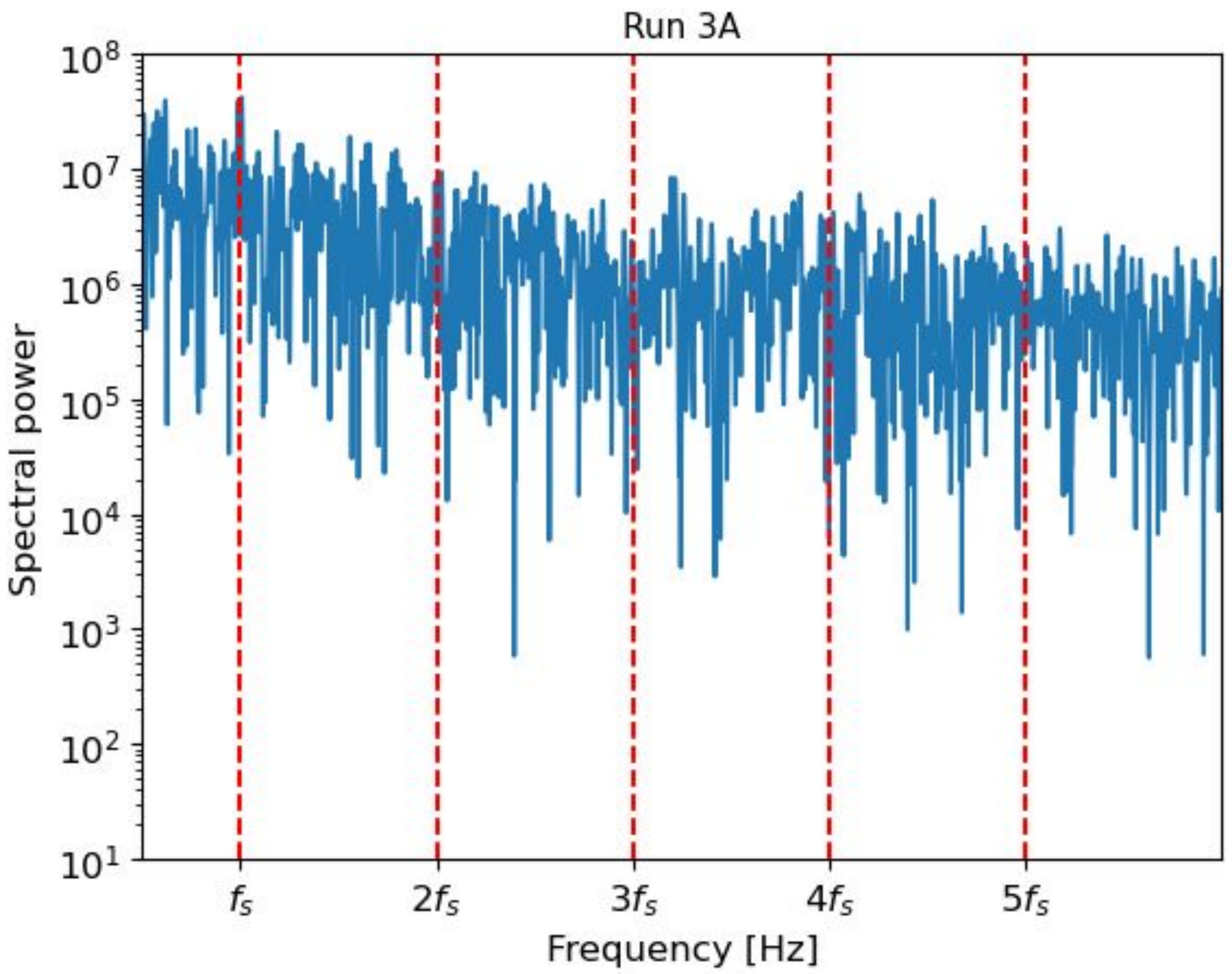

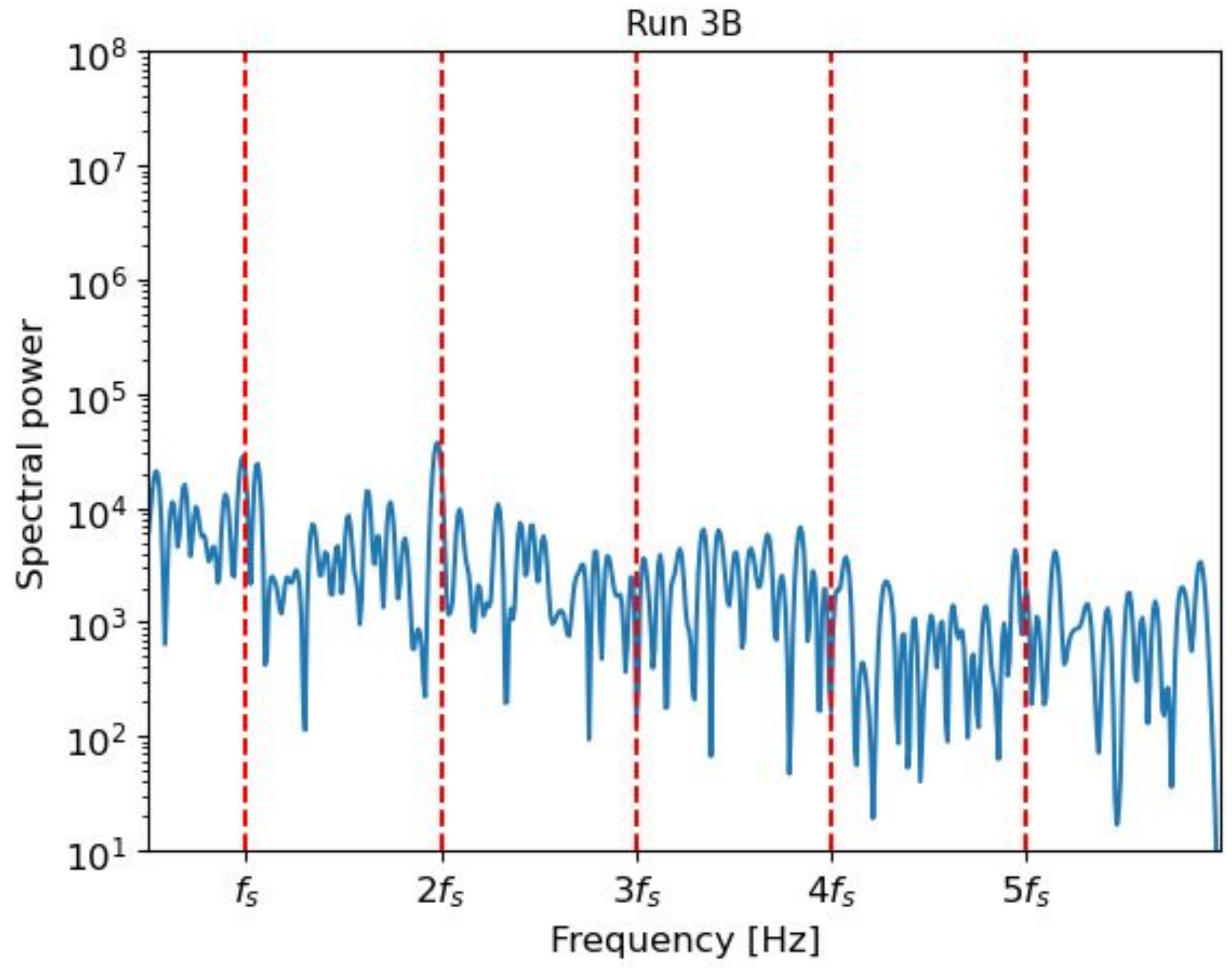

- Conclusion: The Spectral analysis of OOF gain correction vs time shows no distinct peak. Therefore, this systematics does not have an effect on CPTLV analysis

Beam dynamics related systematic uncertainties: Study of Run-by-Run CBO parameter

For combined Run 2+ Run 3a+ Run 3b dataset

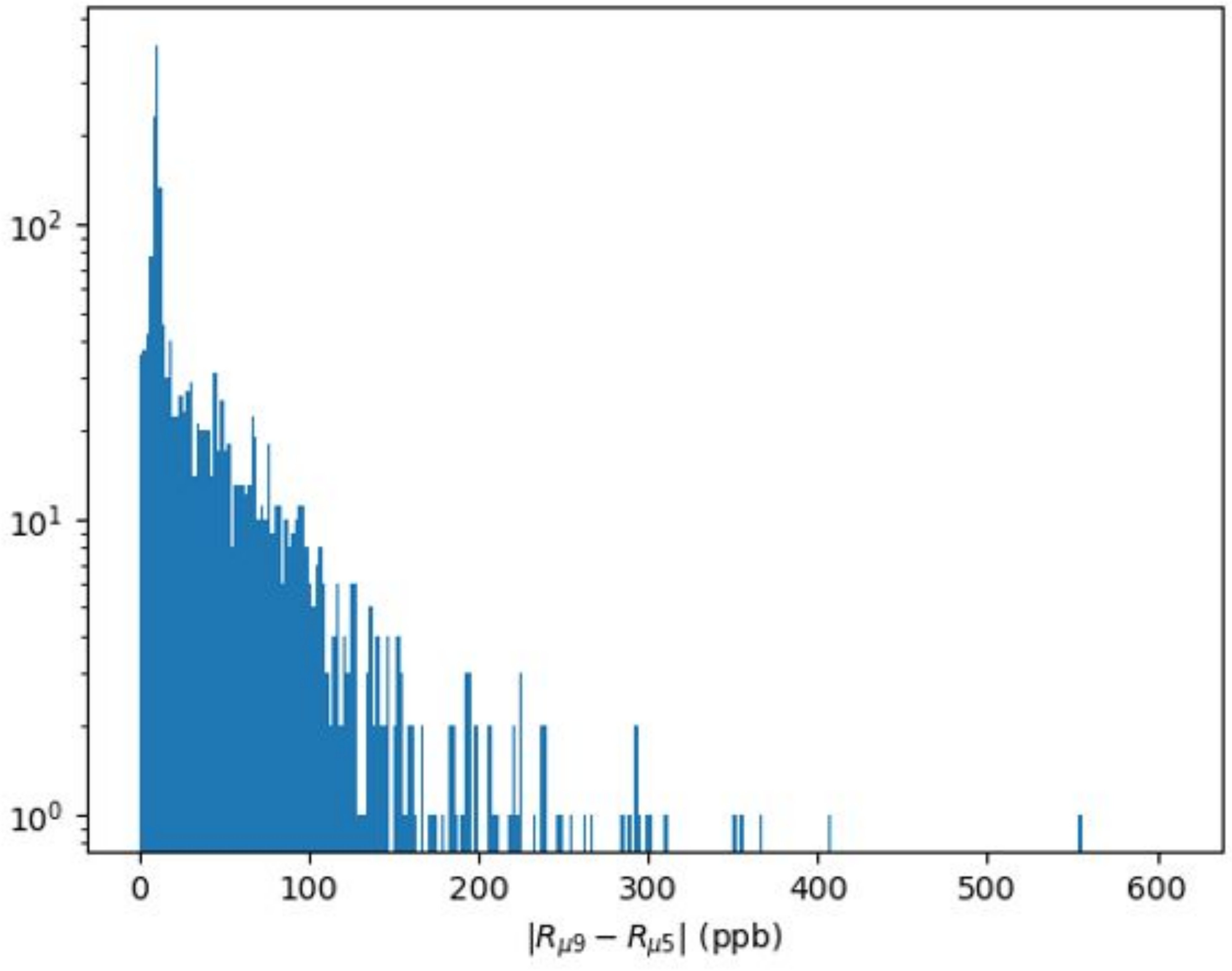

- Conclusion: Distribution of difference in R_μ from 5-parameter fit and 9-parameter fit (including CBO parameters) is clustered between 0-300 ppb, below sensitivity limit.

Beam dynamics related systematic uncertainties:
Study of Run-by-Run Electric Field Correction: C_e

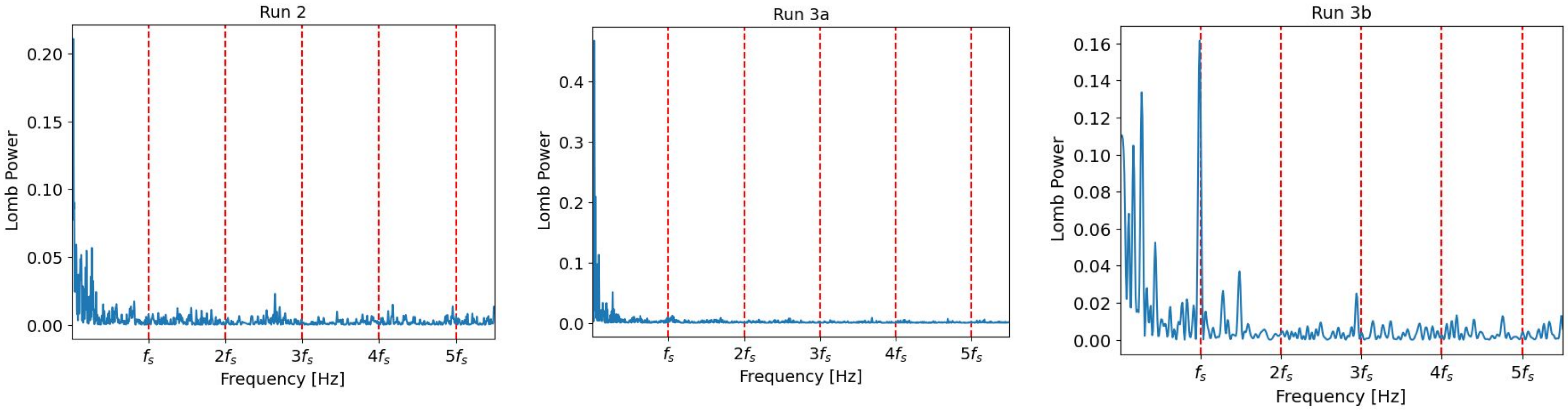

- Conclusion: Only Run 3b has a distinct peak at sidereal frequency. Amplitude of oscillation corresponding to this peak is 11 ppb, below the sensitivity limit.

Study of Run-by-Run Pitch Correction: C_p

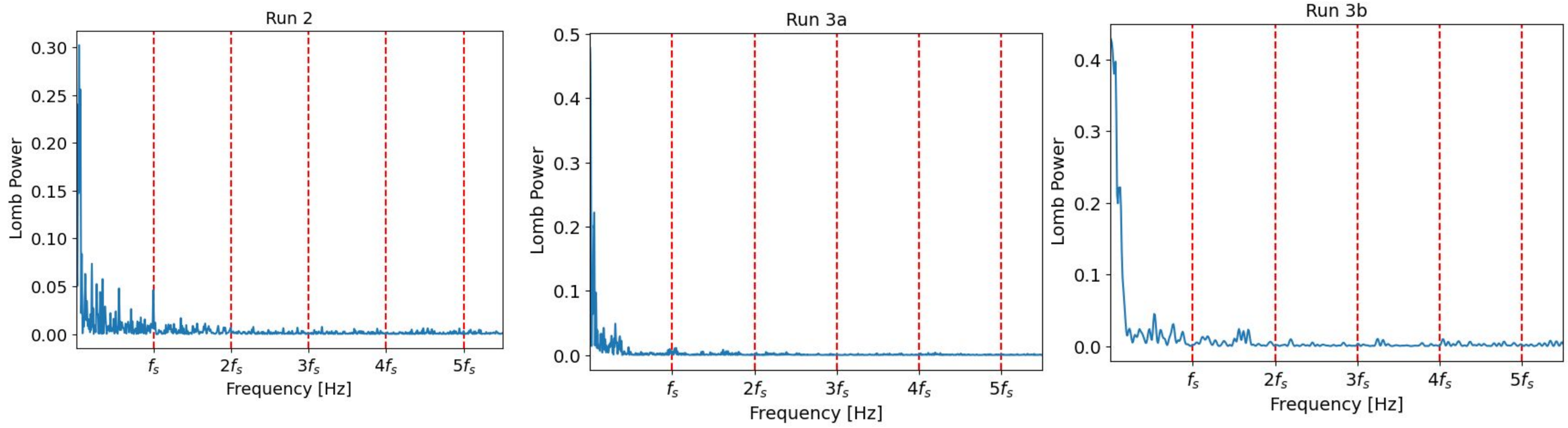

- Conclusion: Only Run 2 has a distinct peak at sidereal frequency. Amplitude of oscillation corresponding to this peak is 0.45 ppb, below the sensitivity limit.

Results

- CPTLV analysis is not yet unblinded for the entire Run 2 and Run 3 dataset.
- The new analysis model has been tested on the preliminary Run 2 dataset. Features of the new analysis framework:
    - Asymmetry-weighted method is used to extract ω_a data, instead of Threshold method.
    - A detailed systematic study is performed which includes gain related, and beam dynamics related systematics along with the magnetic field related systematics.
    - Generalized Lomb-Scargle method is used for the spectral analysis.

Results: Preliminary Run 2

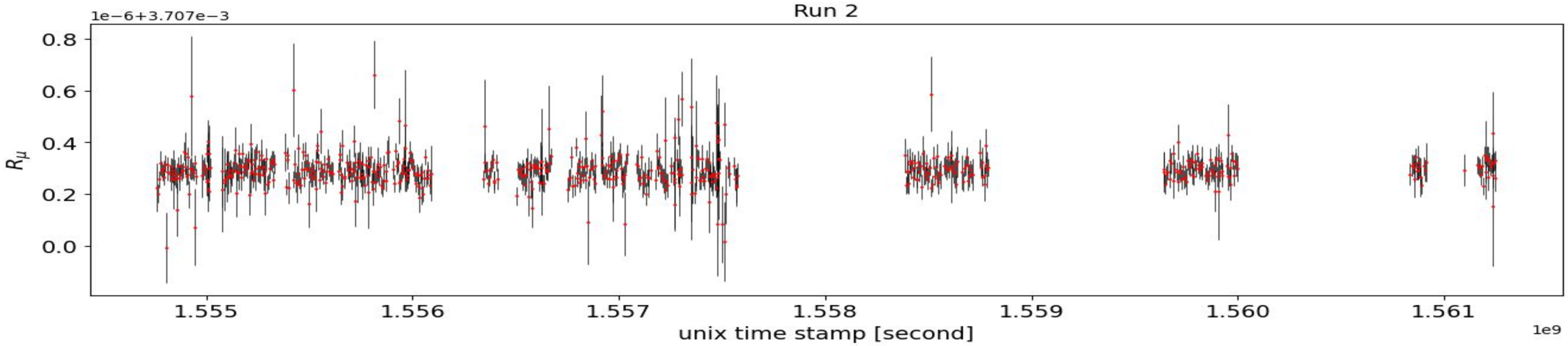

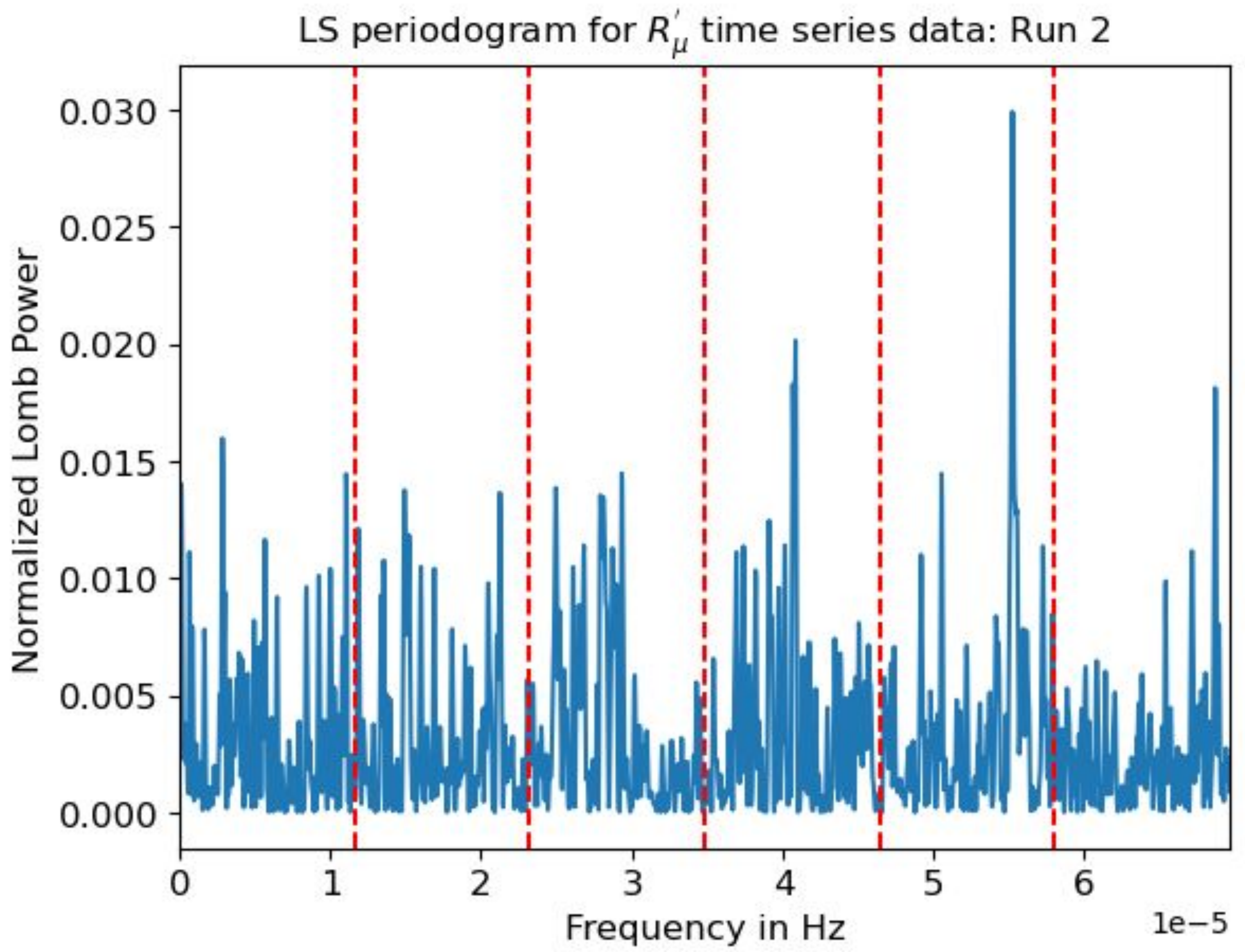

Results: Preliminary Run 2

- 10,000 MC datasets generated with 1.74 ppm sinusoidal signal injected at sidereal frequency. Distribution of Lomb Power at sidereal frequency is plotted for those 10,000 MC datasets.

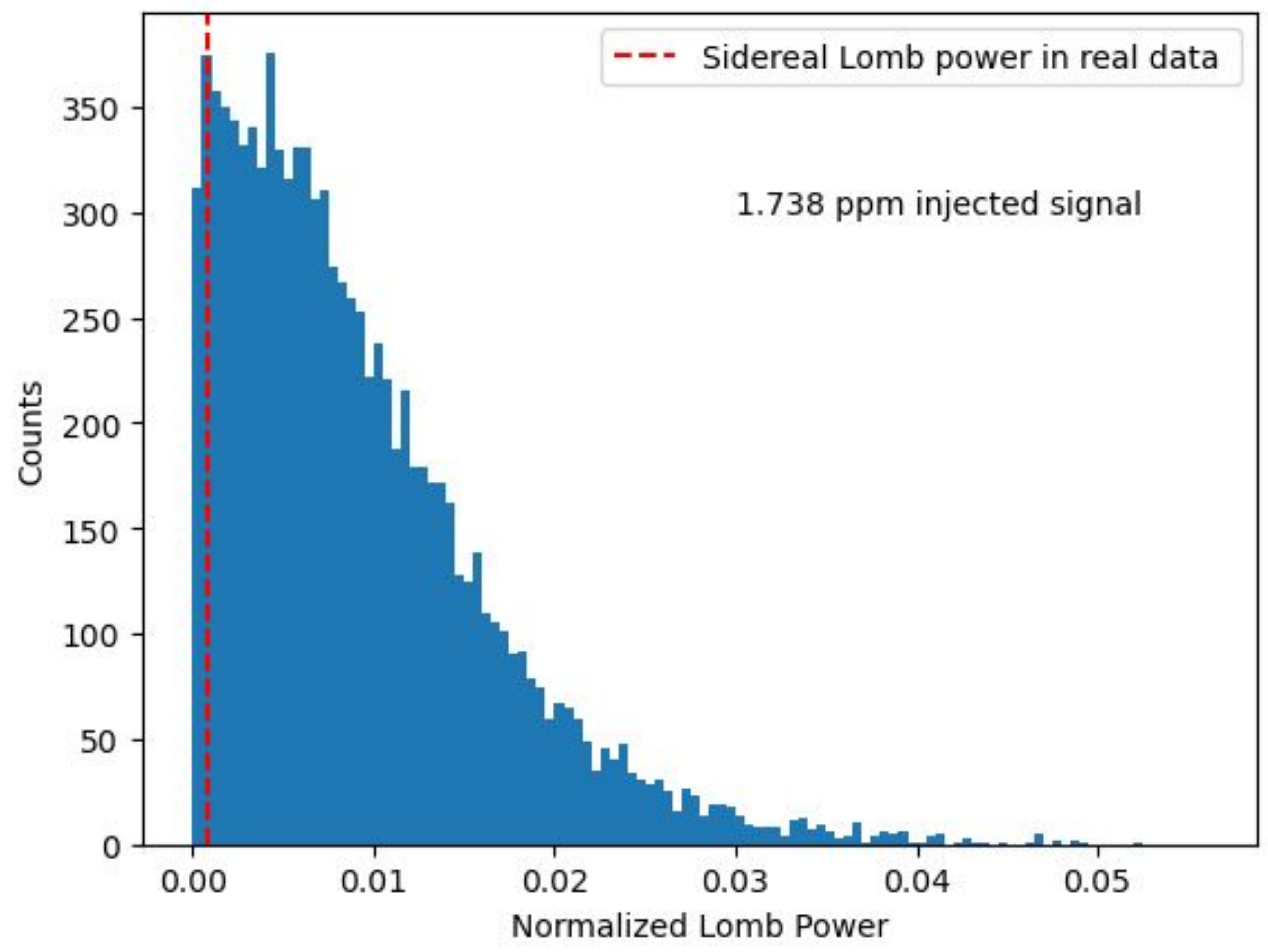

- The red dotted line indicates the Normalized Lomb power at the sidereal frequency in the real Run 2 dataset. Total bin count above the red dotted line is 9502, which indicates confidence level of 95.02%.

Results: Preliminary Run 2

- Sidereal oscillation amplitude at sidereal frequency:

  $$A_1^+ < 1.74\ \mathrm{ppm},\ b_T^{\mu^+} \leq 1.10 \times 10^{-24}\ \mathrm{GeV}$$

  - Previous T-method analysis on Preliminary Run 2 data:
    $A_1^+ < 2.0\ \mathrm{ppm},\ b_T^{\mu^+} \leq 1.3 \times 10^{-24}\ \mathrm{GeV}$

  - Sensitivity has increased due to use of the Asymmetry-weighted method.

- With Run 2 and Run 3 unblinded data, sensitivity limit should subceed $\mathbf{1 \times 10^{-24}\ GeV}$

- With Runs 4-6, sensitivity will improve by about another factor of 2

Prospects: Sidereal Measurement

- Muon g-2 is an extremely sensitive laboratory to test SM / search for ***(and possibly identify!)*** BSM physics.
- Previous studies indicate that sensitivity roughly scales with ω_a uncertainty.
  - E989 uncertainty aiming for x4 improvement compared to BNL E821.
- E989 sensitivity to sidereal variation should be at $\sim 5 \times 10^{-25}$ **GeV** level.
- Performing **first-ever** search for CPTLV at **sidereal harmonic frequencies**
- **First-ever** search for **annual variation**
  - Not done in E821 because 3-month runs were always at the same time of year.
  - E989 data covers ~10 calendar months out of the year

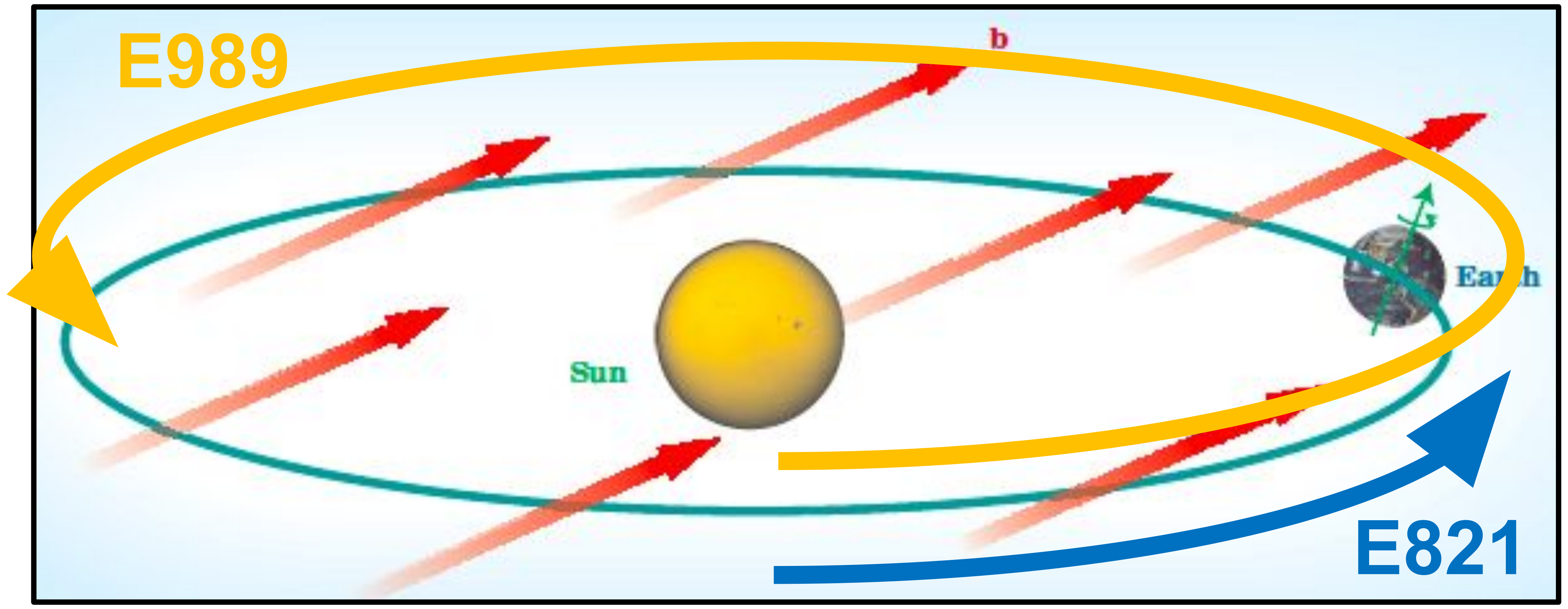

Thanks to the UMiss Muon g-2 Group

Postdocs

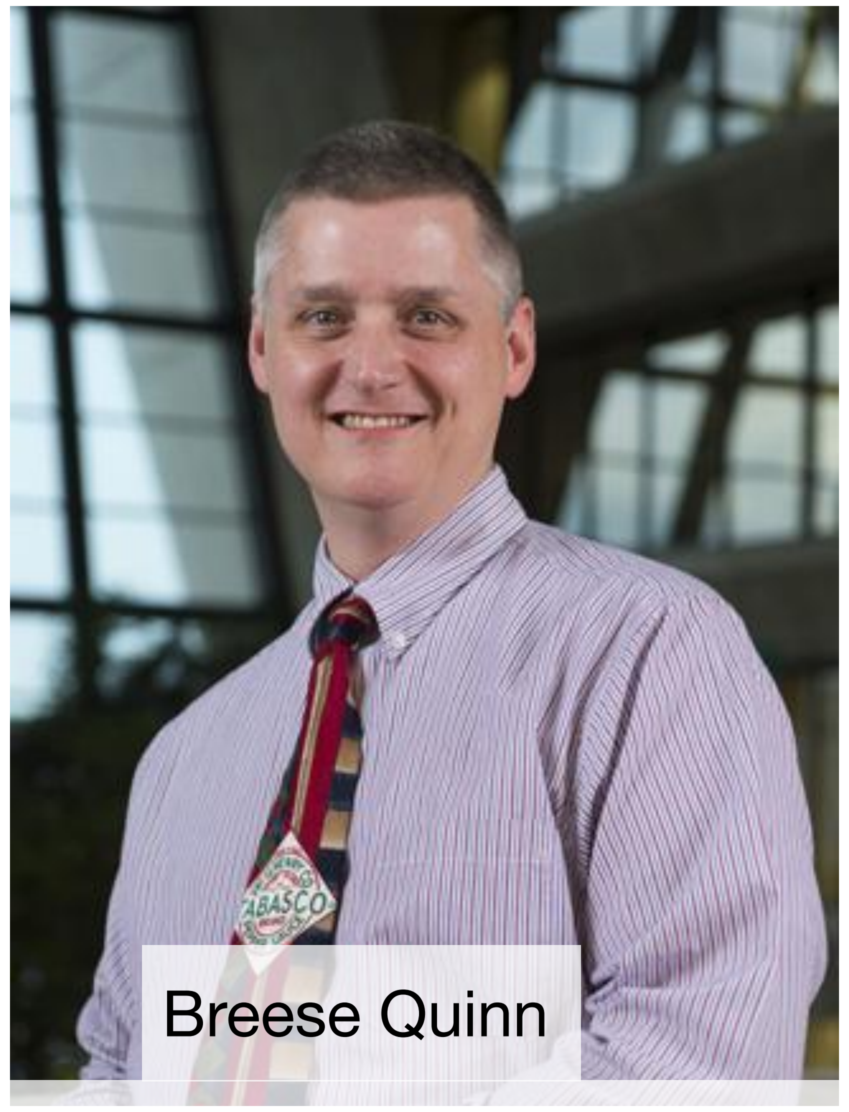

Undergraduate Student

Graduate Students

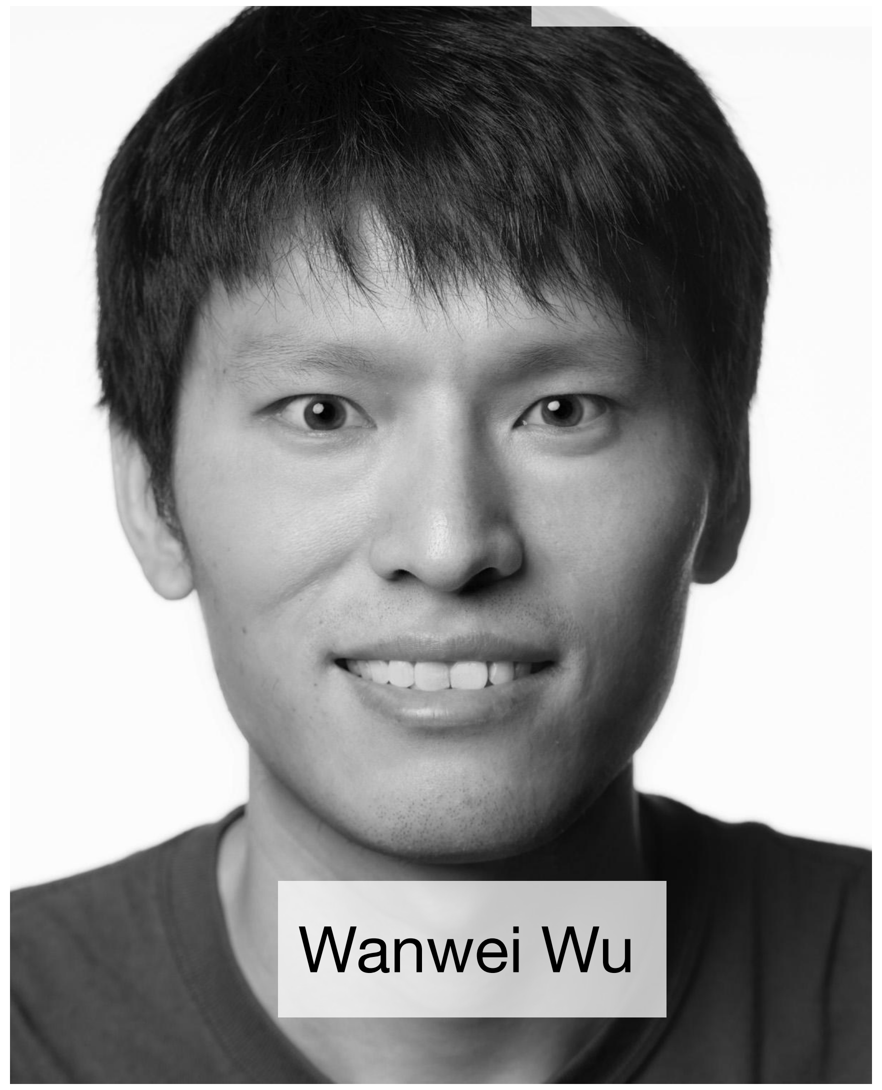

Undergrads Cooper Crawley, Lane Taylor

Acknowledgements

- Department of Energy (USA),
- National Science Foundation (USA),
- Istituto Nazionale di Fisica Nucleare (Italy),
- Science and Technology Facilities Council (UK),
- Royal Society (UK),
- Leverhulme Trust (UK),
- European Union's Horizon 2020,
- Strong 2020 (EU),
- German Research Foundation (DFG),
- National Natural Science Foundation of China,
- MSIP, NRF and IBS-R017-D1 (Republic of Korea)

Thanks also to all engineers, techs and support staffs at all our collaborating institutions for their work which made g-2 successful!!

Thank You, UCL!

Backup Slides